

US010934241B2

(12) United States Patent

(10) Patent No.: US 10,934,241 B2

(45) **Date of Patent:** Mar. 2, 2021

(54) CURCUMINOID-INSPIRED SYNTHETIC COMPOUNDS AS ANTI-TUMOR AGENTS

(71) Applicant: **Kenneth K. Laali**, Jacksonville, FL

(US)

(72) Inventor: Kenneth K. Laali, Jacksonville, FL

(US)

(73) Assignee: University of North Florida Board of

Trustees, Jacksonville, FL (US)

(*) Notice: Subject to any disclaimer, the term of this

patent is extended or adjusted under 35

U.S.C. 154(b) by 0 days.

(21) Appl. No.: 16/010,822

(22) Filed: Jun. 18, 2018

(65) Prior Publication Data

US 2018/0362433 A1 Dec. 20, 2018

Related U.S. Application Data

- (60) Provisional application No. 62/520,788, filed on Jun. 16, 2017.
- (51) Int. Cl. C07C 49/235 (2006.01) C07C 49/255 (2006.01) C07F 5/02 (2006.01)
- (58) Field of Classification Search CPC C07C 49/255; C07C 49/235; C07F 5/022 See application file for complete search history.

(56) References Cited

U.S. PATENT DOCUMENTS

1,009,550 A *	11/1911	Moys B67D 7/163
7.355.081 B2*	4/2008	141/381 Lee C07C 49/248
		568/36 Singh A61K 31/12

OTHER PUBLICATIONS

Gupta, Subash C. et al. Multitargeting by curcumin as revealed by molecular interaction studies. Nat Prod Rep. Nov. 2011; 28(12): 1937-1955.

(Continued)

Primary Examiner — Savitha M Rao Assistant Examiner — Andrew P Lee (74) Attorney, Agent, or Firm — Smith & Hopen, P.A.; Michele L. Lawson

(57) ABSTRACT

Novel CUR—and CUR—BF2 compounds exhibiting antitumor properties are presented. CUR compounds bearing fluorinated moieties with selective fluorine introduction into the α-carbonyl moiety as well as CUR—BF, adducts and CURs with diverse substitution patterns in the phenyl rings including fluorinated substituents (SCF₃, OCF₃, and F) and/or bulky activating groups (OMe, OAc, and OBz) are presented. Fluorinated aryl-pyrazoles and isoxazoles as well as novel CUR and CUR—BF₂ compounds with monocyclic aromatic and bicyclic-heteroaromatic lateral rings, bearing fluorine(s), OCF3, CF3, and SCF3 groups, and their alphacarbonyl-fluorinated analogs, as well as their pyrazole and isoxazole derivatives are presented. The CUR-pyrazoles embody analogs that are fluorinated at the phenyl-pyrazole moiety. The compounds and their derivatives exhibited exceptional cytotoxic and anti-proliferative activity against several cancer cell-lines. Deuterated CUR-BF2 and CUR compounds were also synthesized.

7 Claims, 97 Drawing Sheets

(56) References Cited

OTHER PUBLICATIONS

Minassi, Alberto et al. Dissecting the Pharmacophore of Curcumin. Which Structural Element Is Critical for Which Action? J. Nat. Prod., Feb. 20, 2013, 76: 1105-1112.

Bairwa, Khemraj et al. Recent developments in chemistry and biology of curcumin analogues. RSC Adv., 2014, 4: 13946-13978. Vyas, Alok et al. Perspectives on New Synthetic Curcumin Analogs and their Potential Anticancer Properties. Curr Pharm Des. 2013; 19(11): 2047-2069.

Pillai, G. Radhakrishna et al. Induction of apoptosis in human lung cancer cells by curcumin. Cancer Letters 208 (2004): 163-170.

Lopresti, Adrian L. et al. Multiple antidepressant potential modes of action of curcumin: a review of its anti-inflammatory, monoaminergic, antioxidant, immune-modulating and neuroprotective effects. Journal of Psychopharmacology, 2012, 26(12): 1512-1524.

Perrone, Donatella et al. Biological and therapeutic activities, and anticancer properties of curcumin (Review). Experimental and Therapeutic Medicine, 2015, 10: 1615-1623.

Tan, Kheng-Lin et al. Curcumin Analogues with Potent and Selective Anti-proliferative Activity on Acute Promyelocytic Leukemia: Involvement of Accumulated Misfolded Nuclear Receptor Corepressor (N-CoR) Protein as a Basis for Selective Activity. ChemMedChem 2012, 7: 1567-1579.

Cheng, Ce et al. Improved bioavailability of curcumin in liposomes prepared using a pH-driven, organic solvent-free, easily scalable process. RSC Adv., 2017, 7: 25978-25986.

Zhang, Lili et al. Curcumin-cyclodextrin complexes enhanced the anti-cancer effects of curcumin. Environmental Toxicology and Pharmacology 48 (2016) 31-38.

Yallapu, Murali Mohan et al. Beta-Cyclodextrin-curcumin self-assembly enhances curcumin delivery in prostate cancer cells. Colloids and Surfaces B: Biointerfaces 79 (2010) 113-125.

Liu, Jieying et al. Recent Progress in Studying Curcumin and its Nano-preparations for Cancer Therapy. Current Pharmaceutical Design, 2013, 19, 1974-1993.

Simoni, Daniele et al. Antitumor effects of curcumin and structurally Beta-diketone modified analogs on multidrug resistant cancer cells. Bioorganic & Medicinal Chemistry Letters 18 (2008) 845-849.

Nieto, Carla I. et al. Fluorination Effects on NOS Inhibitory Activity of Pyrazoles Related to Curcumin. Molecules 2015, 20, 15643-15665.

Amolins, Michael W. et al. Synthesis and evaluation of electron-rich curcumin analogues. Bioorg Med Chem. Jan. 1, 2009; 17(1): 360-367.

Labbozzetta, Manuela et al. Lack of nucleophilic addition in the isoxazole and pyrazole diketone modified analogs of curcumin; implications for their antitumor and chemosensitizing activities. Chemico-Biological Interactions 181 (2009) 29-36.

Narlawar, Rajeshwar et al. Curcumin-Derived Pyrazoles and Isoxazoles: Swiss Army Knives or Blunt Tools for Alzheimer's Disease? ChemMedChem 2008, 3, 165-172.

Wan, Sheng Biao et al. Evaluation of curcumin acetates and amino acid conjugates as proteasome inhibitors. International Journal of Molecular Medicine, 2010; 26: 447-455.

Feng, Ling et al. Synthesis and Biological Evaluation of Curcuminoid Derivatives. Chem. Pharm. Bull., 2015; 63(11): 373-881.

Wichitnithad, Wisut et al. Synthesis, Characterization and Biological Evaluation of Succinate Prodrugs of Curcuminoids for Colon Cancer Treatment. Molecules 2011, 16, 1888-1900.

Cheikh-Ali, Zakaria et al. "Squalenoylcurcumin" Nanoassemblies as Water-Disperable Drug Candidates with Antileishmanial Activity. ChemMedChem 2015, 10, 411-418.

Sribalan, Rajendran et al. Synthesis and biological evaluation of new symmetric curcumin derivatives. Bioorganic & Medicinal Chemistry Letters 25 (2015) 4282-4286.

Wada, Koji et al. Novel curcumin analogs to overcome EGFR-TKI lung adenocarcinoma drug resistance and reduce EGFR-TKI-induced GI adverse effects. Bioorganice & Medicinal Chemistry 23 (2015) 1507-1514.

Lin, Li et al. Antitumor agents 247. New 4-ethoxycarboylethyl curcumin analogs as potential antiandrogenic agents. Bioorganic & Medicinal Chemistry 14 (2006) 2527-2534.

Lin, Li et al. Antitumor Agents. 250. Design and Synthesis of New Curcumin Analogues as Potential Anti-Prostate Cancer Agents. J. Med. Chem. 2006, 49, 3963-3792.

Martinez-Cifuentes, Maximiliano et al. Heterocyclic Curcumin Derivatives of Pharmacological Interest: Recent Progress. Current Topics in Medicinal Chemistry, 2015, 15, 1663-1672.

Wang, Jiang et al. Fluorine in Pharmaceutical Industry: Fluorine-Containing Drugs Introduced to the Market in the Last Decade (2001-2011). Chem. Rev., 2014, 114, 2432-2506.

Rao, E. Venkata and P. Sudheer. Revisiting Curcumin Chemistry Part I: A New Strategy for the Synthesis of Curcuminoids. Indian J Pharm Sci. May-Jun. 2011; 73(3): 262-270.

Megna, Bryant W. et al. The aryl hydrocarbon receptor as an antitumor target of synthetic curcuminoids in colorectal cancer. Journal of Surgical Research, Jun. 2017 (213) 16-24.

Elavarasan, S. et al. An Efficient Green Procedure for Synthesis of Some Fluorinated Curcumin Analogues Catalyzed by Calcium Oxide under Microwave Irradiation and Its Antibacterial Evaluation. Journal of Chemistry, vol. 2013, Article ID 640936; 1-8.

Padhye, Subhash et al. Fluorocurcumins as Cyclooxygenase-2 Inhibitor: Molecular Docking, Pharmacokinetics and Tissue Distribution in Mice. Pharmaceutical Research, vol. 26, No. 11, Nov. 2009:2438-2445.

Mimeault, Murielle and Surinder K. Batra. Potential applications of curcumin and its novel synthetic analogs and nanotechnology-based formulations in cancer prevention and therapy. Mimeault and Batra Chinese Medicine 2011, 6:31.

Kamada, Kenji et al. Boron Diflouride Curcuminoid Fluorophores with Enhanced Two-Photon Excited Fluorescence Emission and Versatile Living-Cell Imaging Properties. Chem. Eur. J. 2016, 22, 5219-5232.

Bai, Guifeng et al. Syntheses and photophysical properties of BF2 complexes of curcumin analogues. Org. Biomol. Chem., 2014, 12, 1618-1626.

Aertgeerts, Kathleen et al. Structural Analysis of the Mechanism of Inhibition and Allosteric Activation of the Kinase Domain of HER2 Protein. The Journal of Biological Chemistry, May 27, 2011; vol. 286, No. 21: 18756-18765.

Laali, Kenneth K. et al. Fluoro-curcuminoids and curcuminoid-BF2 adducts: Synthesis, X-ray structures, bioassay, and computational/docking study. Journal of Fluorine Chemistry 191 (2016) 29-41.

Laali, Kenneth K. et al. Novel fluorinated curcuminoids and their pyrazole and isoxazole derivatives: Synthesis, structural studies, Computational/Docking and in-vitro bioassay. Journal of Fluorine Chemistry 206 (2018) 82-98.

Padhye, Subhash et al. New Difluoro Knoevenagel Condensates of Curcumin, Their Schiff Bases and Copper Complexes as Proteasome Inhibitors and Apoptosis Inducers in Cancer Cells. Pharmaceutical Research, vol. 26, No. 8, Aug. 2009, 1874-1880.

* cited by examiner

FIG. 1

FIG. 2

FIG. 4

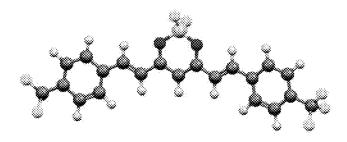


FIG. 5

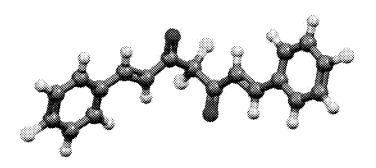


FIG. 6

FIG. 7

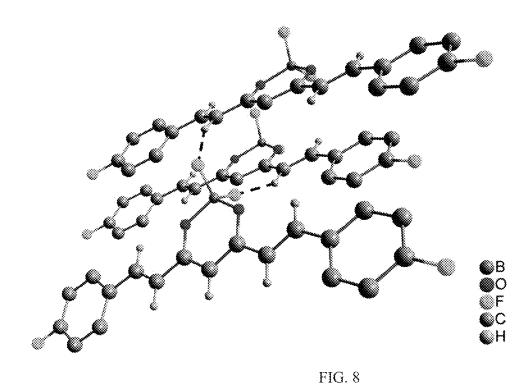


FIG. 9

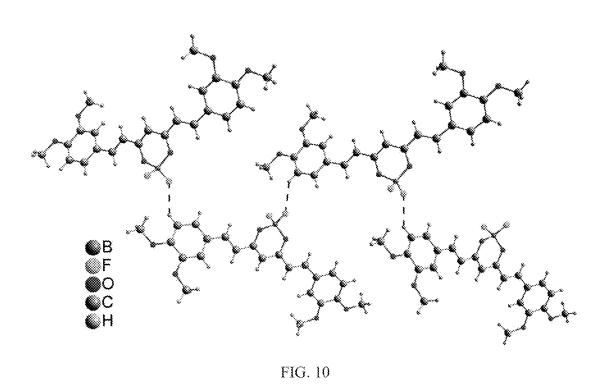


FIG. 11

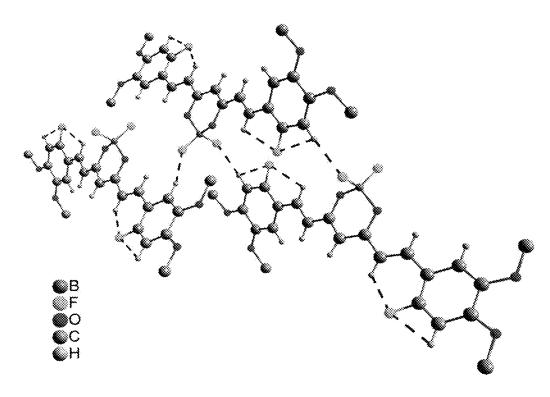


FIG. 12

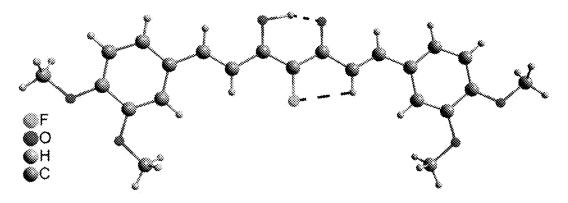


FIG. 13

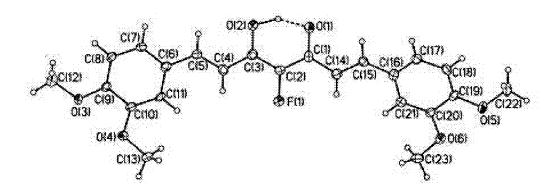


FIG: 14A

FIG. 14B

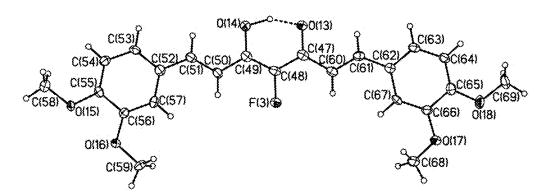


FIG. 14C

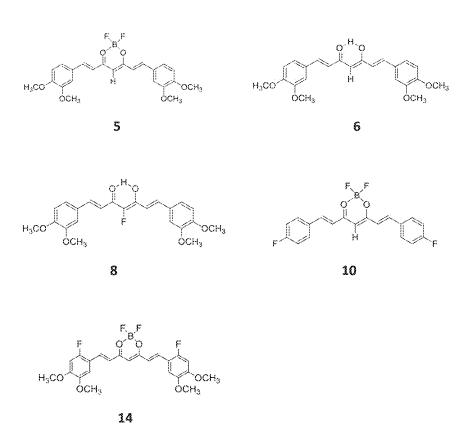
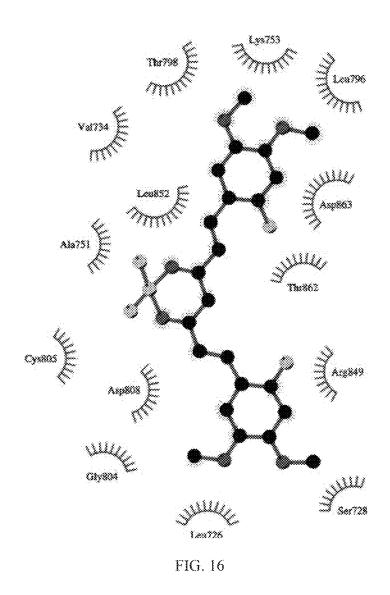


FIG. 15



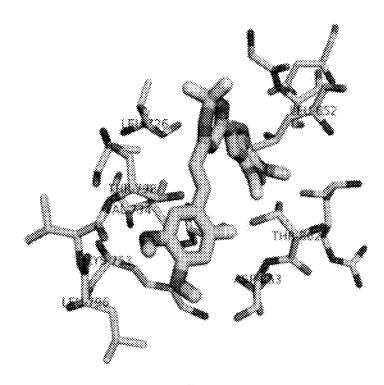
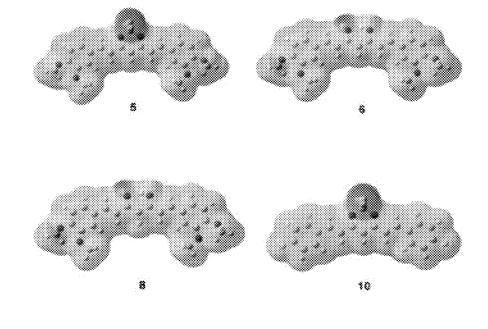


FIG. 17



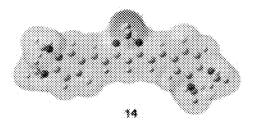


FIG. 18

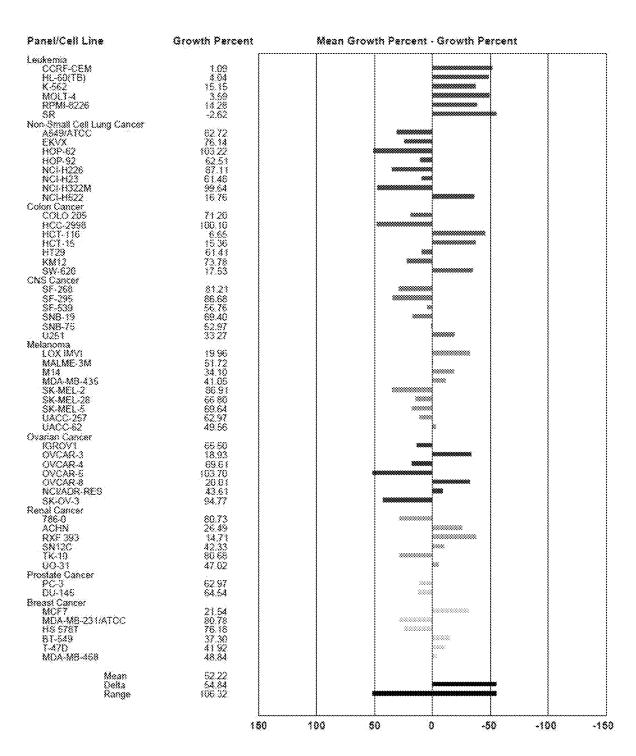


FIG. 19

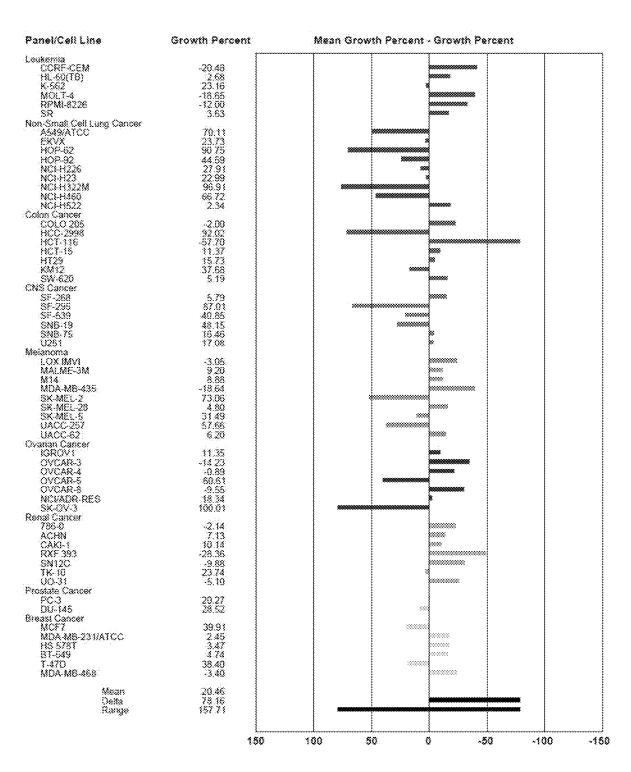


FIG. 20

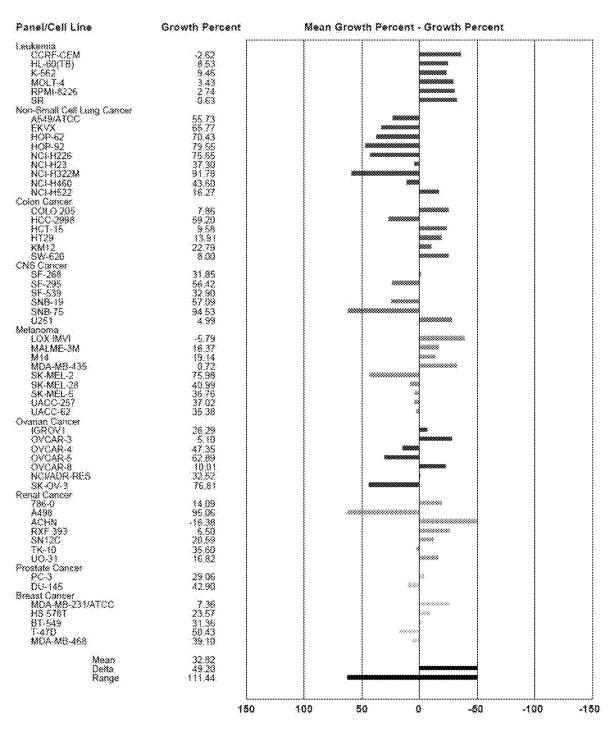


FIG. 21

One Dose Mean Graph		Expe	Experiment ID: 1705OS00			Report Date: May 26, 20	
Panel/Cell Line	Growth Percent	i	Mean Growth I	Percent ·	Growth Perc	cent	
Leukemia							[
CORF-CEM	69.72		1		88		
HL-60(TB)	81.90 77.64	1	1				
K-562 MOLT-4	76.07	- 1	1				}
RPMI-8226	38.93	- 1	1				
SR	40.81	- 1	1				{
Non-Small Cell Lung Cancer		- 1	1				1
A549/ATCC	95.36	- 1	1	900			
EKVX	111.48	1		3000			
HOP-62 HOP-92	101,36 93.05	- 1	1	8			
NCI-H226	100.00	1		9888			
NCI-H23	83.18	1	-		88 I		1
NOI-H322M	101.72	1		90000			
NCI-H460	91.07	1					
NCI-H522 Colon Cancer	93.74	- 1		- 88			
COLO 205	113.96	- 1	1	************			{
HČČ-2998	100.84	1		30000			
HCT-116	17.74	1				000000	
HOT-15	88.48	1	1				
HT29	83.21	1			88 88		
KM12 SVV-620	81,94 89,08	1			r		
CNS Cancer	09.00	1					
SF-268	86.28	1	1		k		
SF-295	97.55	1	1	988			
SF-539	105.97	- 1	1	0000000			{
SNB-19 SNB-75	90.30 115.34	- 1		2000000000			
U251	66.53		1				
Melanoma		1					
LOXIMVI	71.99	}	1				
MALME-3M	98.53	1		2000	l		
M14 MDA-MB-435	79,88 79,17		1		888 888		}
SK-MEL-2	100.99	1	1	38888	m		
SK-MEL-28	100.04		1	9888			
SK-MEL-5	91.39	1		*			
UACC-257	104.08	- 1	1	300000			
UACC-62 Ovanan Cancer	75,89	- 1	1		SSSSS		1
IGROV1	80.60	- 1	1		888		}
OVCAR-3	88.05	1					
OVCAR-4	97.30	- 1	1	988			{
OVCAR-5	117.63	- 1		***********			
OVCAR-8	95.98	1	1	988 300000			
NCI/ADR-RES SK-OV-3	103,80 118,59	- 1	1	90000000			
Renal Cancer	1	1	1				
786-0	87.22	1	1		†		
ACHN	101.94	}	1	30000	[1
CAKI-1 RXF 393	95,97 104.08	}	Į.	888 200000			1
SN12C	94.18	}	1	300000	[1
TK-10	100.77	1	I	30000			
UO-31	73.14	1	1				
Prostate Cancer	200	- 1	ł		200		
PC-3 DE-145	81.00	- 1	1	3668	***		}
DU-145 Breast Cancer	97,22	- 1	ł	5000			
MCF7	52.11	- 1	1		000000000000000000000000000000000000000		1
MDA-MB-231/ATCC	52.11 99.81	1	ł	33988			
HS 578T	98.23	1	1	35555			1
BT-549 T-470	82,46 77,96	1	ł		*** ****		1
MDA-M8-468	180.18	1		50000			
			1				
Mean Delta	88:72 70:98	1				nanon:	
Range	100.85			***********		010101	
	150	10	0 50		-50	-18	30 -15

FIG. 22

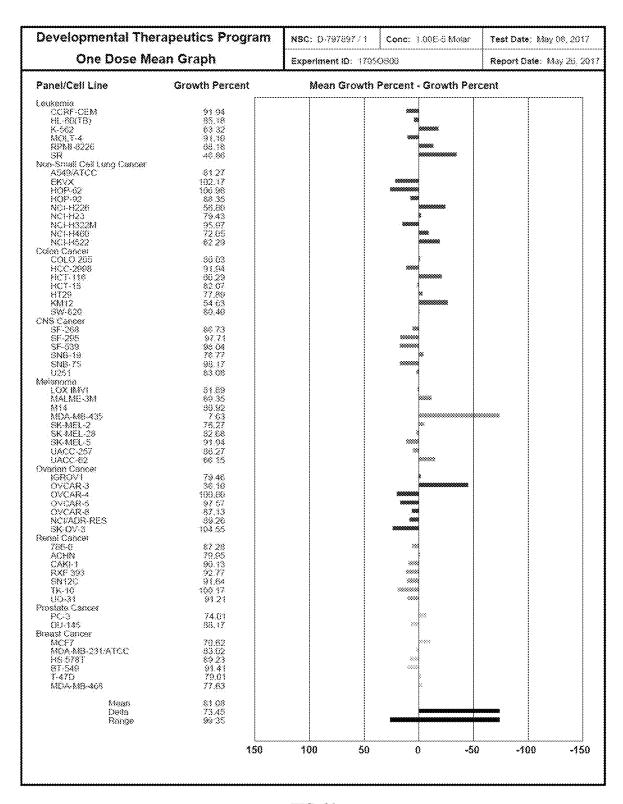
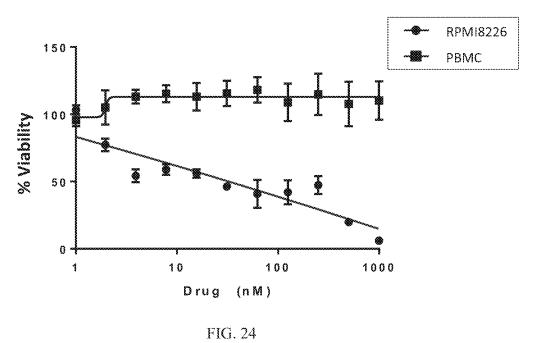


FIG. 23



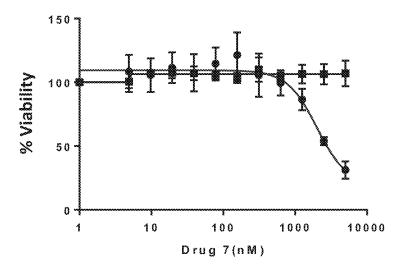


FIG. 25

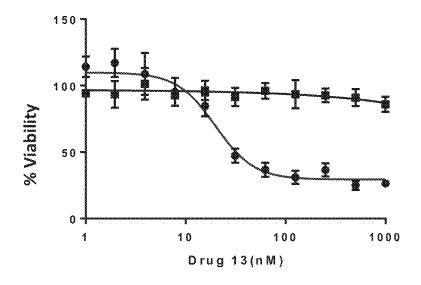


FIG. 26

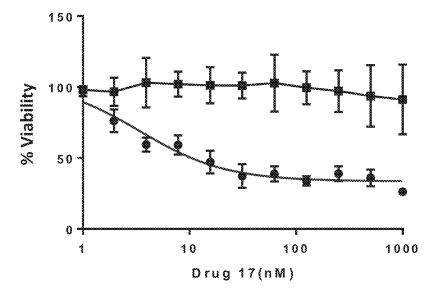


FIG. 27

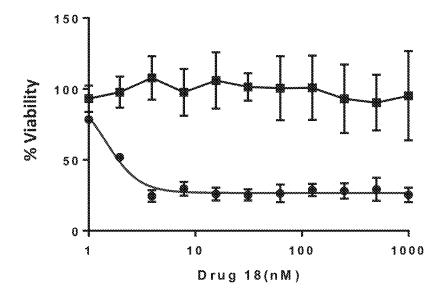


FIG. 28

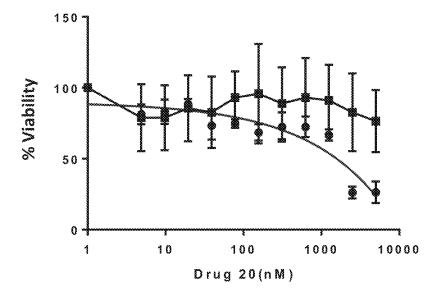


FIG. 29

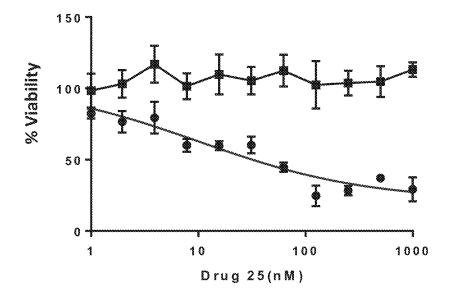


FIG. 30

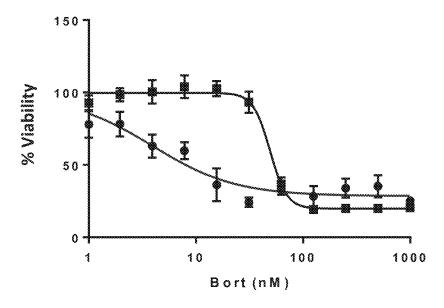


FIG. 31

FIG. 32

FIG. 33

FIG. 34

FIG. 35

Banking energies for Careamannels

Currenninalds	Autoback Vina (kink/mot)*						
	18082	Protessione	VEGR2	BRAF	8CL2		
Racovo indultitor	-31.4 (SW)	– 7.8 (Bergemaik) – 7.8 (Inaccentik) 8.5 (Carlinecck)	– V.2 (Artioth) – IOS (Scortenib) -89 (Legystonib)	-9.3 (Venus skaith) -12.9 (Eubaskaith)	-8.3 (Naviociae) -8.2 (Veneteriae)		
	<i></i> 7.8	-72	~7.A	±8,6:	478°		
	-83	·~8.3	~8.2.	~90 8	~&X°		
	-24		-4.4	÷ 7. ≱:	-58		
	-85	-4 7.6	-83°	# 8. \$	+8X°		
"L L" Çûr " ,	-75	7.2	+3.00 J	-7.6	-62		
	-73	≟ 8 .8	¥73 8	-8.3	4 88		
~~~ ~~~~~	-8.6	-9.9	-10.1	-187	- 9.9		
δ δ 	~ ta.s:	~18.3	~11.7	<b>~312</b> 0	÷8.3⊹		
	~38.4	-9.6	~18.4	4.01	~9.8		
	-38,8	-9.4	-113	-107	2 <del>8</del> 80		
	-9.8	-82	-38.7	-9.8	-8.á		
	~10.5	-£\$	~11.8	÷ 4.8	<b>-23</b>		
60 1 Ven	-10.6	- <b>+%&amp;</b> .	÷18.9.	-10.2	<b>8.</b> Ž		
	-10.7	# <b>*</b>	-12.3	-10.6	-16.0		
	~* <b>%</b> \$	<b>~?</b> ₺ .	~10.3	<b>~\$</b> .?∶	~738 ]		
	-30.4	-8.5	-11.5	-9.8	÷738		

FIG. 36

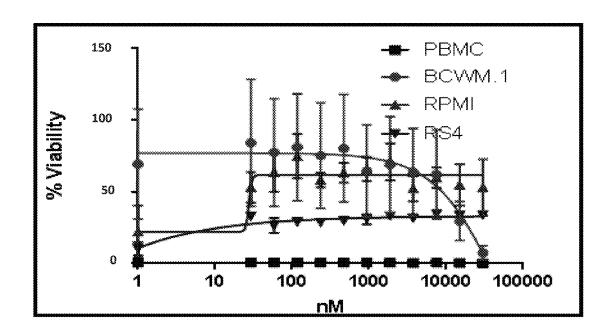
Concessoriopids	Amotivak Vina (keal/med)*						
	888382	Projessor	VIEFR2	BRAF	BC12		
. C. T. T. 13	-8:4	~\$.7	~ 9.4	-8.7	~6.3		
	- tø.t	~8.7	~18.2	~ §.\$	₩ <b>7</b> .3		

^{*} Most stable binding mode (more favorable values in bold).

FIG. 36 Cont.

	<u>Control</u>	<u>WM</u>	<u>MM</u>	ALL
Compound	PBMC	BCWM.1	RPMI 8226	RS4;11
7	7812	3884	6584	7171
6	516.5	473.9	500.4	506.7
9	17647	15289	26.33	1018
8	21701	8765	14914	11126
11	240.8	269.5	235.6	305.8
10	615.3	1541	1419	1888
15	6159	6985	12114	9911
14	1267	2242	1923	954.5
17	15315	9902	9867	15113
16	669,3	1422	1344	934.6
13	587.6	2225	2508	2408
12	54.97	371.3	550.6	450.9
5	30000	56644	27.69	30000
4	14444	15784	14930	12034
3	18943	7475	8898	8117
2	4058	6533	14332	7751

A



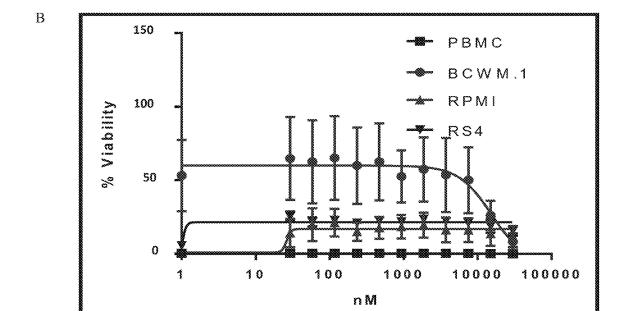


FIG. 38A-B

FIG. 39

 $R^3 = R^4 = OMe$ ;  $R^6 = F$ ;  $R^3 = R^5 = H$  [Ar¹ = Ph; p-OCF3-Ph; m-CF3-Ph; 3,5-F2-Ph; p-CN-Ph]

 $R^4 = SCF3$ ;  $R^2 = R^3 = R^5 = R^6 = H [Ar^1 = Ph; m-CF3-Ph]$ 

 $R^4 = F$ ;  $R^2 = R^3 = R^5 = R^6 = H$  [Ar¹ = Ph; m-CF3-Ph; p-OCF3-Ph; 3,5-F2-Ph; p-CN-Ph]

 $R^4 = CF3$ ;  $R^2 = R^3 = R^5 = R^6 = H [Ar^1 = Ph]$ 

 $R^2 = R^3 = R^4 = OMe; R^5 = R^6 = H [Ar^1 = Ph; p-OCF3-Ph]$ 

 $R^3 = R^4 = R^5 = OMe; R^2 = R^6 = H [Ar^1 = Ph; p-CF3-Ph; 3,5-F2-Ph]$ 

FIG. 41

FIG. 42

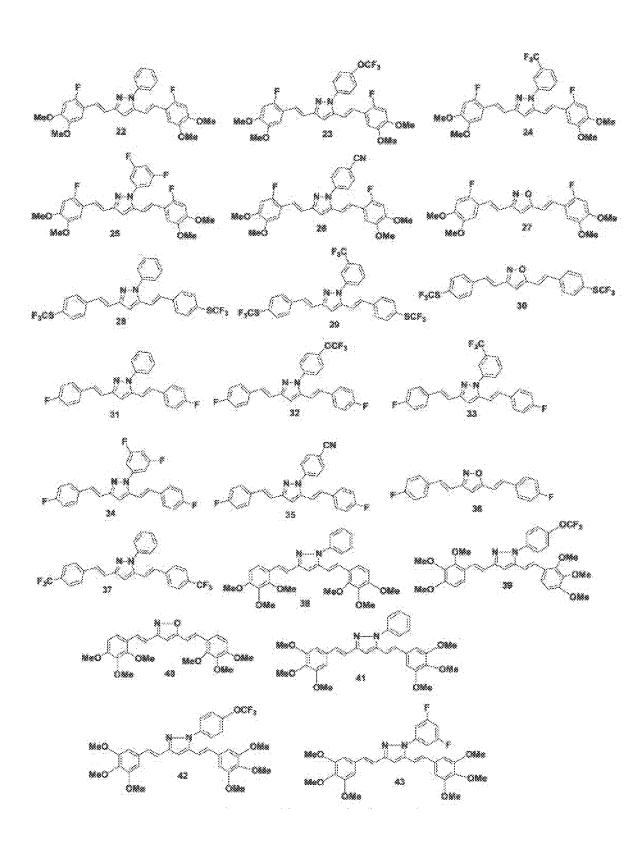


FIG. 43

Mar. 2, 2021

lsoxazoles"	HER2	Professome	VEGFR2	BRAF	BC1-3
Known inhibiter	-11.4(5Y8)	-7.8 (Bortezomin) -7.8 (Exacemin) -8.5 (Carilizomin)	9.? (Axionib) -18.8 (Soraionib) -8.9 (Lenvatiob)	9.3 (Ventural(cob) -12.9 (Pabrasenib)	-8.3 (Navitoclas -8.2 (Venetoclas
	8 - 8 - 9.2 Sc.7 - 7.3 (W.Y) - 8.6	-7.9 -7.8 -8.5	-8.7 -7.8 -8.1	-8 9 -8.4 -8.5	-6.7 -7.4 -5.6
1-11 <b>81</b> -01.9 004 1-11 <b>81</b> -01.9 004 1-11 <b>81</b> -01.9 004	****	-7. <b>8</b>	-2, <b>8</b> :	*	-6.9
	8 - 8 - (13 SC) - 10.0 CC) - 10.0	-8.7 -8.9 -9.3	-18.8 -9.7 -9.8	.3.9 .3.6 .5.8	-66 -72 - <b>83</b>
	9.4	-7.4	+18.8	-9.8	-80
<b>"</b> :4,0~ ¹³³ 0,4;	8 - 11 - 11.7 SCF: - 18.5 OCT: - 18.8	-3.8 -9.8 -9.3	-10.5 -9.8 -9.8	.9.9 .9.4 .9.5	-7.3 -7.8 -3.2
1,0 ¹² 0,4;	-9,7	*2	-18.8	.9.2	-8.2
	8 - 11 - 18.5 SUF: - 18.2 OUT: - 18.3	-8.9 -8.5 -9.2	.9.6 .3.8 .9.2	9.4 8.8 9.3	-7.1 3.7 -8.2
· p · ii			3.4	*!	7.5
	-19.7	-9.8	-16.4	-18,4	-8.4
	-18.6	-8.9	-18.8	-18.4	**.i
* 	-33.7	-9.4	-11.0	-16.4	-6.8

^{*}Most askite binding mode (more favorable values in brid).

Wyblighted compounds (or highlighted substitutents) are those that match with wotherhed campainds.

FIG. 45

FIG. 46

Synthesis of S-methylated curcuminoid dications salts

Mar. 2, 2021

S-methylated benzthiophene-2 CUR dication salt

A similar strategy is used for the preparation of isomeric 3-CUR dication salts

S-methylated benzthiophene-3 CUR BF2 dication salt

S-methylated benzthiophene-3 CUR dication salt

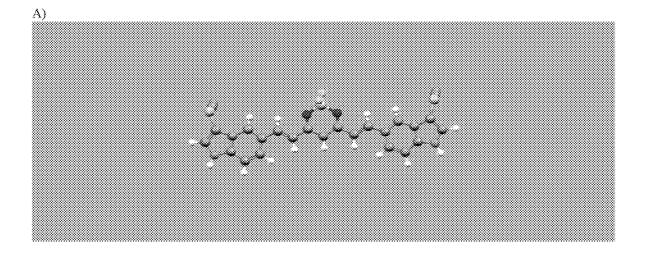
FIG. 47

FIG. 48

FIG. 49

FIG. 50

FIG. 51



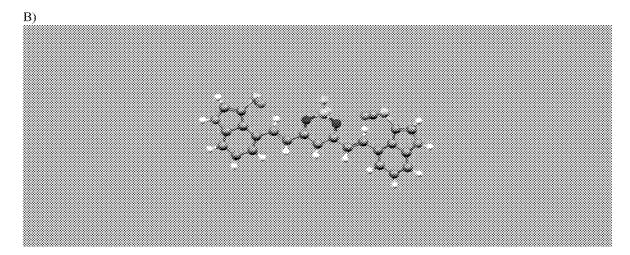
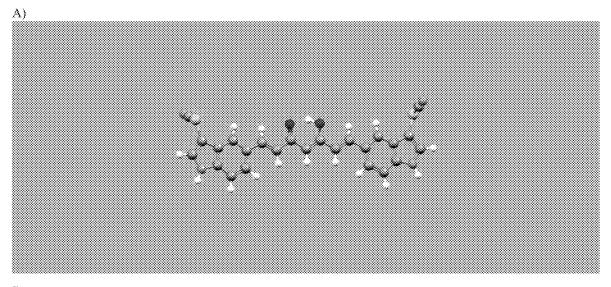


FIG. 52A-B



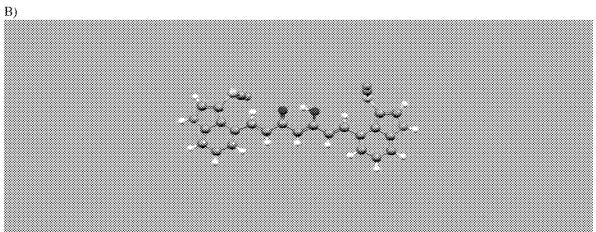


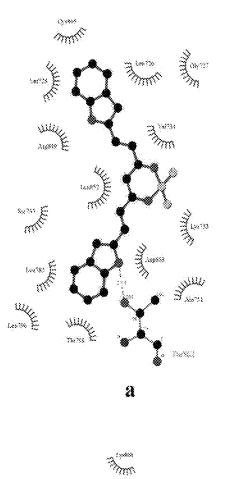
FIG. 53A-B

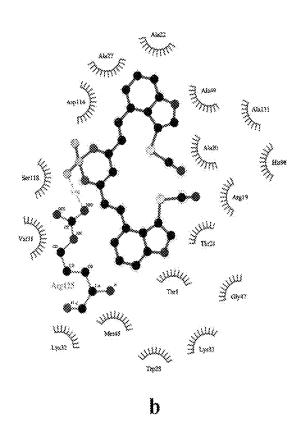
FIG. 54

FIG. 55

FIG. 56

FIG. 57





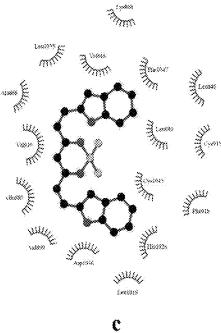
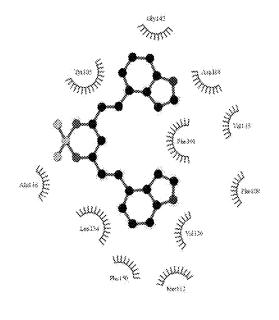


FIG. 58A-D



d

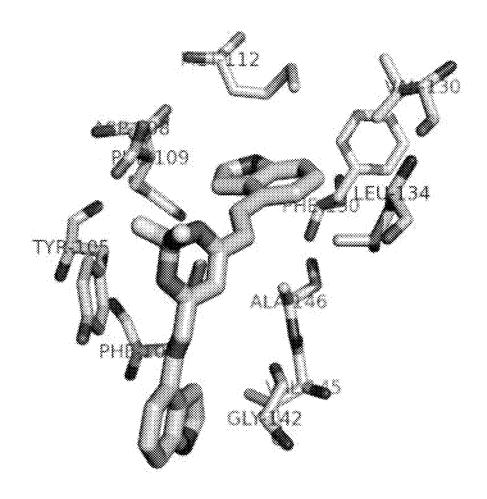


FIG. 59

FIG. 60

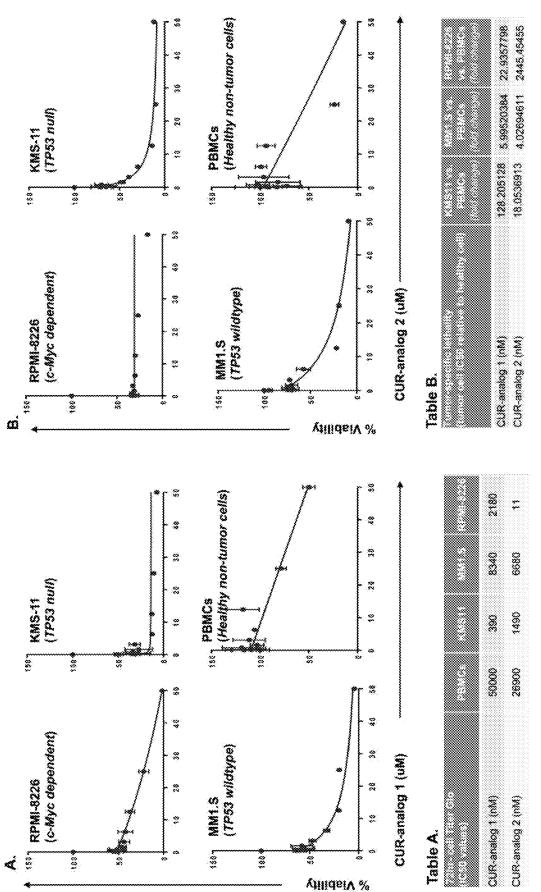
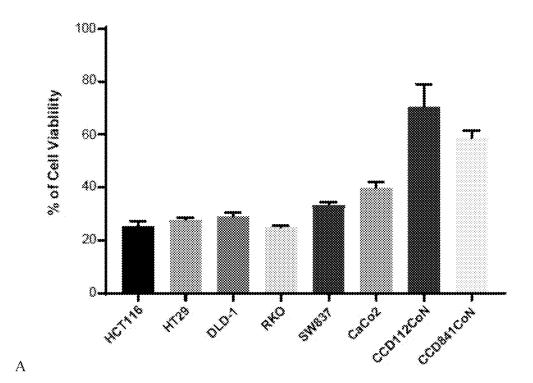
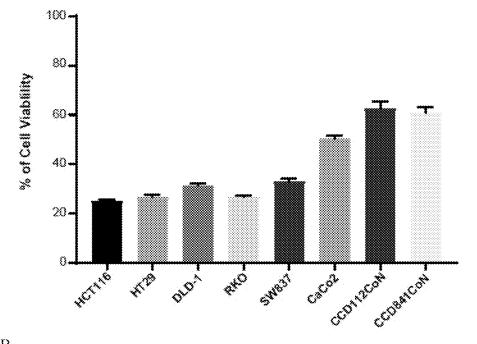


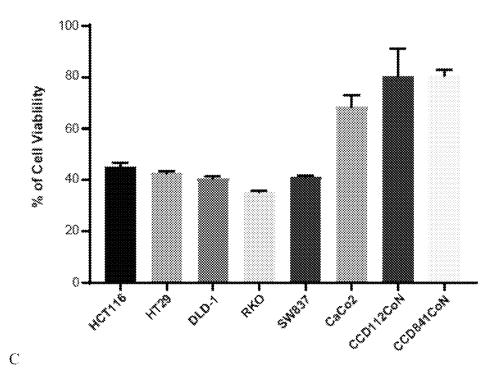
FIG. 61A-B

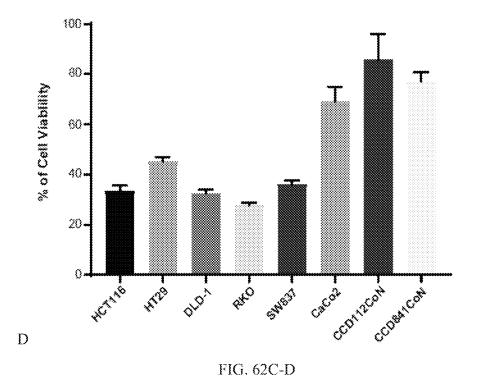


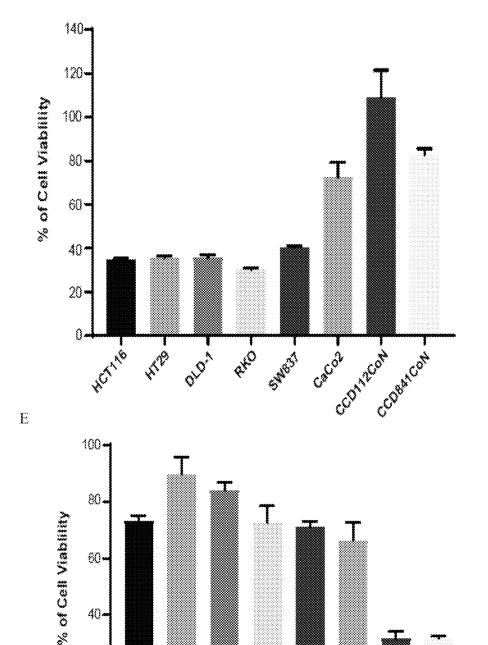


В

FIG. 62A-B







F

40.

20•

FIG. 62E-F

**→** 

Cacol Alcon acon

est C

digi,

A AND

	Organism	Tessee	Morphology	Disease	ATCC-Cat.
HCTIIE	iuran	color	epithelia	Colorectal carcinoma	CCL-247
HT29	iuman	color	epithelia	Colorectal adenocarcinoma	HT8-38
000-1	iuman	color	epithelia	Dukes' type C, colorectal adenocarcinoma	CC1-221
8KO	luman .	colon	epithelial	Carchoma	CRL-2577
SW837	janen	rection	epithelial	Grade IV, adenocarcinoma	CC1-235
Caco2	human	00/00	epithelial-like	Colorectal adenocarcinoma	HTE-37
CCD112CoN	human	colon	foroblast	Normal	CRL-1541
CCD841CoN	lurar	color	epithelia	Normal	CRL-1790

FIG. 64

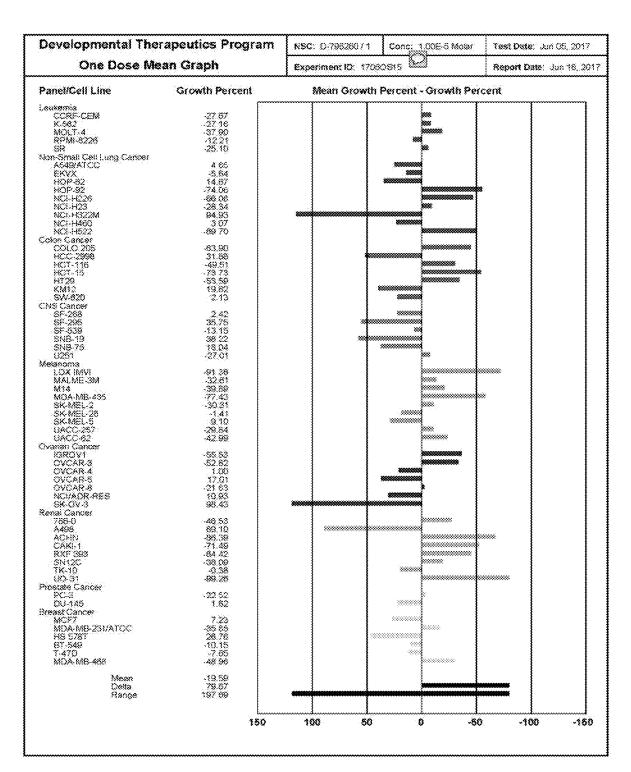


FIG. 65

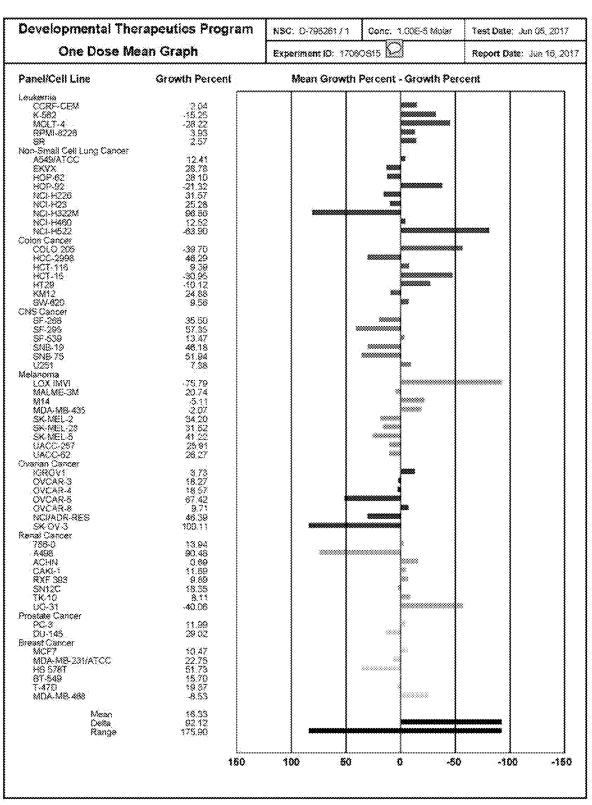


FIG. 66

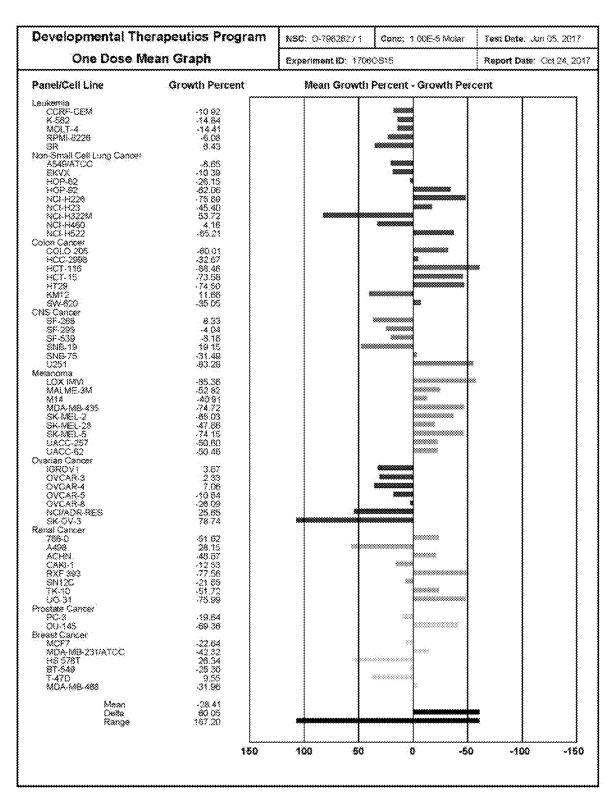


FIG. 67

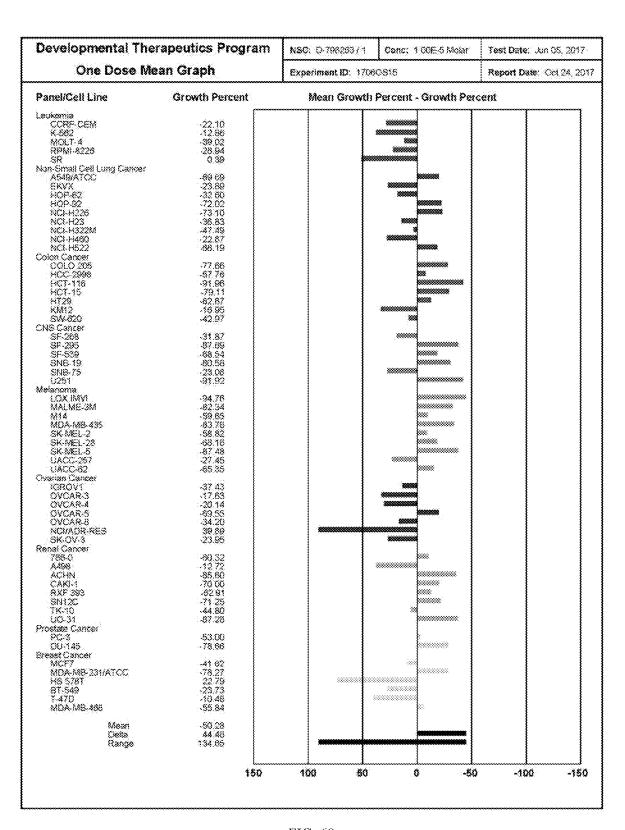


FIG. 68

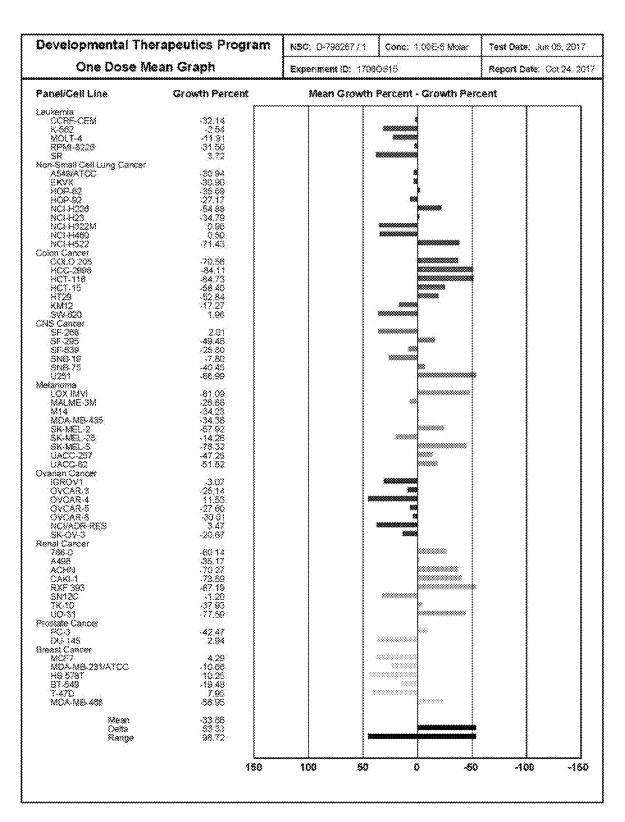
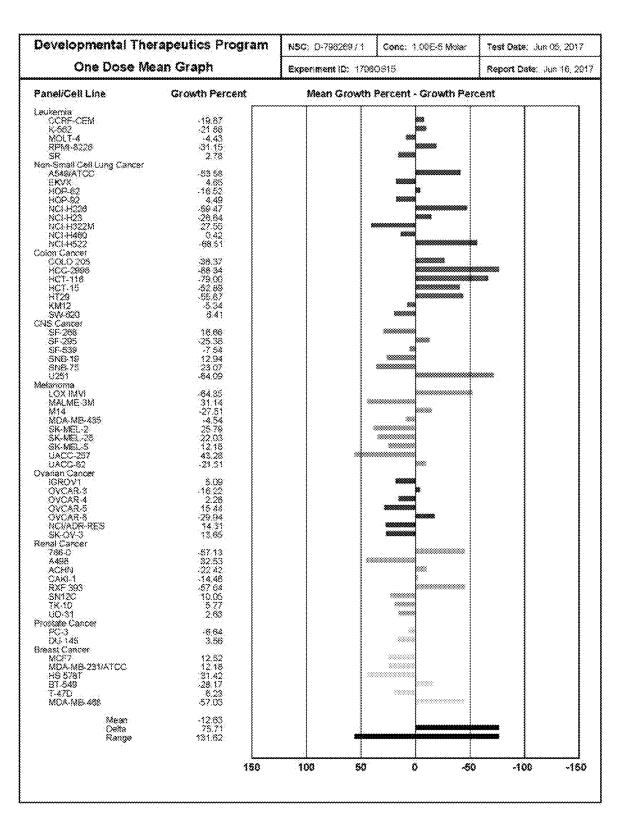


FIG. 69



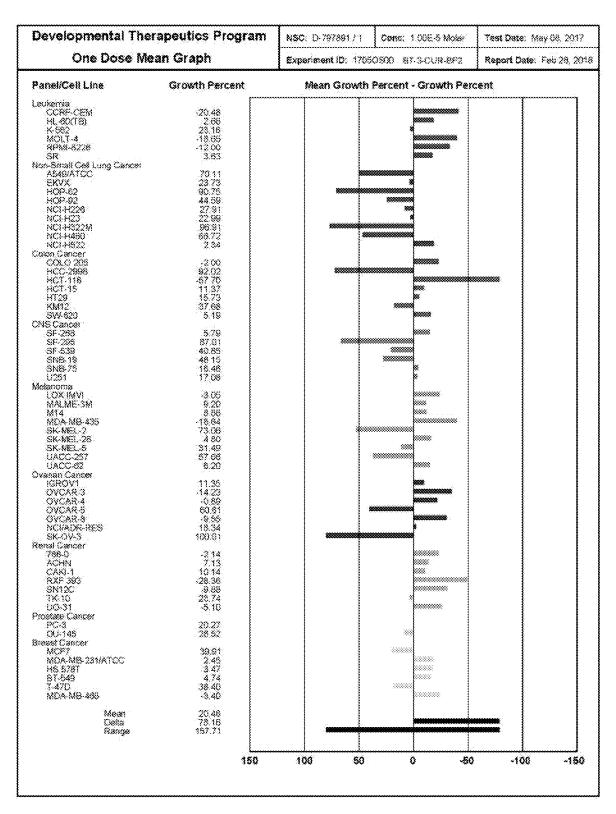


FIG. 71

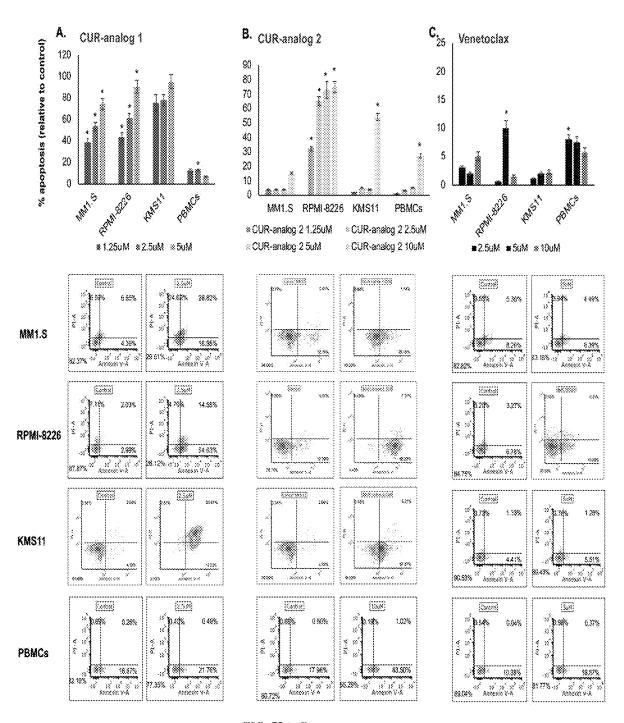


FIG. 72A-C

FIG. 73

A

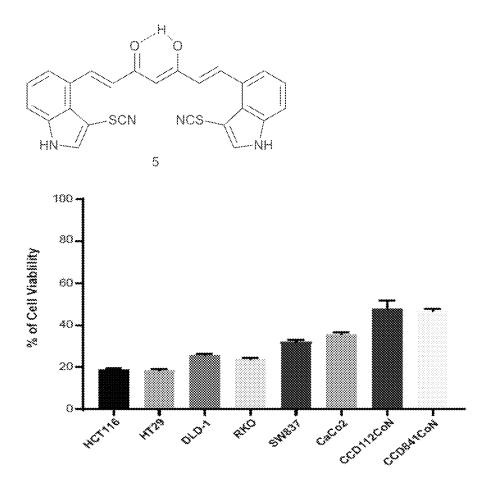


FIG. 74A

В

FIG. 74B

 $\mathbf{C}$ 

FIG. 74C

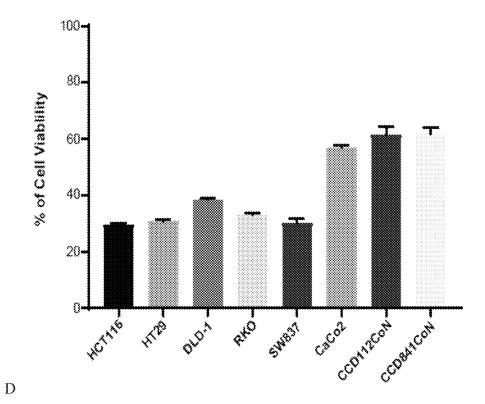


FIG. 74D

E

FIG. 74E

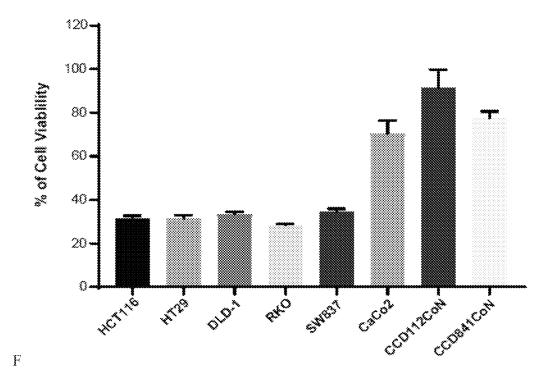
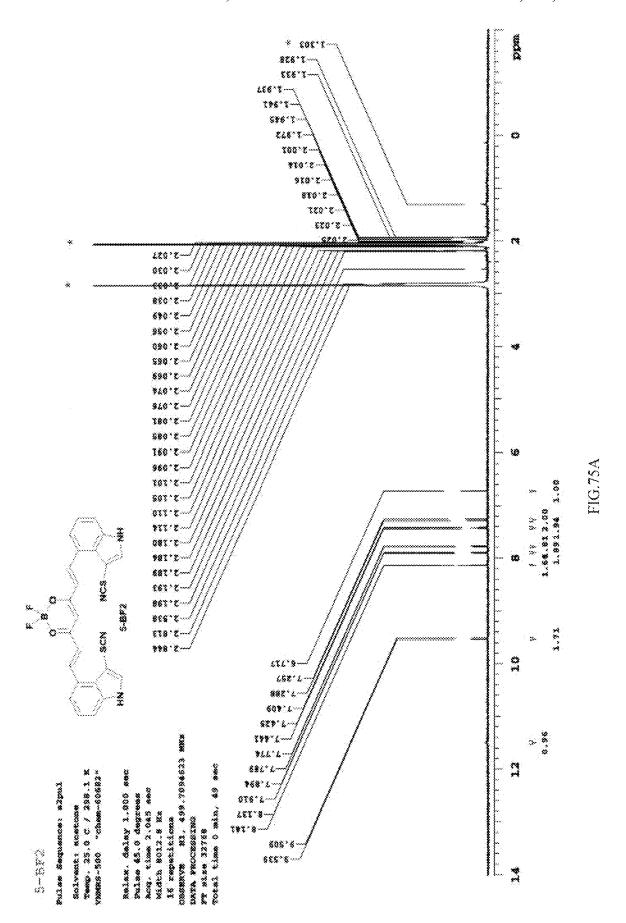
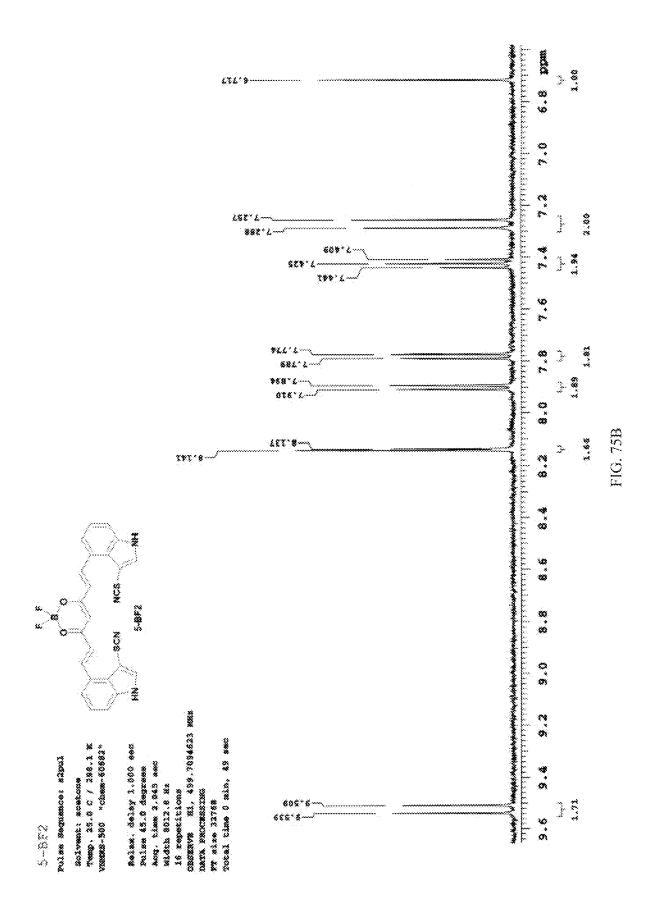
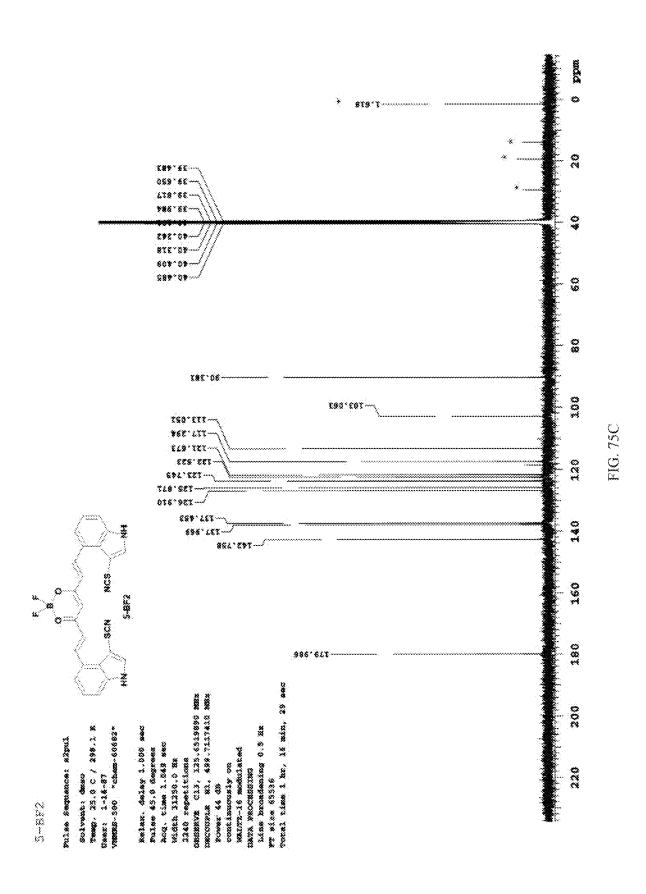
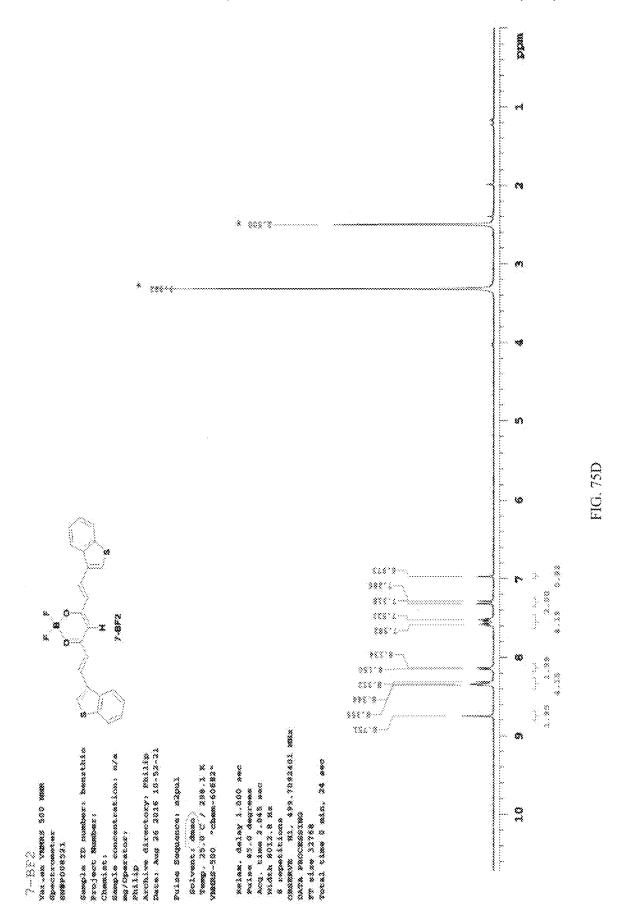


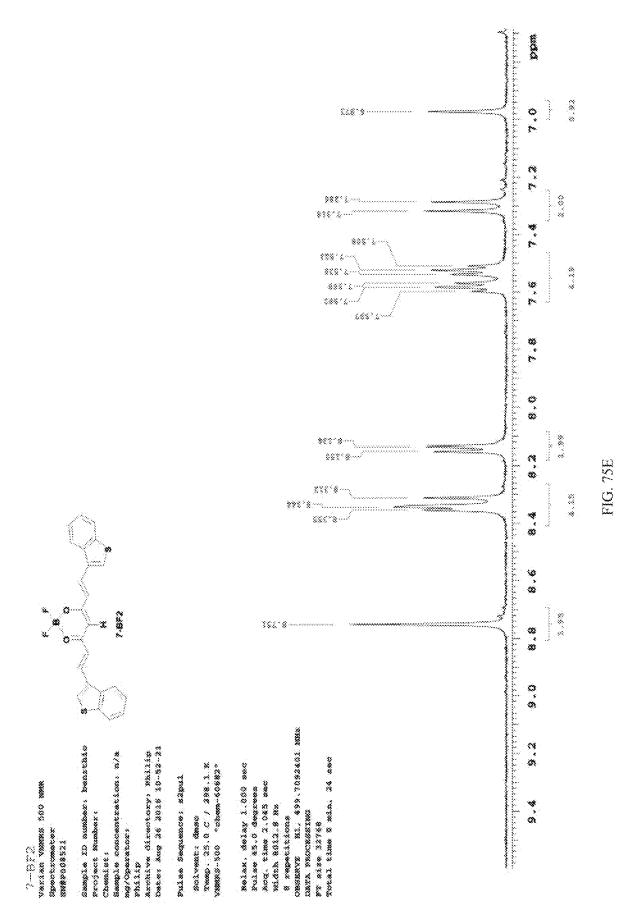
FIG. 74F

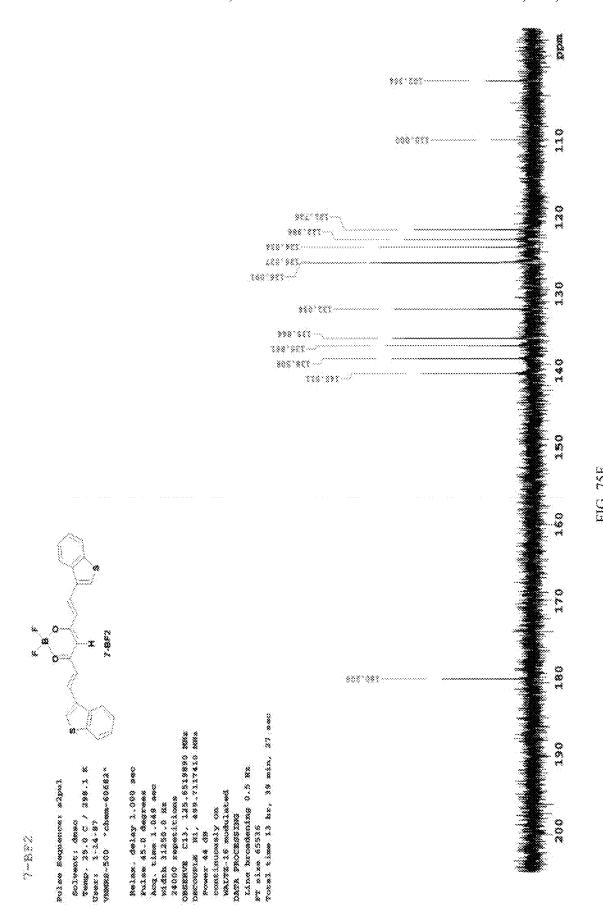


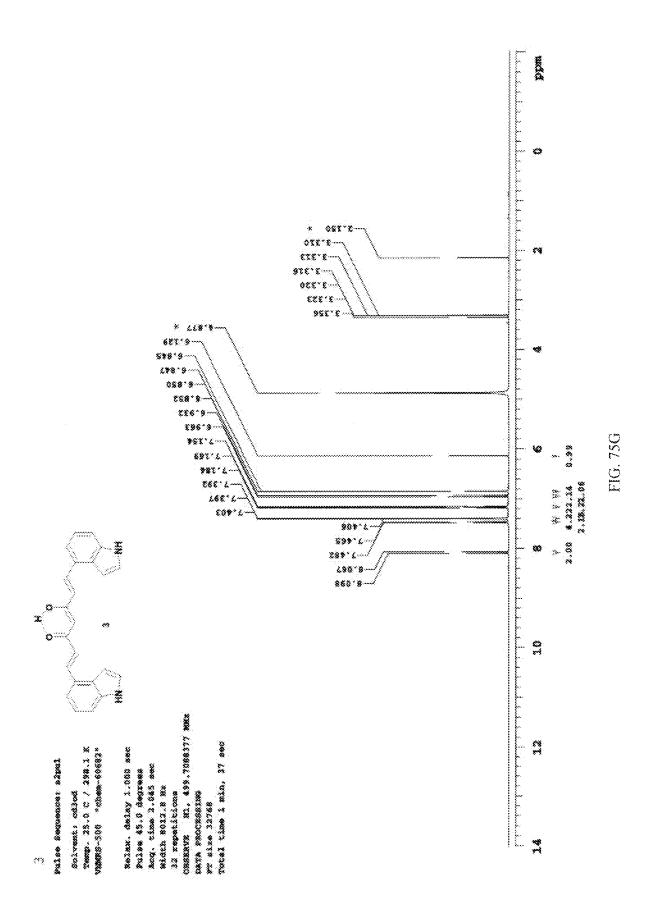


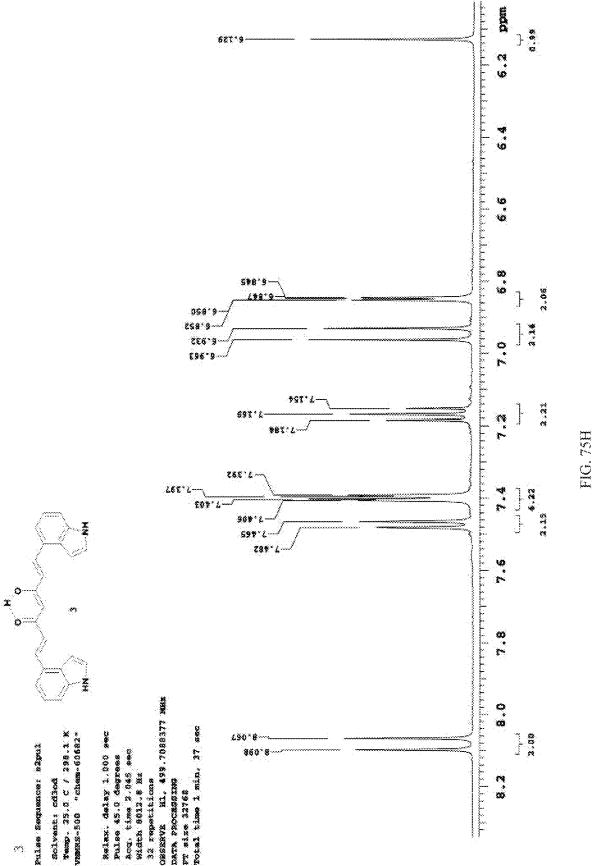


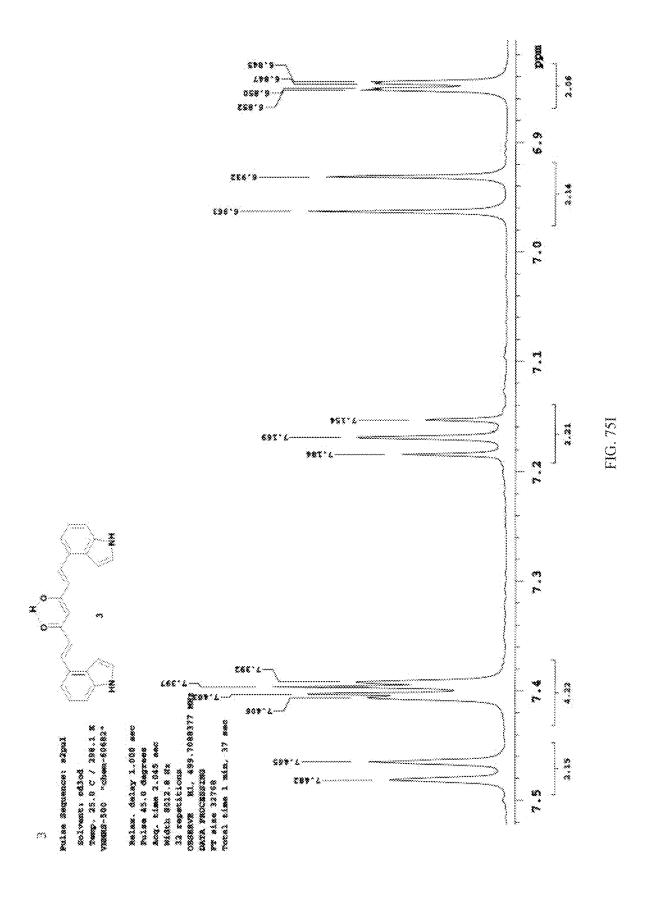


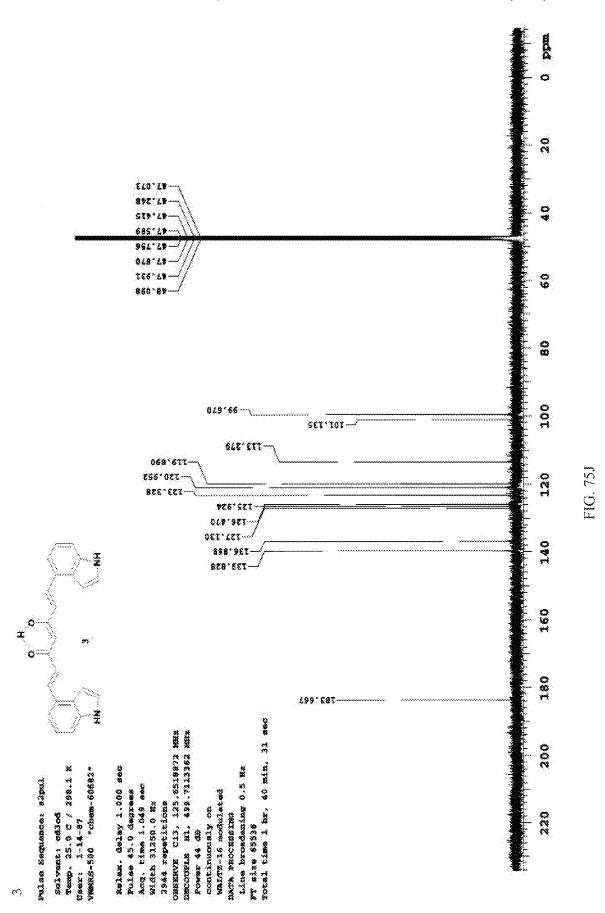


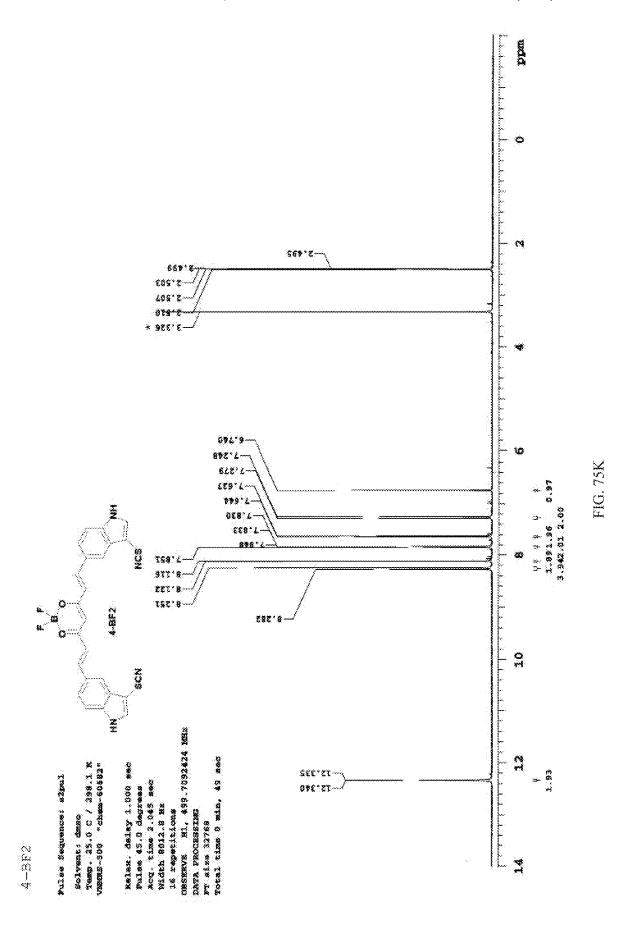


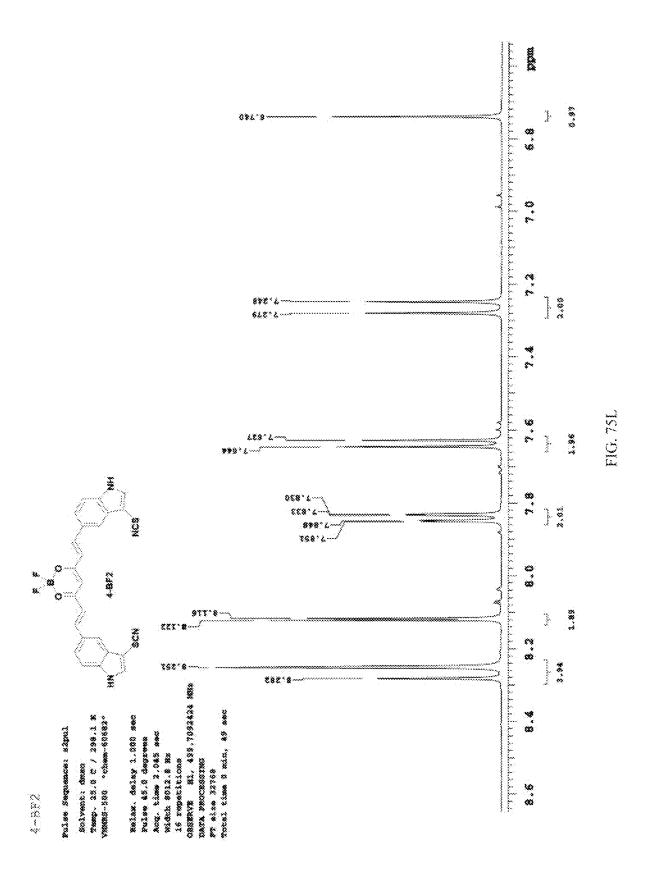


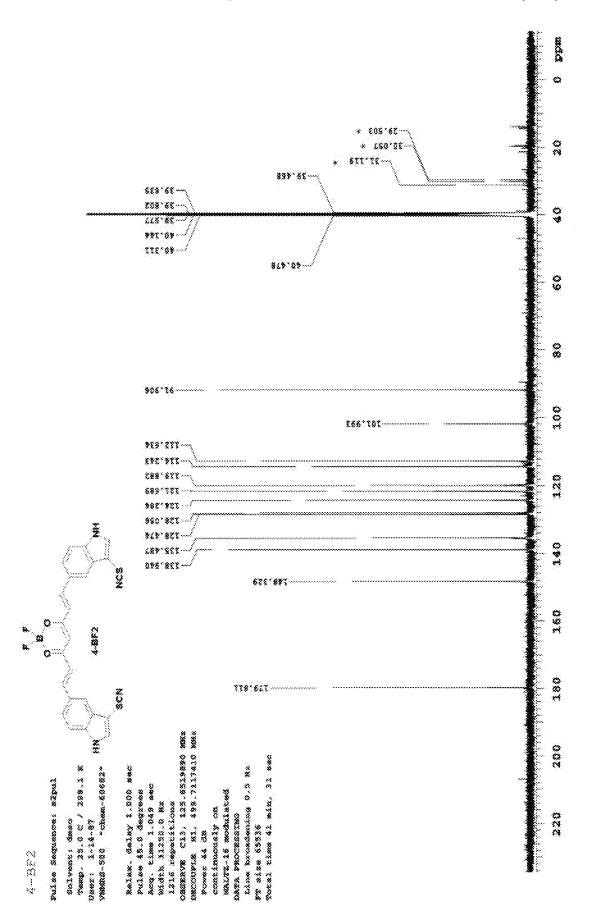




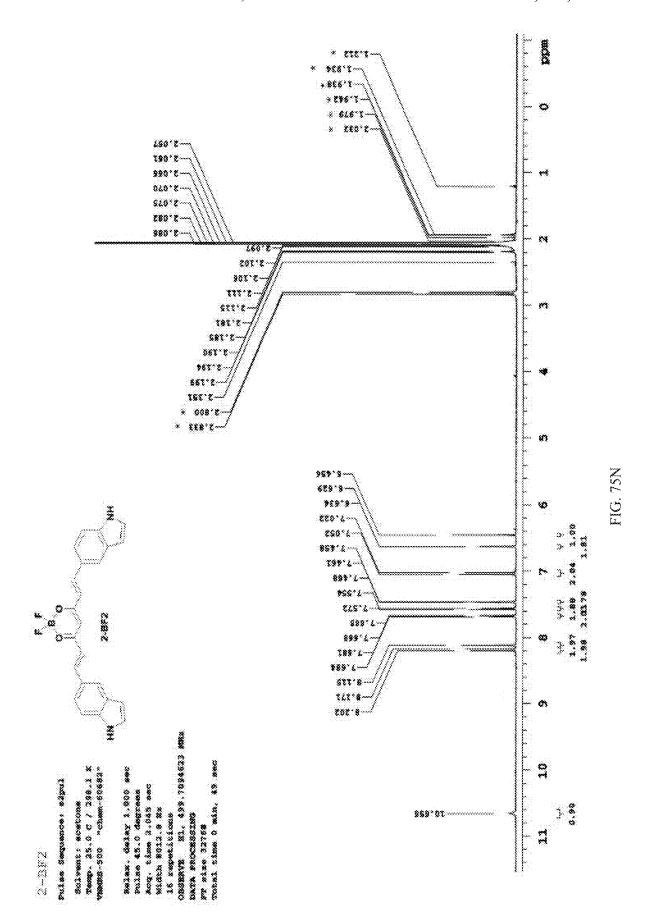


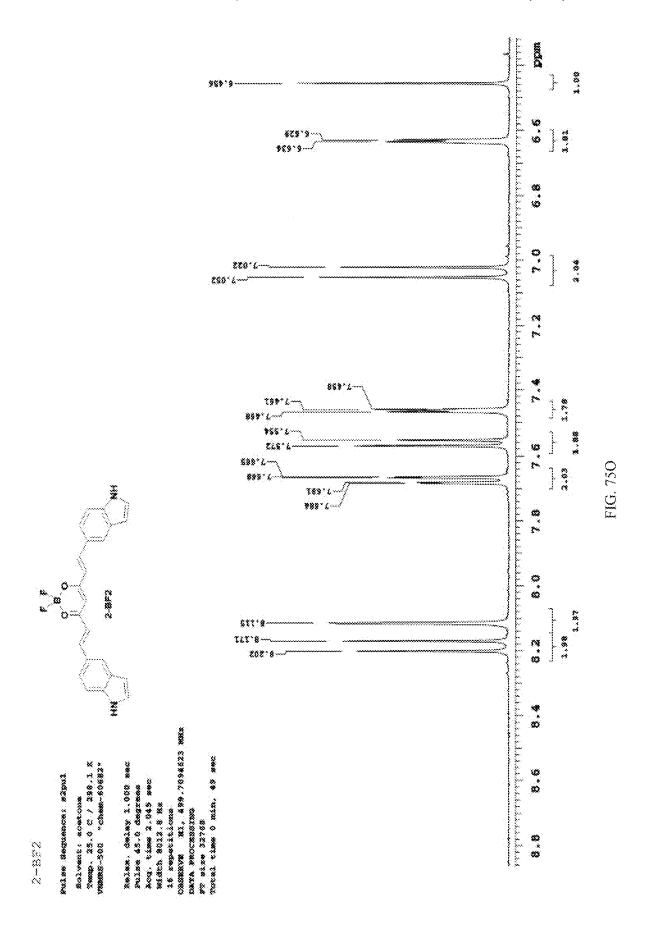


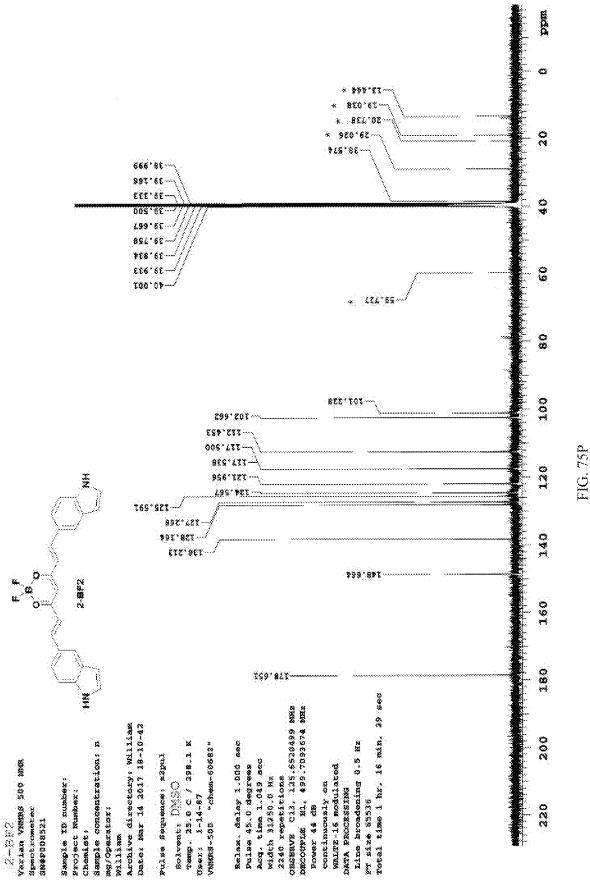


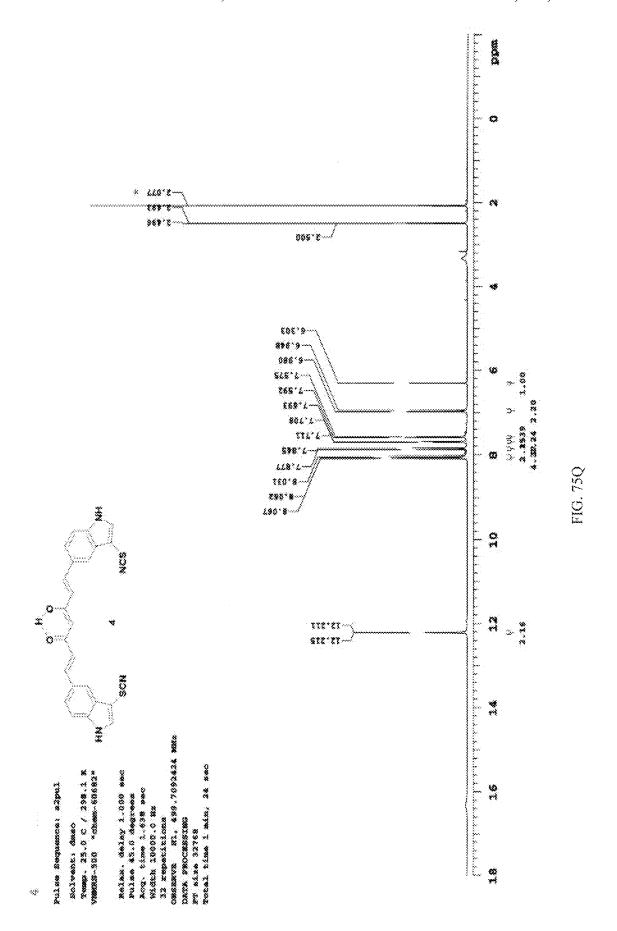


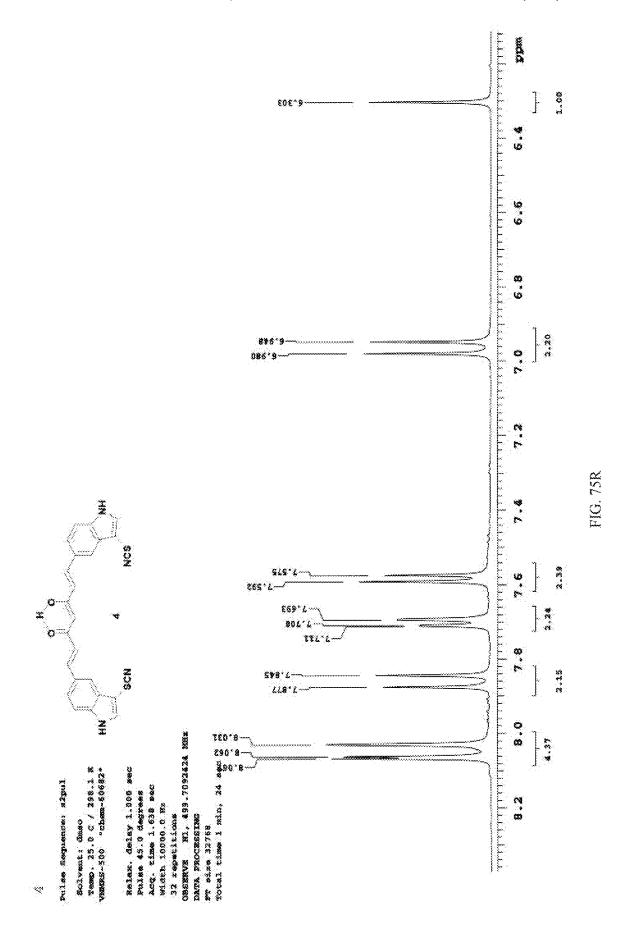
IG. 75M

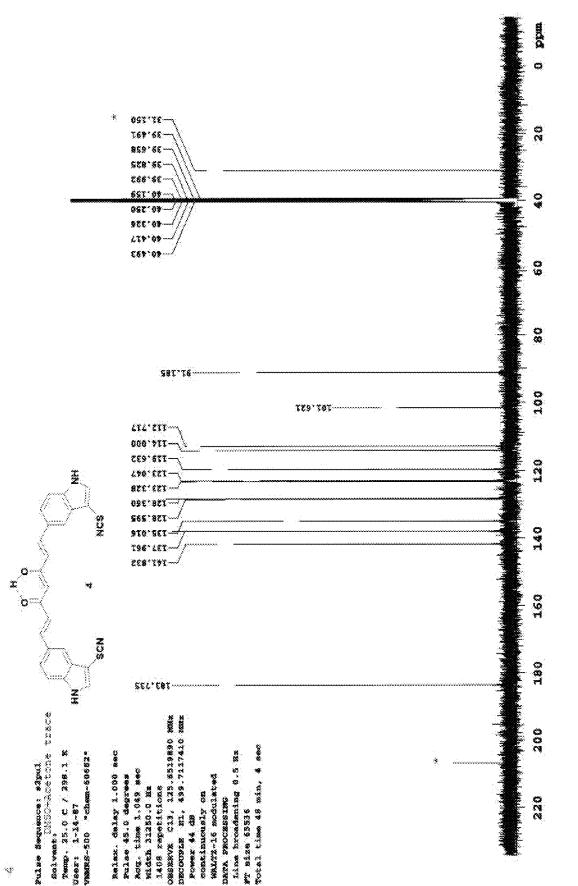




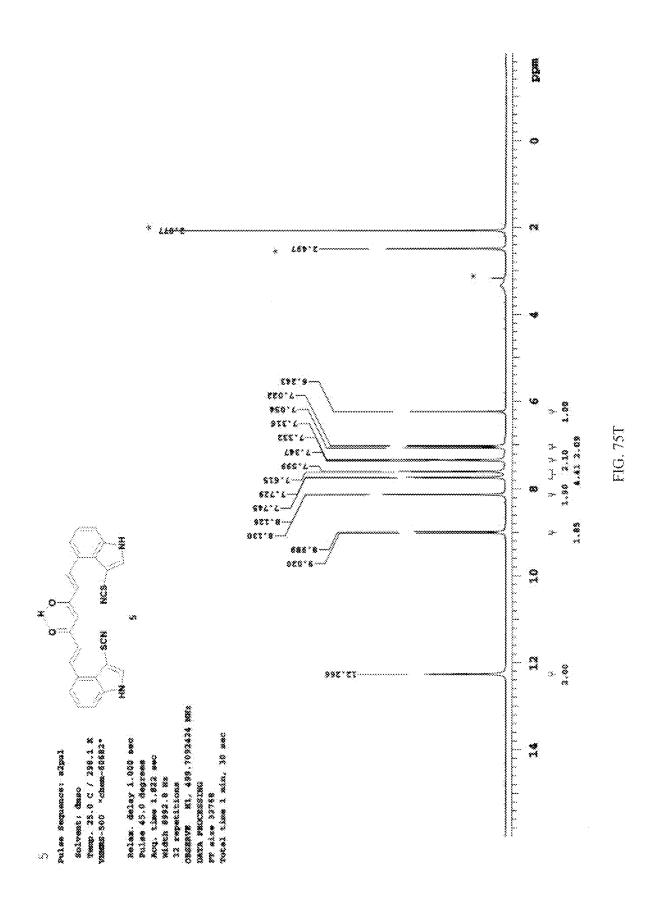


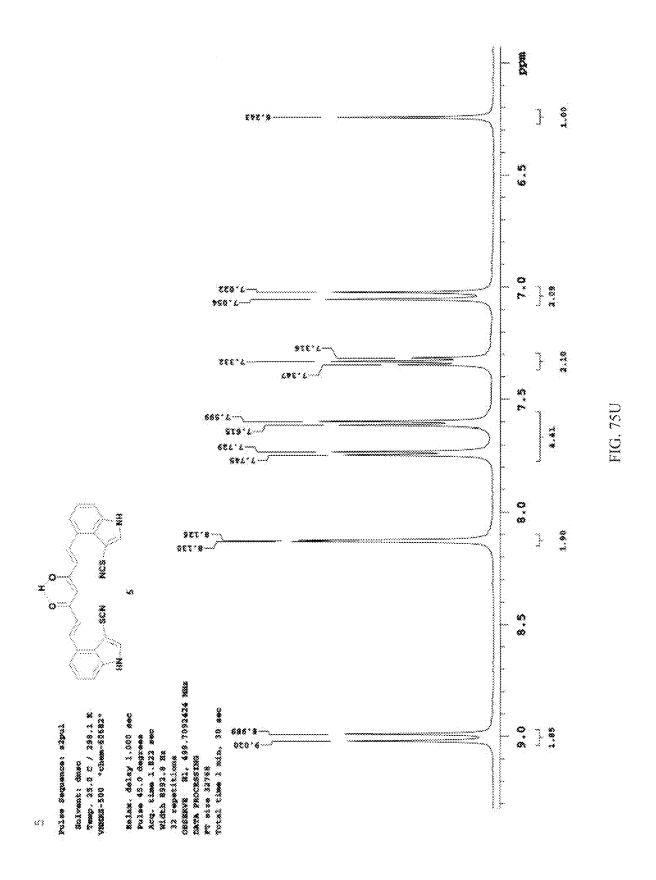


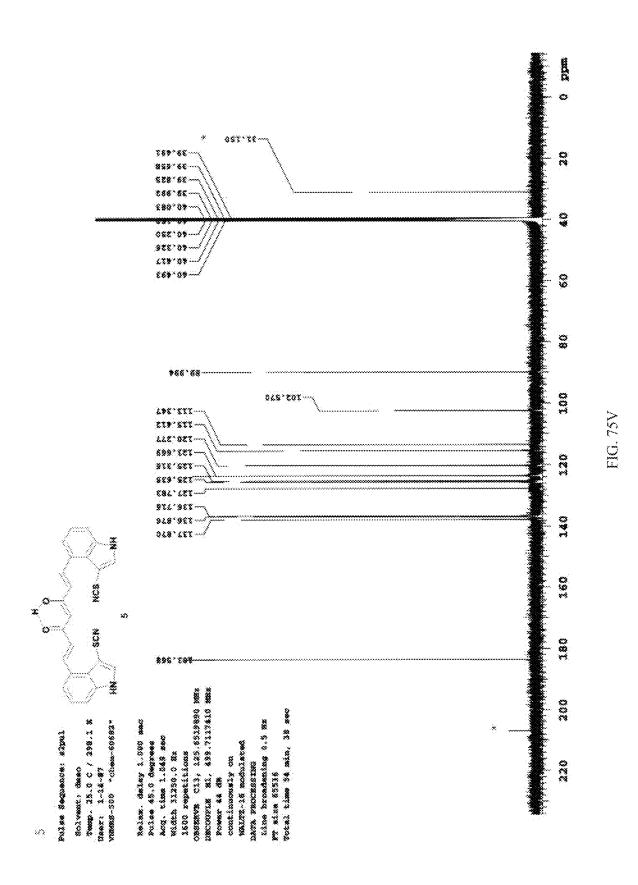


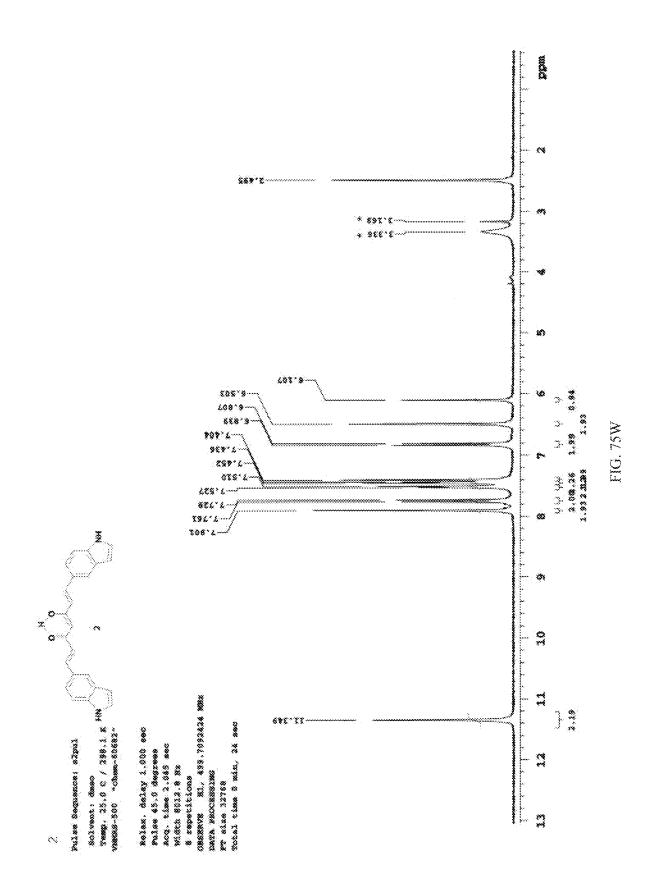


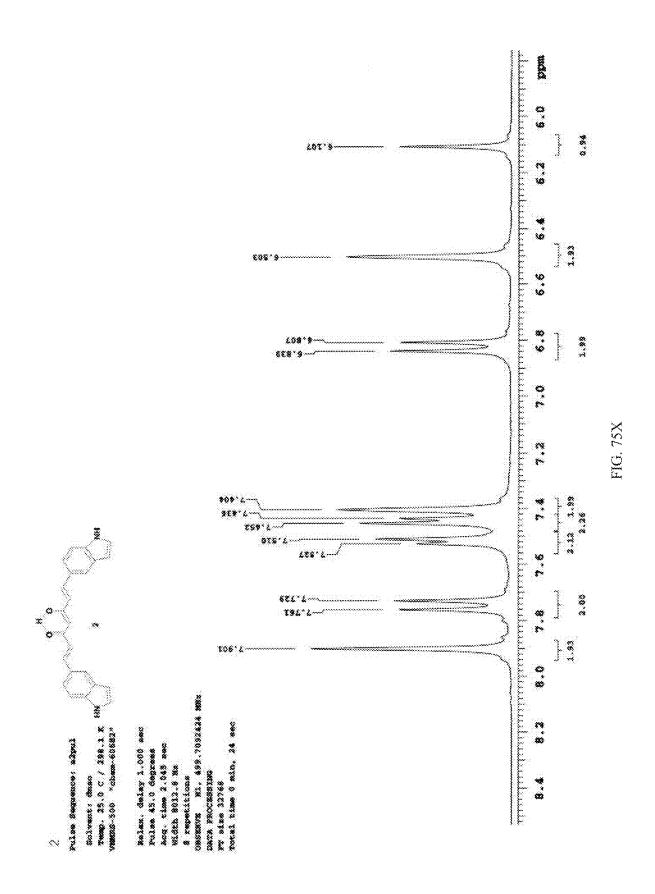
IG. 75S

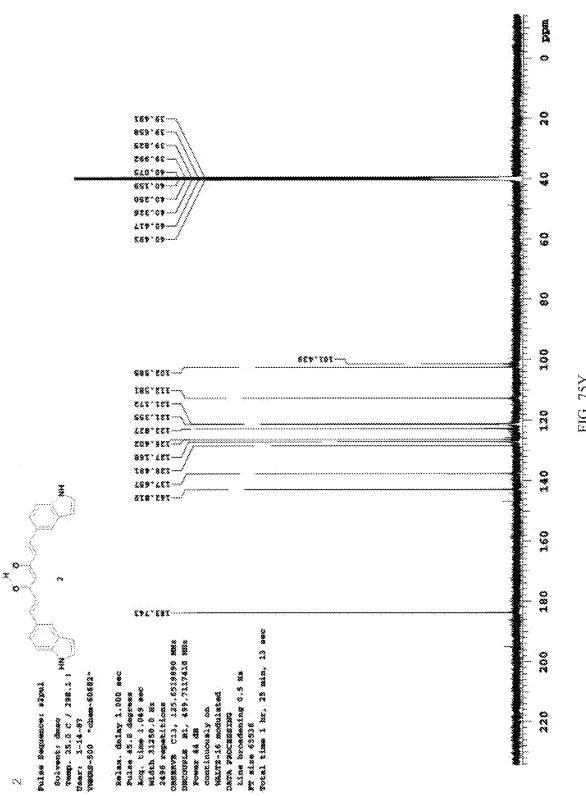


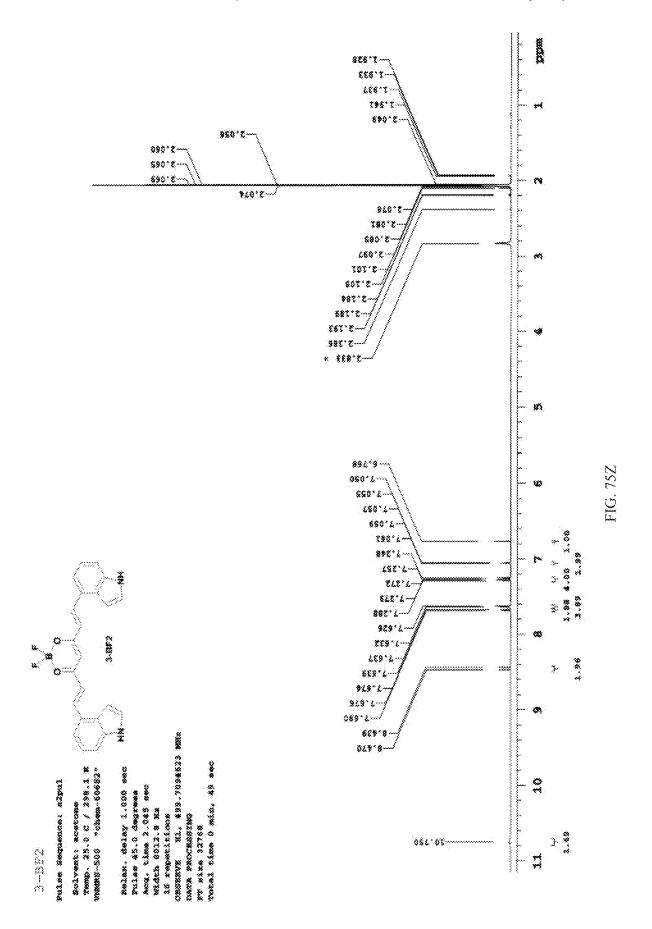


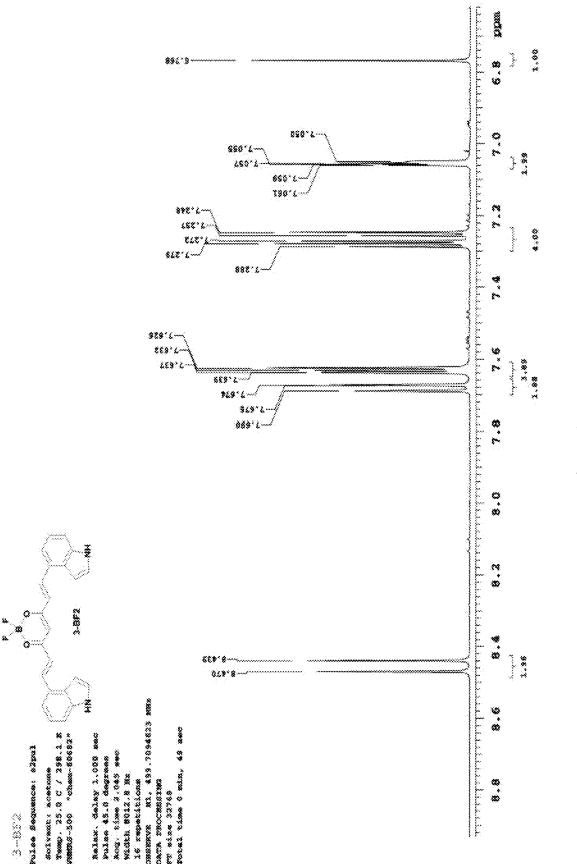












1G. 75AA

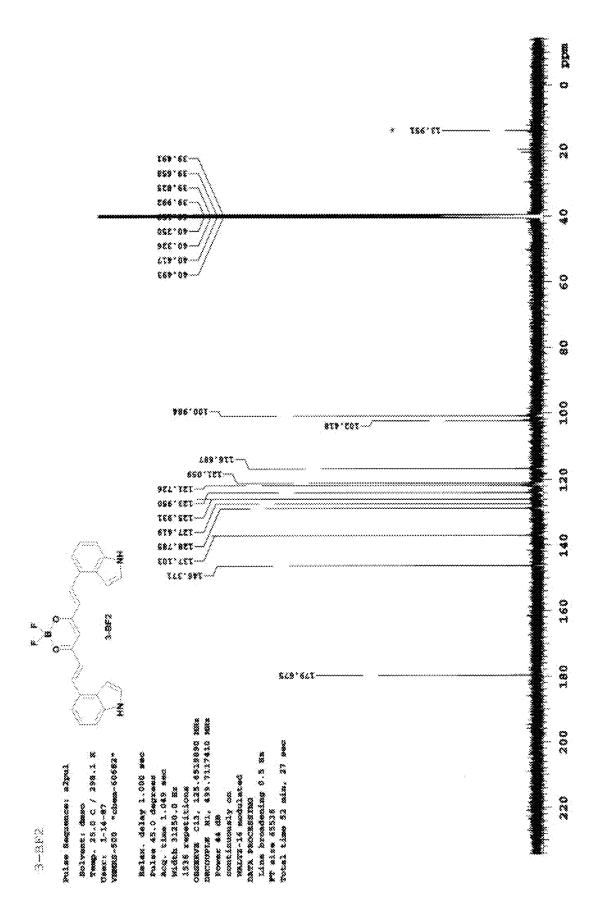
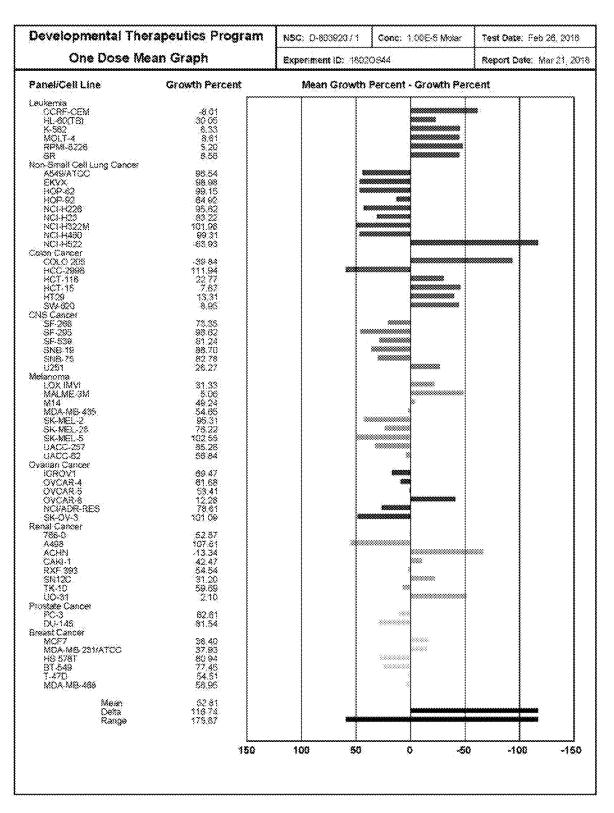


FIG. 75BB

### Deuterated and Non-Deuterated CUR-BF2 and CUR

FIG. 76

FIG. 77



# CURCUMINOID-INSPIRED SYNTHETIC COMPOUNDS AS ANTI-TUMOR AGENTS

### CROSS REFERENCE TO RELATED APPLICATIONS

This application is a nonprovisional of and claims priority to U.S. Provisional Application No. 62/520,788 entitled "Novel Curcuminoid-Inspired Synthetic Compounds (with Potent Cytotoxicity and Anti-Proliferative Properties) as ¹⁰ Anti-Tumor Agents", filed Jun. 16, 2017, the contents of which are hereby incorporated by reference into this disclosure.

#### FIELD OF THE INVENTION

The invention relates to antitumor agents. More specifically, the invention relates to a series of new CUR— and CUR—BF2 compounds with monocyclic aromatic and bicyclic-heteroaromatic lateral rings, bearing diverse substituents including fluorine(s), OCF3, CF3, and SCF3 groups (to increase polarity and lipophilicity), and their alpha-carbonyl-fluorinated analogs, as well as their pyrazole and isoxazole derivatives. The invention also relates to heterocyclic CUR—BF2 adducts and CUR compounds 25 based on indole, benzothiophene, and benzofuran along with their aryl-pyrazoles.

#### BACKGROUND OF THE INVENTION

Parent compound curcumin 1 (FIG. 1) is a non-toxic phenolic natural product. The central core of 1 is a conjugated  $\beta$ -keto-enolic moiety that can participate in hydrogen bonding, act as Michael acceptor, and coordinate to metal ions, while its hydrophobic phenyl domains are potential 35 sites for  $\pi$ - $\pi$  interactions with the aromatic side chains in amino acids, and the phenolic OH groups are capable of H-bonding interactions. (S. C. Gupta, et al., *Nat. Prod. Rep.* 2011, 28, 1937-1955).

Combination of these structural features, and its ability to 40 influence multiple signaling molecules made it very challenging to unravel the biological profile of CUR and to identify its pharmacophore, despite extensive studies aimed at improving its pharmacokinetic profile and potency. (A. Minassi, et al., *J. Nat. Prod.* 2013, 76, 1105-1112; K. 45 Bairwa, et al., *RSC. Adv.* 2014, 4, 13946-13978; A. Vyas, et al., *Curr. Pharm. Des.* 2013, 19, 2047-2069).

Whereas potential health benefits of 1 and its anti-cancer, anti-inflammatory, antioxidant and anti-mutagenic effects are extensively studied and documented, unfavorable bio-50 physicochemical features namely poor solubility, low absorption, low bioavailability, and rapid metabolism have so far prevented the development of a CUR-based anti-cancer drug. (G. R. Pillail, et al., *Cancer Letters* 2004, 208, 163-170; A. L. Loprestil, et al., *J. Psychopharmacology* 55 2012, 26, 1512-1524; D. Perrone, et al., *Experimental and Therapeutic Medicine* 2015, 10, 1615-1623; K.-L. Tan, et al., *ChemMedChem* 2012 7, 1567-1579).

To address these shortcomings, extensive research has focused on synthesis of structurally modified CURs. These 60 included changes in the aryl substitution patterns, synthesis of unsymmetrical CUR compounds by introducing two different aryl groups, introduction of diverse substituents at the central methylene carbon, as well as more drastic structural modifications such as converting the 1,3-diketone 65 moiety to prazoles and isoxazoles, or complete deconstruction to monocarbonyl derivatives in order to prepare CUR

2

mimics. These highly diverse structural modifications and their biological activity outcomes were summarized in a 2014 review. (K. Bairwa, et al., RSC. Adv. 2014, 4, 13946-13978). Considering drug delivery aspects, encapsulation into water-soluble hosts, conjugation with nanoparticles, polymeric micelles, or liposomes have been explored as possible methods to deliver curcumin to cancer cells. (M. Mimeault, et al., Chin. Med. 2011, 6, 31; C. Cheng, et al., RSC Adv. 2017, 7, 25978-25986; L. Zhang, et al., Environ. Tox. Pharm. 2016, 48, 31-38; M. M. Yallapu, et al., Colloids and Surfaces B: Biointerfaces 2010, 79, 113-125; J. Liu, et al., Curr. Pharm. Des. 2013, 19, 1974-1993).

Structural modifications have included introduction of enaminone, oxime, and dienone, and replacement of the 15 central moiety with pyrazole and isoxazole rings. (D. Simoni, et al., Biorg. Med. Chem. Lett., 2008, 18, 845-849; K.-L. Tan, et al., ChemMedChem, 2012, 7, 1567-1579; C. L. Nieto, et al., Molecules, 2015, 20, 15643-15665; M. W. Amolins, et al., Bioorg. Med. Chem., 2009, 17, 360-367; M. Labbozzetta, et al., Chem. Biol. Interact., 2009, 181, 29-36; R. Narlawar, et al., ChemMedChem, 2008, 3, 165-172). It is noteworthy that many of these synthetic modifications represent significant departure from CUR's original skeleton. Other studies have reported improved bioactivity by transforming the phenolic OH in CUR to acetates and amino acid conjugates, cinnamic and succinyl esters, other types of esters, and acetamides. (S. B. Wan, et al., Int. J. Mol. Med., 2010, 26, 447-455; L. Feng, et al., Chem. Pharm. Bull., 2015, 63, 873-881; W. Wichitnithd, et al., Molecules, 2011, 16, 1888-1900; Z. Cheikh-Ali, et al., ChemMedChem, 2015, 10, 411-418; R. Sribalan, et al., Bioorg. Med. Chem. Lett., 2015, 25, 4282-4286). Introduction of ester or  $\alpha$ ,  $\beta$ -unsaturated ester linkers into the active methylene region has been used to prepare curcuminoid libraries as potential antitumor agents for lung and prostate cancer. (K. Wada, et al., Bioorg. Med. Chem., 2015, 23, 1507-1514; L. Lin, et al., Bioorg. Med. Chem., 2006, 14, 2527-2534; L. Lin, et al., J. Med. Chem., 2006, 49, 3964-3972).

Studies of heterocyclic curcuminoids have so far mainly focused on systems in which the diketo-linker was replaced with piperid-4-one, tetrahydrothiopyran-4-one, or terahydropyran-4-one moieties. There are also limited examples in which phenyl rings were replaced with thiophene, pyrrole, or pyridine, while maintaining the 1,3-keto-enolic structural motif. Synthetic progress along with the pharmacological properties of these compounds have been reviewed. (M. Martinez-Cifuentes, et al., *Curr. Topic. Med. Chem.* 2015, 15, 1663-1672).

Selective fluorine introduction into pharmaceuticals is a powerful strategy for improving metabolic stability and physiochemical properties, but this approach has remained greatly under-utilized with respect to curcuminoids. (J. Wang, et al., *Chem. Rev.*, 2014, 114, 2432-2506; H.-J. Bohm, et al., *ChemBioChem*, 2004, 5, 637-643).

Since the standard approach for the assembly of symmetrical CUR analogs is via a "double aldol" condensation of aldehydes with acetylacetone, ring fluorinated derivatives can be synthesized via this route, however very few examples have been reported, and with limited NMR data. (E. V. Rao, et al., *Indian. J. Pharm. Sci.*, 2011, 73, 262-270; B. W. Megna, et al., *J. Surg. Res.*, 2017, 213, 16-24; S. Elavarasan, et al., *Journal of Chemistry*, 2013, 1-8; (a) S. Padhye, et al., *Pharm. Res.*, 2009, 26, 1874-1880; (b) S. Padhye, et al., *Pharm. Res.*, 2009, 26, 2438-2445).

Examples of curcuminoids bearing a single fluorine at the active methylene position (along with an ester linker or a methyl group) have been very rare. (L. Lin, et al., *Bioorg*.

*Med. Chem.*, 2006, 14, 2527-2534; L. Lin, et al., *J. Med. Chem.*, 2006, 49, 3964-3972). The reported methods required additional steps, namely deprotonation (NaH/DMF) followed by fluorination, as well as additional steps for protection and deprotection of the phenolic OH in the 5 case of parent CUR.

Considering the importance of the 1,3-diketo moiety in the CUR skeleton for interaction with target proteins, development of methods for direct fluorine introduction into the active methylene position is highly desirable, but no such 10 methods have been reported.

It is also noteworthy that despite extensive bioassay studies on curcuminoids, the potential of CUR—BF2 complexes as anti-proliferation agents has remained largely unexplored. (S. C. Gupta, et al., Nat. Prod. Rep. 2011, 28, 1937-1955; A. Vyas, et al., Curr. Pharm. Des. 2013, 19, 2047-2069; M. Mimeault, et al., Chin. Med. 2011, 6, 1-19). Review of the published literature shows that these compounds are usually treated as "intermediates" en-route to curcuminoids, and only few examples exist in which they 20 have been characterized, albeit with limited NMR data, except in two independent recent studies, where a series of CUR—BF₂ complexes bearing various donor end-groups were synthesized and their photophysical properties were explored. ((E. V. Rao, et al., Indian. J. Pharm. Sci., 2011, 73, 25 262-270; K. Kamada, K., et al., Chem. Eur. J., 2016, 22, 5219-5232; G. Bal, et al., Org. Biomol. Chem., 2014, 12, 1618-1626; K. Aertgeerts, et al., J. Biol. Chem., 2011, 286, 18756-18765).

In order to address the shortcomings of the previous work,  30  the inventors have used selective fluorine introduction as a strategy to increase metabolic stability and polarity, producing a library of "CUR-inspired" compounds bearing fluorinated moieties which employ practical methods for selective fluorine introduction into the  $\alpha$ -carbonyl moiety, as  35  described in Laali 2016, herein incorporated in its entirety into this application. (K. K. Laali, et al., *J. Fluorine.Chem.*, 2016, 191, 29-41).

The inventors have also synthesized a library of CUR—  $BF_2$  adducts and CURs with diverse substitution patterns in  40  the phenyl rings. To that end, fluorinated substituents (SCF $_3$ , OCF $_3$ , and F) were introduced in an effort to improve lipophilicity and metabolic stability, whereas bulky activating groups (OMe, OAc, and OBz) were introduced as a way to tune steric/electronic effects. To gauge the potential role  45  of the enolic moiety in interaction with proteins, a library of fluorinated aryl-pyrazoles and isoxazoles were also synthesized and characterized, as described in Laali, 2018, herein incorporated in its entirety into this application. (K. K. Laali, et al., *J. Fluorine. Chem.* 2018, 206, 82-98).

The inventors have also synthesized novel heterocyclic CURs and CUR—BF₂ adducts based on indole, benzothiophene and benzofuran as well as their aryl-pyrozoles. The inventors have shown that the novel compounds presented favorable binding affinities, in some cases more favorable than currently known inhibitors, for various cancers including multiple myeloma and colorectal cancer. The novel compounds exhibited high anti-proliferative and apoptotic activity against cancer cells while exhibiting significantly lower cytotoxicity in normal cells.

#### SUMMARY OF INVENTION

In an embodiment, the invention discloses the synthesis, isolation, and characterization (including by X-ray analysis) of a series of new CUR—and CUR—BF2 compounds with monocyclic aromatic and bicyclic-heteroaromatic lateral

4

rings, bearing diverse substituents including fluorine(s), OCF3, CF3, and SCF3 groups (to increase polarity and lipophilicity), and their alpha-carbonyl-fluorinated analogs, as well as their pyrazole and isoxazole derivatives. The CUR-pyrazoles synthesized embody analogs that are fluorinated at the phenyl-pyrazole moiety.

Inspired by the earlier fluorination study of carbonyl compound, the inventors report here the synthesis of novel curcuminoids that are mono- and difluorinated at the methylene position by direct one-pot fluorination with Selectfluor (F-TEDA-BF₄) without using a base or additive (see FIG. 2). In addition to parent CUR (1) and its symmetrical O-dimethylated analog (DMC; 6), symmetrical curcuminoids bearing fluorines (11 and 14) and trifluoromethyl groups (20) in the phenyl rings were also synthesized, and subsequently mono- and difluorinated at the active methylene position, seen in FIG. 2. The corresponding curcuminoid-BF2 adducts which serve as synthetic intermediates en-route to these curcuminoids were isolated and characterized. The X-ray crystal structures were obtained for CUR-BF₂ adducts 5, 10, and 14, and for the F—CUR 8. The cell growth inhibitory and apoptosis inducing effects of these compounds were examined by in-vitro assays against leukemia (MOLT-4), prostate cancer (PC3 and LNCap), as well as lung (A549) and breast cancer (MDA231) cell lines. A selected group of compounds were screened by the NCI 60 cell panel. Computational docking studies were also performed on CUR-BF2 adducts and fluorinated curcuminoids to compare their binding energies in HER2 protein relative to a well-known ligand (SYR), versus trends from bioactivity data for breast cancer (IC₅₀ MDA231), and in proteasome in comparison with bioassay data in leukemia (IC₅₀ MOLT-

Further, the inventors have synthesized a library of heterocyclic CUR—BF2 and CUR compounds based on indole, benzothiophene, and benzofuran, including several examples of their aryl-pyrazole derivatives. Computational/ docking studies were performed on 20 heterocyclic CUR-BF₂ and CUR compounds to compare binding efficiency to target proteins involved in specific cancers, namely HER2, proteasome, VEGFR, BRAF, and BCL-2 versus known inhibitor drugs. The majority presented very favorable binding affinities that were comparable and in some cases more favorable than the known-inhibitors. The indole-based CUR—BF2 and CUR compounds and their bis-thiocyanato derivatives exhibited high anti-proliferative and apoptotic activity by in-vitro bioassay against a panel of 60 cancer cell lines, and more specifically against multiple myeloma (MM) cell lines (KMS11, MM1.S, and RPMI-8226) with significantly lower IC50s versus healthy PBMC cells. The indolebased CUR—BF₂ adducts and their bis-thiocyanato derivatives exhibited significantly higher anti-proliferative activity in human colorectal cancer cells (HCT116, HT29, DLD-1, RKO, SW837, and Caco2) compared to parent curcumin, while showing significantly lower cytotoxicity in normal cells (CCD112CoN and CCD841CoN).

In one aspect of the invention, a composition is presented which may be used in the treatment or prophylaxis of cancer which included identifying a cancerous tumor or growth in the patient and administering a therapeutically effective amount of a composition comprising formula (I) or (II):

30

40

45

65

(I)

where  $R_4$  is O, a pyrazole formed with  $R_5$ , O associated with a difluoroboron adduct,

$$N-N$$
 or  $N-O$   $R_4$   $R_5$   $R_4$   $R_5$ 

where  $R_5$  is OH, O associated with a difluoroboron adduct,

$$N-N$$
 or  $N-O$   $R_4$   $R_5$   $R_4$   $R_5$ 

where  $R_6$  is H, F, or unsubstituted forming a double bond at  $\bullet$ :

where  $R_7$  is H, or F;

where R₅ is

H₃C N

where R₉ is

 $R_2$   $R_3$   $R_4$   $R_6$   $R_7$   $R_7$   $R_8$   $R_8$   $R_9$   $R_9$ 

$$\begin{array}{c} R_{5} \\ R_{6} \\ R_{7} \end{array}$$

where * is a double bond or a single bond; wherein * is a double bond when at least one of  $R_6$  and  $R_7$  is unsubstituted or a single bond when  $R_6$  is fluorine or hydrogen and  $R_7$  is fluorine; where * is a double bond or a single bond; wherein * is a double bond when * is a single bond; where  $R_1$  is o-OCH3, m-OCH3, o-F, H;

where R₂ is o-OCH₃, m-OCH₃, H, m-OCF₃,

at a meta position,

$$R_2$$
 NH, or  $R_2$  NH;

where R₃ is p-F, p-OCH₃, m-CF₃, p-CF₃, p-SCF₃, p-OH,

at a para position,

at a para position,

where  $R_{10}$  is H, phenyl, 4-benzonitrile,

and

where  $R_{11}$  is SCN.

In some embodiments, there may be at least one deuterated substituent on the aryl which may be a deuterated methoxy such as R—O—CD₃.

In some embodiments, there may be at least one deuterated substitution on the aryl with the at least one substitution being a plurality of deuterated substitutions which may be at the meta positions.

In another aspect of the invention, a composition is presented which may be used in the treatment or prophylaxis of cancer which included identifying a cancerous tumor or 30 growth in the patient and administering a therapeutically effective amount of a composition comprising formula (I):

$$R_1 \xrightarrow{R_2} R_3$$

where * is a double bond or a single bond;

wherein * is a single bond when * is a double bond; where * is a double bond or a single bond;

wherein * is a double bond when * is a single bond; where R, is

$$\mathbb{R}^5$$
,  $\mathbb{R}^5$ , or  $\mathbb{R}^7$ ;

where  $R_2$  is O, a pyrazole formed with  $R_3$ , or O associated with a difluoroboron adduct;

where  $R_3$  is OH or O associated with a difluoroboron adduct;

where R₄ is

$$\mathbb{R}^{5}$$
, or  $\mathbb{R}^{5}$ ,  $\mathbb{R}^{5}$ ,  $\mathbb{R}^{5}$ 

where  $R_5$  is H or SCN;

where  $R_6$  is H or CH3; and

where  $R_7$  is H or CH3.

#### BRIEF DESCRIPTION OF THE DRAWINGS

For a fuller understanding of the invention, reference should be made to the following detailed description, taken in connection with the accompanying drawings, in which:

FIG. 1. Tautomerism in curcumin—exclusive presence of the enol tautomer

FIG. 2. List of curcuminoid compounds.

FIG. 3 Synthesis and isolation of F2-CUR (3) and F—CUR (4).

FIG. **4**. Synthetic sequence for the preparation of CUR—BF₂ compounds and curcuminoids.

FIG. 5. Optimized structure of  $(CF_3)_2$ —CUR— $BF_2$  19 by (1) 35 B3LYP/6-311+G(d,p).

FIG. 6. Optimized structure of 12 by B3LYP/6-311+G(d,

FIG. 7. Thermal ellipsoid plot of 10. Thermal ellipsoids are drawn at 50% probability. Selected inter-atomic distances (Å) and angles (°): B(1)-F(4) 1.372(6), B(1)-F(3) 1.383(6), B(1)-O(2) 1.470(6), B(1)-O(1) 1.477(6), O(1)-C (9) 1.303(5), O(2)-C(11) 1.307(5); F(4)-B(1)-F(3) 110.7(4), F(4)-B(1)-O(2) 109.2(4), F(3)-B(1)-O(2) 108.1(4), F(4)-B (1)-O(1) 108.1(4), F(3)-B(1)-O(1) 108.2(4), O(2)-B(1)-O(1) 112.5(4).

FIG. **8**. Crystal packing diagram of 10. Selected hydrogen atoms have been removed for clarity. Compound 10 crystallizes in the monoclinic space group P2_f/n. The asymmetric unit corresponds to one molecule with a total of four molecules in each cell. Each molecule interacts with an adjacent molecule via two H—F contacts (2.2813(26) and 2.3582(25) Å).

FIG. **9**. Thermal ellipsoid plot of 5. Thermal ellipsoids are drawn at 50% probability. Selected inter-atomic distances (Å) and angles (°): B(1)-F(1) 1.382(9), B(1)-F(2) 1.365(8), B(1)-O(1) 1.477(8), B(1)-O(2) 1.488(8), O(1)-C(1) 1.313 (7), O(2)-C(3) 1.322(7); F(2)-B(1)-F(1) 111.3(5), F(2)-B(1)-O(1) 107.9(6), F(1)-B(1)-O(1) 109.5(6), F(2)-B(1)-O(2) 108.4(6), F(1)-B(1)-O(2) 107.9(6), O(1)-B(1)-O(2) 111.7 (6) (5).

FIG. 10. Crystal packing diagram of 5. Compound 5 crystallizes in the monoclinic space group P2/c. The asymmetric unit corresponds to one molecule with a total of four molecules in each cell. Each molecule interacts with an adjacent molecule via one H—F contact (2.4455(31) Å).

FIG. 11. Thermal ellipsoid plot of 14. Thermal ellipsoids are drawn at 50% probability. Selected inter-atomic dis-

8

tances (Å) and angles (°): B(1)-F(1) 1.368(5), B(1)-F(2) 1.382(5), B(1)-O(2) 1.477(5), B(1)-O(1) 1.480(5), O(1)-C (1) 1.318(4), O(2)-C(3) 1.306(4), F(1)-B(1)-F(2) 111.1(3), F(1)-B(1)-O(2) 108.7(3), F(2)-B(1)-O(2) 109.0(3), F(1)-B (1)-O(1) 108.3(3), F(2)-B(1)-O(1) 108.9(3), O(2)-B(1)-O(1) 110.8(3).

FIG. 12. Crystal packing diagram of 14. Selected hydrogen atoms have been removed for clarity. Compound 14 crystallizes in the triclinic space group Pt. The asymmetric unit corresponds to one molecule with a total of two molecules in each cell. Each molecule interacts with two adjacent molecules via two H—F contacts of 2.2674(19) and 2.3567(29) Å. The molecule also contains two intramolecular H—F contacts with distances of 2.4602(21) and 2.5059 (21) Å.

FIG. 13 Ball and stick plot of 8. Compound 8 crystallizes in the triclinic space group Pt. The asymmetric unit corresponds to three crystallographically nonequivalent molecules with a total of six molecules in each unit cell. 8a, 8b, 20 and 8c are illustrated in FIGS. 14a-c respectively. The same gross structural features are found in all three molecules. No significant intermolecular contacts are observed. The molecule contains intramolecular hydrogen bonding and one H—F contact with a distance of 2.4455(31) Å;

FIG. **14**A-B (A) Thermal ellipsoid plot of 8a. Thermal ellipsoids are drawn at 50% probability; (B) Thermal ellipsoid plot of 8b. Thermal ellipsoids are drawn at 50% probability.

FIG. 14C Thermal ellipsoid plot of 8c. Thermal ellipsoids are drawn at 50% probability.

FIG. 15. List of lead curcuminoids identified based on bioassay.

FIG. **16**. Binding mode in the active site of HER2 of compound 14 as a model curcuminoid analog (2D-plot).

FIG. 17. Binding mode in the active site of HER2 of compound 14 as a model curcuminoid analog (3D-plot).

FIG. 18. Electrostatic potential maps for the most active curcuminoid derivatives.

FIG. 19. Dose mean graph of 1,7-bis(2,3,6-trimethoxy-phenyl)hepta-1,4,6-triene-3,5-dione for various cancer cell lines at  $1\times10^{-5}$  M.

FIG. 20. Dose mean graph of 1,7-bis(3-benzothiophene) hepta-1,4,6-triene-3,5-dione for various cancer cell lines at  $45 \times 10^{-5}$  M.

FIG. 21. Dose mean graph of bis(2,3,4-trimethoxy)hepta-1,4,6-triene-3,5-dione boron-difluoride adduct for various cancer cell lines at  $1\times10^{-5}$  M.

FIG. **22**. Dose mean graph of bis(4-Trifluoromethylthio) 50 CUR. It shows high anti-proliferative potency against HCT-116

FIG. 23. Dose mean graph of bis(6-Fluoro-3,4-dimethoxy)CUR-isoxazole adduct. It shows notable anti-proliferative potency against Melanoma MDA-MB-433 cell line. 55

FIG. **24.** IC $_{50}$  graph for 1,7-bis(3-benzothiophene)hepta-1,4,6-triene-3,5-dione in cancer cells (RPMI8226) and healthy cells (PBMC).

FIG. 25.  $\overrightarrow{\text{IC}}_{50}$  graph for 1,7-bis(3,4-dimethoxyphenyl) hepta-1,6-diene-3,5-dione in cancer cells (RPMI8226) and 60 healthy cells (PBMC).

FIG. 26.  $IC_{50}$  graph for 1,7-bis(2,3,4-trimethoxyphenyl) hepta-1,4,6-triene-3,5-dione in cancer cells (RPMI8226) and healthy cells (PBMC).

FIG. 27. IC $_{50}$  graph for 1,7-bis(2-benzothiophene)hepta- 65 1,4,6-triene-3,5-dione in cancer cells (RPMI8226) and healthy cells (PBMC).

FIG. **28**. IC₅₀ graph for 1,7-bis(2-benzothiophene)hepta-1,4,6-triene-3,5-dione-boron-diffuoride adduct in cancer cells (RPMI8226) and healthy cells (PBMC).

FIG. **29**. IC₅₀ graph for 1,7-bis(3-trifluoromethoxyphenyl)hepta-1,4,6-triene-3,5-dione-boron-difluoride adduct in cancer cells (RPMI8226) and healthy cells (PBMC).

FIG. 30.  $IC_{50}$  graph for 1,7-bis(3,4-dibenzyloxyphenyl) hepta-1,4,6-triene-3,5-dione in cancer cells (RPMI8226) and healthy cells (PBMC).

FIG. **31**. IC₅₀ graph for bortezomib in cancer cells (RPMI8226) and healthy cells (PBMC).

FIG. 32. List of mono- and di-substituted curcuminoid compounds and difluoroboron-curcuminoid adducts.

FIG. 33. List of tri-substituted curcuminoid compounds and difluoroboron-curcuminoid adducts.

FIG. **34**. List of selectively fluorinated curcuminoid compounds and difluoroboron-curcuminoid adducts.

FIG. 35 is a consolidated list of CUR and CUR—BF2 compounds of FIGS. 32-34.

FIG. 36. is a table listing binding affinities for CURs of FIG. 35.

FIG. 37 is a table of tumor-cell specific cytotoxicity by cell viability assay to determine EC50 (concentration at which 50% of the cells remain viable). These assays indicated that curcuminoids 9 and 5 of FIG. 35 were highly effective against RPMI-8226 (multiple myeloma cell line) while exhibiting significantly less cytotoxicity in peripheral blood mononuclear cells (PBMCs) from healthy donors (non-tumor control cells).

Structure of 9:

FIG. **38**A-B is a series of graphs depicting EC50 curve plots for compounds 5 (A) and 9 (B) of FIG. **35** respectively. PBMCs (non-cancer cells, controls); BCWM (BCWM.1 WM cell line); RPMI (RPMI-8266, MM cell line); RS4 (RS4; 11, ALL cell line).

FIG. 39 is a list of CURs from FIG. 35 with anti-tumor activity based on NCI-60 immunoassay.

FIG. **40** is a scheme depicting the synthesis of CUR-pyrazoles and CUR-isoxazoles.

FIG. **41** is a list of pyrazole curcuminoid compounds, 1,2-oxazole curcuminoid compounds.

FIG. 42. List of pyrazole curcuminoid compounds, 1,2oxazole curcuminoid compounds, and difluoroboron-curcuminoid adducts.

FIG. 43 is a list of CUR-pyrazoles and CUR-isoxazoles.

FIG. 44 is a table listing binding affinities for CUR- 5 pyrazoles and CUR-isoxazoles of FIG. 43.

FIG. 45 is a list of indole-based curcuminoid compounds, thiocyano-curcuminoid compounds and difluoroboron-curcuminoid adducts.

FIG. 46 is a list of benzothiophene-curcuminoid com- 10 pounds, benzofuran-curcuminoid compounds, and difluoroboron-curcuminoid adducts.

FIG. 47. Reaction schemes to produce curcuminoid-based and curcuminoid-boron difluoride adduct di-cation salts.

FIG. 48 is a schematic for the formation of CUR—BF₂ 15 from indole-5-aldehyde.

FIG. 49 is a schematic of MW-assisted synthesis of curcuminoid 2.

FIG. 50 is a schematic of 3-BF₂ and 3 from indole-4aldehyde.

FIG. 51 is a schematic of the synthesis of bis-thiocyanato CUR—BF₂ and CUR compounds.

FIG. 52A-B are optimized structures of 4-BF₂ and 5-BF₂ by B3LYP/6-311+G(d,p).

FIG. 53A-B are optimized structures of compounds 4 and 25 5 by B3LYP/6-311+G(d,p).

FIG. 54 is a schematic depicting isolation of 6a-BF₂ and its decomplexation to 6a.

FIG. **55** is a schematic of the synthesis of 6-BF₂/6a-BF₂ and decomplexation to 6.

FIG. 56 is a schematic of heterocyclic CUR—BF, and CUR based on benzothiophene and benzofuran.

FIG. 57 is a schematic of heterocyclic CUR-acylpyrazoles based on benzothiophene and benzofuran.

FIG. 58A-D are a series of images depicting the most 35 favorable binding interactions in the active sites of the studied enzymes. (a) 9-BF2 in HER2; (b) 5-BF2 in proteasome; (c) 9-BF₂ in VEGFR2; (d) 3-BF₂ in BCL-2.

FIG. 59 is a 3D Representation of 3-BF₂ in BC1-2.

FIG. 60 is an image depicting compounds with high 40 anti-proliferative and apoptotic activity based on NCI-60 assay.

FIG. 61A-B is a series of images depicting indole-based CUR analogs are significantly more toxic to tumor cells than to healthy cells. Cell proliferation and viability were deter- 45 mined in multiple myeloma (MM) cancer cell lines (RPMI-8226, KMS-11, MM1.S) as well as in peripheral blood mononuclear cells (PBMCs) from healthy donors that were exposed to various concentrations of (A) CUR-analog 1 (3-BF₂) and (B) CUR-analog 2 (CUR 2) for 72 hours using 50 the CellTiter Glo 2.0 assay. The inhibitory concentration of CUR-analog 1 and 2 at which 50% of MM cell lines and PBMCs remained viable after 72 hours (IC50) was determined and is presented in Table A. Calculated fold changes in IC50 between MM cell lines relative to healthy PBMCs 55 assay for the associated compound. are presented in Table B.

FIG. 62A-F are a series of graphs depicting cell-viability assay for 5-BF₂ (A), 4-BF₂ (B), 3-BF₂ (C), 7-BF₂ (D), 2-BF₂ (E), curcumin (F).

FIG. 63 is a table depicting the cell lines employed in the 60 study of FIG. 62.

FIG. 64 is a list of indole-based CUR—BF2 and CUR compounds

FIG. 65 is a dose mean graph of indole-5-CUR-BF2-SCN for various cancer cell lines at  $1 \times 10^{-5}$  M.

FIG. 66 is a dose mean graph of indole-5-CUR—SCN for various cancer cell lines at  $1 \times 10^{-5}$  M.

FIG. 67 is a dose mean graph of indole-4-CUR-BF2-SCN for various cancer cell lines at  $1 \times 10^{-5}$  M.

FIG. 68 is a dose mean graph of indole-4-CUR-SCN for various cancer cell lines at  $1 \times 10^{-5}$  M.

FIG. 69 is a dose mean graph of indole-4-CUR—BF2 for various cancer cell lines at  $1\times10^{-5}$  M.

FIG. 70 is a dose mean graph of indole-5-CUR—BF2 for various cancer cell lines at  $1 \times 10^{-5}$  M.

FIG. 71 is a dose mean graph of

for various cancer cell lines at  $1 \times 10^{-5}$  M.

FIG. 72A-C is a series of images depicting CUR-analogs induce apoptosis in multiple myeloma tumor cells but are significantly less toxic to healthy cells. Apoptotic cell death in multiple myeloma (MM) cancer cell lines (RPMI-8226, KMS-11, MM1.S) as well as peripheral blood mononuclear cells (PBMCs) from healthy donors that were exposed to various concentrations of (A) CUR-analog 1 (Indole-4 CUR—BF₂) and (B) CUR-analog 2 (Indole-5 CUR) or (C) the FDA-approved Bcl-2 inhibitor (venetoclax, used for comparison) was assessed. Bar graphs show % of apoptotic cells (annexin-V+PI positive cells) normalized to basal apoptosis observed in control (DMSO-treated) cells. Below each bar graph are representative scatterplots showing % of apoptotic cells exposed to DMSO (control) or CUR-analogs/ venetoclax. *p<0.05, shows concentrations where a statistically significant difference was noted compared to DMSOtreated cells.

FIG. 73 is a list of compounds tested against CRC cells. FIG. 74A is a graph depicting comparative CRC viability assay for the associated compound.

FIG. 74B is a graph depicting comparative CRC viability assay for the associated compound.

FIG. 74C is a graph depicting comparative CRC viability assay for the associated compound.

FIG. 74D is a graph depicting comparative CRC viability assay for the associated compound.

FIG. 74E is a graph depicting comparative CRC viability assay for the associated compound.

FIG. 74F is a graph depicting comparative CRC viability

FIG. 75A is representative NMR spectra for the bioactive compound 5-BF2.

FIG. 75B is representative NMR spectra for the bioactive

compound 5-BF2. FIG. 75C is representative NMR spectra for the bioactive

compound 5-BF2. FIG. 75D is representative NMR spectra for the bioactive compound 7-BF2.

FIG. 75E is representative NMR spectra for the bioactive compound 7-BF2.

FIG. 75F is representative NMR spectra for the bioactive compound 7-BF2.

FIG. 75G is representative NMR spectra for the bioactive compound 3.

FIG. 75H is representative NMR spectra for the bioactive compound 3.

FIG. 751 is representative NMR spectra for the bioactive 5 compound 3.

FIG. 75J is representative NMR spectra for the bioactive compound 3.

FIG. 75K is representative NMR spectra for the bioactive compound 4-BF2.

FIG. 75L is representative NMR spectra for the bioactive compound 4-BF2.

FIG. 75M is representative NMR spectra for the bioactive compound 4-BF2.

FIG. 75N is representative NMR spectra for the bioactive  15  compound 2-BF2.

FIG. **75**O is representative NMR spectra for the bioactive compound 2-BF2.

FIG. **75**P is representative NMR spectra for the bioactive compound 2-BF2.

FIG. 75Q is representative NMR spectra for the bioactive compound 4.

FIG. 75R is representative NMR spectra for the bioactive compound 4.

 $\widehat{\text{FIG}}$ . 75S is representative NMR spectra for the bioactive  25  compound 4.

FIG. **75**T is representative NMR spectra for the bioactive compound 5.

FIG. 75U is representative NMR spectra for the bioactive compound 5.

FIG. 75V is representative NMR spectra for the bioactive compound 5.

FIG. 75W is representative NMR spectra for the bioactive compound 2.

FIG. 75X is representative NMR spectra for the bioactive ³⁵ compound 2.

FIG. **75**Y is representative NMR spectra for the bioactive compound 2.

FIG. 75Z is representative NMR spectra for the bioactive compound 3-BF2.

FIG. 75AA is representative NMR spectra for the bioactive compound 3-BF2.

FIG. **75**BB is representative NMR spectra for the bioactive compound 3-BF2.

FIG. **76** is an image depicting deuterated versus non-deuterated CUR—BF2 and CUR compounds synthesized for comparative bioactivity study.

FIG. 77. List of deuterated curcuminoid compounds, and difluoroboron-curcuminoid adducts.

FIG. **78**. Reaction scheme to produce deuterated CUR—BF₂ compounds and deuterated curcuminoids, and strategies to introduce SCN and SeCN groups into the alpha carbonyl position.

FIG. 79 is a dose mean graph of

$$\begin{array}{c} & & & & \\ & & & \\ & & & \\ & & & \\ & & & \\ & & & \\ & & & \\ & & & \\ & & & \\ & & & \\ & & & \\ & & & \\ & & & \\ & & & \\ & & \\ & & & \\ & & \\ & & \\ & & \\ & & \\ & & \\ & & \\ & & \\ & & \\ & & \\ & & \\ & & \\ & & \\ & & \\ & & \\ & & \\ & & \\ & & \\ & & \\ & & \\ & & \\ & & \\ & & \\ & & \\ & & \\ & & \\ & & \\ & & \\ & & \\ & & \\ & & \\ & & \\ & & \\ & & \\ & & \\ & & \\ & & \\ & & \\ & & \\ & & \\ & & \\ & & \\ & & \\ & & \\ & & \\ & & \\ & & \\ & & \\ & & \\ & & \\ & & \\ & & \\ & & \\ & & \\ & & \\ & & \\ & & \\ & & \\ & & \\ & & \\ & & \\ & & \\ & & \\ & & \\ & & \\ & & \\ & & \\ & & \\ & & \\ & & \\ & & \\ & & \\ & & \\ & & \\ & & \\ & & \\ & & \\ & & \\ & & \\ & & \\ & & \\ & & \\ & & \\ & & \\ & & \\ & & \\ & & \\ & & \\ & & \\ & & \\ & & \\ & & \\ & & \\ & & \\ & & \\ & & \\ & & \\ & & \\ & & \\ & & \\ & & \\ & & \\ & & \\ & & \\ & & \\ & & \\ & & \\ & & \\ & & \\ & & \\ & & \\ & & \\ & & \\ & & \\ & & \\ & & \\ & & \\ & & \\ & & \\ & & \\ & & \\ & & \\ & & \\ & & \\ & & \\ & & \\ & & \\ & & \\ & & \\ & & \\ & & \\ & & \\ & & \\ & & \\ & & \\ & & \\ & & \\ & & \\ & & \\ & & \\ & & \\ & & \\ & & \\ & & \\ & & \\ & & \\ & & \\ & & \\ & & \\ & & \\ & & \\ & & \\ & & \\ & & \\ & & \\ & & \\ & & \\ & & \\ & & \\ & & \\ & & \\ & & \\ & & \\ & & \\ & & \\ & & \\ & & \\ & & \\ & & \\ & & \\ & & \\ & & \\ & & \\ & & \\ & & \\ & & \\ & & \\ & & \\ & & \\ & & \\ & & \\ & & \\ & & \\ & & \\ & & \\ & & \\ & & \\ & & \\ & & \\ & & \\ & & \\ & & \\ & & \\ & & \\ & & \\ & & \\ & & \\ & & \\ & & \\ & & \\ & & \\ & & \\ & & \\ & & \\ & & \\ & & \\ & & \\ & & \\ & & \\ & & \\ & & \\ & & \\ & & \\ & & \\ & & \\ & & \\ & & \\ & & \\ & & \\ & & \\ & & \\ & & \\ & & \\ & & \\ & & \\ & & \\ & & \\ & & \\ & & \\ & & \\ & & \\ & & \\ & & \\ & & \\ & & \\ & & \\ & & \\ & & \\ & & \\ & & \\ & & \\ & & \\ & & \\ & & \\ & & \\ & & \\ & & \\ & & \\ & & \\ & & \\ & & \\ & & \\ & & \\ & & \\ & & \\ & & \\ & & \\ & & \\ & & \\ & & \\ & & \\ & & \\ & & \\ & & \\ & & \\ & & \\ & & \\ & & \\ & & \\ & & \\ & & \\ & & \\ & & \\ & & \\ & & \\ & & \\ & & \\ & & \\ & & \\ & & \\ & & \\ & & \\ & & \\ & & \\ & & \\ & & \\ & & \\ & & \\ & & \\ & & \\ & & \\ & & \\ & & \\ & & \\ & & \\ & & \\ & & \\ & & \\ & & \\ & & \\ & & \\ & & \\ & & \\ & & \\ & & \\ & \\ & & \\ & & \\ & & \\ & \\ & & \\ & & \\ & & \\ & & \\ & & \\ & & \\ & & \\ & & \\ & & \\ & & \\ &$$

for various cancer cell lines at 1×10⁻⁵M.

14

# DETAILED DESCRIPTION OF THE PREFERRED EMBODIMENT

In the following detailed description of preferred embodiments, reference is made to the accompanying drawings, which form a part hereof, and within which are shown by way of illustration specific embodiments by which the invention may be practiced. It is to be understood that other embodiments may be utilized and structural changes may be made without departing from the scope of the invention.

Unless otherwise defined, all technical and scientific terms used herein have the same meaning as commonly understood by one of ordinary skill in the art to which this invention belongs. Although any methods and materials similar or equivalent to those described herein can be used in the practice or testing of the present invention, some potential and preferred methods and materials are described herein. All publications mentioned herein are incorporated herein by reference in their entirety to disclose and describe the methods and/or materials in connection with which the publications are cited. It is understood that the present disclosure supercedes any disclosure of an incorporated publication to the extent there is a contradiction.

All numerical designations, such as pH, temperature, time, concentration, and molecular weight, including ranges, are approximations which are varied up or down by increments of 1.0 or 0.1, as appropriate. It is to be understood, even if it is not always explicitly stated that all numerical designations are preceded by the term "about". It is also to be understood, even if it is not always explicitly stated, that the reagents described herein are merely exemplary and that equivalents of such are known in the art and can be substituted for the reagents explicitly stated herein.

The term "about" or "approximately" as used herein refers to being within 1 or more than 1 standard deviations, per the practice in the art. Alternatively, "about" can mean a range of up to 20% of a given value.

Concentrations, amounts, solubilities, and other numerical data may be expressed or presented herein in a range format. It is to be understood that such a range format is used merely for convenience and brevity and thus should be interpreted flexibly to include not only the numerical values explicitly recited as the limits of the range, but also to include all the individual numerical values or sub-ranges encompassed within that range as if each numerical value and sub-range is explicitly recited. As an illustration, a numerical range of "about 1 to about 5" should be interpreted to include not only the explicitly recited values of about 1 to about 5, but also include the individual values and sub-ranges within the indicated range. Thus, included in this numerical range are individual values such as 2, 3, and 4 and sub-ranges such as from 1-3, from 2-4 and from 3-5, etc. This same principle applies to ranges reciting only one numerical value. Furthermore, such an interpretation should apply regardless of the range or the characteristics being described.

As used herein, the term "comprising" is intended to mean that the products, compositions and methods include the referenced components or steps, but not excluding others. "Consisting essentially of" when used to define products, compositions and methods, shall mean excluding other components or steps of any essential significance. Thus, a composition consisting essentially of the recited components would not exclude trace contaminants and pharma-

ceutically acceptable carriers. "Consisting of" shall mean excluding more than trace elements of other components or steps.

As used in the specification and claims, the singular form "a", "an" and "the" include plural references unless the 5 context clearly dictates otherwise.

The pharmaceutical compositions of the subject invention can be formulated according to known methods for preparing pharmaceutically useful compositions. Furthermore, as used herein, the phrase "pharmaceutically acceptable car- 10 rier" means any of the standard pharmaceutically acceptable carriers. The pharmaceutically acceptable carrier can include diluents, adjuvants, and vehicles, as well as implant carriers, and inert, non-toxic solid or liquid fillers, diluents, or encapsulating material that does not react with the active 15 ingredients of the invention. Examples include, but are not limited to, phosphate buffered saline, physiological saline, water, and emulsions, such as oil/water emulsions. The carrier can be a solvent or dispersing medium containing, for example, ethanol, polyol (for example, glycerol, propylene 20 glycol, liquid polyethylene glycol, and the like), suitable mixtures thereof, and vegetable oils. Formulations are described in a number of sources that are well known and readily available to those skilled in the art. For example, Remington's Pharmaceutical Sciences (Martin E W [1995] 25 Easton Pennsylvania, Mack Publishing Company, 19th ed.) describes formulations which can be used in connection with the subject invention.

The compounds used in the present invention may be administered individually, or in combination with or concurrently with one or more other compounds used in other embodiments of the present invention. Additionally, compounds used in the present invention may be administered in combination with or concurrently with other therapeutics for cancer.

Examples of cancers benefited by the present invention include, but are not limited to, myelomas; leukemias; lymphomas; sarcomas; carcinomas; myelodysplastic syndrome; brain cancer; cancer of the nervous system including gliomas, meningioma, medulloblastoma, schwannoma, and 40 epidymoma; lung cancer including non-small cell lung cancer and small cell lung cancer; breast cancer; prostate cancer; testicular cancer; bladder cancer; bone marrow cancer; cervical cancer; chronic lymphocytic leukemia; colorectal cancer; esophageal cancer; hepatocellular cancer; lym- 45 phoblastic leukemia; follicular lymphoma; lymphoid malignancies of T or B cell origin; melanoma and other skin cancers; myelogenous leukemia; myeloma; oral cancer; ovarian cancer; spleen cancer; pancreatic cancer; stomach cancer; colorectal cancer; renal cell carcinoma; and head and 50 neck carcinoma.

As used herein, "non-fluorinated aryls" or "non-fluorinated aryl compounds" means a molecule lacking one or more fluorine atoms directly connected to an aryl on the molecule

As used herein, "fluorinated aryls" or "fluorinated aryl compounds" means a molecule possessing one or more fluorine atoms directly connected to an aryl on the molecule.

As used herein, "aryl" means an aromatic hydrocarbon substituent or radical molecule possessing an aromatic 60 hydrocarbon.

As used herein, "boron-difluoride adduct" means a borondifluoride moiety (BF₂) associated with the oxygen atoms of a keto-enol.

As used herein, "patient" means members of the animal 65 kingdom, including mammals, such as but not limited to, primates including humans, gorillas and monkeys; rodents,

16

such as mice, fish, reptiles and birds. The patient may be any animal requiring therapy, treatment, or prophylaxis, or any animal suspected of requiring therapy, treatment, or prophylaxis. The term treatment, as used in this definition only, is intended to mean that regiment described is continued until the underlying disease is resolved, whereas therapy requires that the regiment alleviate one or more symptoms of the underlying disease. Prophylaxis means that regiment is undertaken to prevent a possible occurrence, such as where a high risk of cancer is identified, but tumors or other cancerous growths have not been found. "Patient" and "subject" are used interchangeably herein.

The term "administration" or "administering" is used to describe the process in which the curcuminoid or derivative is provided to the patient. The composition may be administered in various ways including oral, intragastric, and parenteral (referring to intravenous and intra-arterial and other appropriate parenteral routes), among others.

Administration will often depend upon the amount of compound administered, the number of doses, and duration of treatment. In an embodiment, multiple doses of the agent are administered. The frequency of administration of the agent can vary depending on any of a variety of factors, such as timing of treatment from previous treatments, objectives of the treatment, i.e., weight loss or treatment of cancer or neurological disease, and the like. The duration of administration of the agent, e.g., the period of time over which the agent is administered, can vary, depending on any of a variety of factors, including patient response, desired effect of treatment, etc.

The amount of the agent contacted (e.g., administered) can vary according to factors such as the degree of susceptibility of the individual, the age, sex, and weight of the individual, idiosyncratic responses of the individual, the dosimetry, and the like. Detectably effective amounts of the agent of the present disclosure can also vary according to instrument and film-related factors. Optimization of such factors is well within the level of skill in the art.

The "therapeutically effective amount" for purposes herein is thus determined by such considerations as are known in the art. A therapeutically effective amount of individual curcuminoid compound or salt formed from curcuminoid compound, derivatives, or any combination thereof is that amount necessary to provide a therapeutically effective result in vivo. The amount of curcuminoid compound or salt, derivatives, or any combination thereof must be effective to achieve a response, i.e. prophylaxis or treatment. In accordance with the present invention, a suitable single dose size is a dose that is capable of preventing or alleviating (reducing or eliminating) a symptom in a patient when administered one or more times over a suitable time period. As used herein, alleviating includes reducing cancerous growths, limiting spread or metastasis of cancerous cells, or limiting growth of cancerous or precancerous bodies. One of skill in the art can readily determine appropriate single dose sizes for systemic administration based on the size of a mammal and the route of administration.

## Example 1—CUR Inspired Compounds Bearing Fluorinated Moieties

Studies were performed to identify suitable solvents for the reaction of 1 with Selectfluor. Experiments were performed by using 0.1 mmol of CUR and 1.1 and 2.1 equivalents of Selectfluor, and the progress of the reactions were monitored by ¹⁹F NMR (and by TLC). ¹⁹F NMR provided a convenient and direct method to gauge chemoselectivity in

different solvents. Apart from F—CUR and  $F_2$ —CUR, formation of CUR—BF $_2$  adduct was observed in some solvents, notably in water and in acetone under microwave irradiation (more in section 2.2). Presence of a distinct doublet at  $\delta$  –195 ppm (J $_{HF}$ =50 Hz) signified the 1,3-diketotautomer of F—CUR present in different proportions in some solvents. Application of microwave (MW) increased the proportion of CUR—BF $_2$  adduct in acetone as solvent,

to be inefficient. (E. V. Rao, et al., *Indian. J. Pharm. Sci.*, 2011, 73, 262-270). Instead, the curcuminoid-BF₂ adducts and their corresponding curcuminoids were synthesized as outlined in Scheme 1. A microwave-assisted method reported for decomplexation of curcumin-quinolone hybrids was adopted but modified by addition of sodium oxalate. (S. Raghavan, et al., *Bioorg. Med. Chem. Lett.*, 2015, 25, 3601-3605.). Sodium oxalate serves as a bidentate ligand and chelating agent to preferentially coordinate with BF₂,

TABLE 1

Solvent ^{b,c}	¹⁹ F NMR signal at –115 ppm (s) F ₂ -CUR	¹⁹ F NMR signal at –140 ppm (s) CUR-BF ₂	¹⁹ F NMR signal at –176 ppm (s) F-CUR	¹⁹ F NMR signal at –195 ppm (d) Diketo-tautomer of F-CUR
Acetonitrile/r.t. ^d	_	11%	55%	34%
Methanol/r.t.e	100%	_	_	_
Ethanol/reflux ^d	61%	33%	6%	_
DMF/reflux ^d	21%	_	43%	36%
THF/r.t. ^d	24%	27%	32%	17%
THF/MW ^d	15%	36%	24%	25%
Acetone/r.t.e	66%	3%	23%	8%
Acetone/MW ^d	24%	64%	6%	6%
Water/refluxe	_	100%	_	_

Reported percentages are based on relative integrals of these species in  19 F NMR (not taking into account signals due to unreacted Selectfluor and its byproducts);

seen in Table 1.

Based on these studies, MeOH was selected as solvent of choice for direct difluorination of curcuminoids, whereas MeCN was chosen for monofluorination.

To minimize the formation of other species observed in  $^{19}\mathrm{F}$  monitoring study in MeCN solvent, the monofluorinations were performed at  $0^{\circ}$  C. and continued at r.t. A noteworthy feature in these studies was that competing ring fluorination products were not detected, and further fluorination beyond the formation of  $F_2$ —CUR was not observed in a control experiment using excess Selectfluor (4 equiv.). Based on these studies compounds 3 and 4 of FIG. 2 were synthesized and isolated according to the scheme shown in FIG. 3.

The base-catalyzed "double aldol" condensation of aldehydes with acetyl acetone serves as a standard method to assemble the curcumin skeleton. Earlier methods employing boric oxide or boric acid as additive had drawbacks with respect to reproducibility, and a more reliable method involving the reaction of acetylacetone-BF₂ complex with aldehydes followed by hydrolysis of the complex was developed. (E. V. Rao, et al., *Indian. J. Pharm. Sci.*, 2011, 73, 262-270). Microwave-assisted one-pot methods that employed calcium oxide, and boric acid/sodium sulfate as additives in toluene solvent had also been reported. (S. Elavarasan, et al., *Journal of Chemistry*, 2013, 1-8; M. G. Shioorkar, et al., *Der Chemie Sinica*, 2015, 6, 110-113).

In the present study, the inventors found the reported hydrolytic/decomplexation process involving multiple steps possibly forming sodium-difluoro(oxalato)borate which is a known compound. (J. Chen, et al., *Chem. Commun.*, 2015, 51, 9809-9812).

In initial studies of solvent effect on fluorination selectivity using Selectfluor, shown in Table 1, formation of curcumin-BF $_2$  adduct was unexpectedly observed under microwave irradiation in acetone or in water. Whereas the method represents an interesting alternative for the synthesis of CUR—BF $_2$  adducts, in practice the isolated yields of this MW-assisted method were lower (see experimental) as compared to the method outlined in FIG. 4, and it was therefore not used in subsequent reactions.

By using the method outlined in FIG. **4**, symmetrical curcuminoids 6, 11, 15, and 20 were synthesized, as seen in FIG. **2**. As with parent 1, these curcuminoids are also exclusively present in the enolic form (NMR). In addition, the corresponding  $CUR - BF_2$  adducts 5, 10, 14, and 19, seen in FIG. **2**, were isolated in high yields and fully characterized (see exp. section).

The X-ray structures for CUR—BF2 adducts 5, 10, and 14, seen in FIGS. 7-13, confirm the symmetrical coordination of BF2 to the two oxygens in the enolic configuration. The asymmetric unit in CUR—BF2 5 corresponds to one molecule with a total of four molecules in each cell. Each molecule interacts with an adjacent molecule via one H—F contact as seen in FIG. 10 and Table 2.

18

 $[^]b\mathrm{R.T.}$  reactions were allowed to run overnight and reflux temp was limited to 70° C.;

^cMW conditions: 200 W until temp reached 140° C.:

^dSelectfluor (1.1 equiv.);

eSelectfluor (2.1 equiv.).

TABLE 2

	Summary of crystallog	raphic data for compo	unds 10, 5, 8 and 14			
	Compound					
	10	5	8	14		
Empirical formula	C ₁₉ H ₁₃ BF ₄ O ₂	C ₂₃ H ₂₃ BF ₂ O	C ₂₃ H ₂₃ O ₆	C ₂₃ H ₂₁ BF ₄ O ₆		
M	360.10	444.22	414.41	480.21		
Crystal System	Monoclinic	Monoclinic	Triclinic	Triclinic		
Space group	P2 _p /n	P2/c	Pi	Pi		
a/Å	5.1465(11)	8.0474(9)	11.7860(15)	9.605(2)		
b/Å	12.696(3)	17.115(2)	14.5631(17)	9.724(2)		
c/Å	25.312(5)	15.2867(17)	17.659(2)	12.941(3)		
$\alpha$ / $^{\circ}$	_	_	97.683(3)	72.264(5)		
β/°	95.343(5)	90.983(5)	93.743(3)	84.108(6)		
γ/°			91.750(3)	67.346(5)		
$V/A^3$	1646.8(6)	2105.1(4)	2995.1(6)	1062.2(4)		
$\rho_{calcd} \ ({ m g \ cm}^{-3})$	1.452	1.402	1.379	1.501		
T/K	105(2)	105(2)	105(2)	105(2)		
Z	4	4	6	2		
$\mu/\text{mm}^{-1}$	0.122	0.111	0.105	0.129		
Crystal size (mm)	$0.20 \times 0.15 \times 0.05$	$0.30 \times 0.05 \times 0.05$	$0.15 \times 0.04 \times 0.04$	$0.30 \times 0.05 \times 0.05$		
Reflections collected:	-					
Total	13015	11202	36284	10942		
Unique	2747	3607	10590	3705		
R _{int} ,	0.0810	0.0534	0.0949	0.0535		
Final R ₁ , wR ₂	0.1079, 0.2257	0.0636, 0.1433	0.0643, 0.1459	0.0590, 0.1471		

 $\begin{array}{l} R_1 = \Sigma[|F_0| - |F_c|]/\Sigma|F_0|, \ wR_2 = \big[\Sigma[w(|F_0|^2 - |F_c|^2)^2]/\Sigma[w(|F_0|^2)^2]\big]^{1/2} \\ R = \Sigma||F_0| - |F_0|/\Sigma|F_0|, \ R_w = \big[\Sigma w \ (|F_0| - |F_0|)^2/\Sigma w \ F_0^2\big]^{1/2} \end{array}$ 

Whereas attempts to obtain X-ray quality crystals for the bis-trifluoromethyl-CUR—BF $_2$  adduct 19 were unsuccessful, its DFT-optimized structure, as seen in FIG. 5, fully agrees with a symmetrically BF $_2$ -coordinated adduct.

Synthesis of  $\alpha$ -Carbonyl Fluorinated Curcuminoids and Structural Features

The corresponding α-carbonyl difluorinated analogs (7, 12, 16, and 21 of FIG. 2) were synthesized in good to moderate isolated yields by using 2.1 equivalents of Select-fluor, following the same procedure applied to fluorination of parent 1, seen in FIG. 1. These compounds exhibit distinctive two-bond C/F coupling with the carbonyls, giving rise to a ~28 Hz triplet in ¹³C NMR (see experimental). The DFT optimized structure of tetrafluorinated curcuminoid 12, as seen in FIG. 6, shows notable conformational changes resulting from tautomerization.

The  $\alpha$ -carbonyl monofluorinated analogs (8, 13, 17, and 22 of FIG. 2) were synthesized by reaction with 1.1 equivalent of Selectfluor in MeOH (analogous to synthesis of 4; FIG. 3). Concomitant formation of the difluorinated analogs was observed in the crude reaction mixtures in the monofluorination reactions, which could be minimized by running the reactions initially 0° C., then warming to r.t. and continuing to stir at room temperature.

The  $\alpha$ -carbonyl monofluorinated compounds exhibit a distinctive two-bond C/F coupling with the carbonyls, giv- 55 ing rise to a 20-23 Hz doublet in  13 C NMR. The 1,3-diketone tautomer can be readily recognized by the presence of a  $\sim$ 50 Hz doublet in  19 F and  1 H NMR due to geminal H/F coupling.

Whereas the monofluorinated curcuminoids 4, 13, 17, and 60 22 (FIG. 2) are exclusively present in the enolic form, compound 8 (FIG. 2) was present as a 75:25 (enol to ketone) tautomeric mixture (by ¹⁹F NMR).

Interestingly, the X-ray structure of 8 shows only the enolic tautomer and exhibits intramolecular hydrogen bonding and one H—F contact with a distance of 2.44 Å, as seen in FIG. 13. The asymmetric unit for 8 corresponds to three

crystallographically nonequivalent molecules with a total of six molecules in each unit cell.

A notable feature in the X-ray crystallographic data is absence of any significant  $\pi$ - $\pi$  stacking. Intermolecular interactions appear to be predominantly through short H—F contacts.

Cell Growth Inhibitory Effects Against Human Cancer Cells—Bioassay

To evaluate the cell growth inhibitory and apoptosis inducing effects of the fluorinated curcuminoids and their BF₂ adducts, in-vitro bioassay tests were performed on four different cancer cell lines namely: MOLT-4 (human leukemia suspension cancer cell line), PC3 and LNCap (human androgen sensitive and insensitive prostate cancer cell lines respectively), A549 (lung cancer), and MDA231 (breast cancer), and the results are sketched in Table 3.

Based on the magnitude of IC50 values, seen in Table 3, compounds 5, 6, 8, 10 and 14, depicted in FIG. **15**, exhibited high potencies toward multiple cancer cell lines, with measured activities at low micro-molar concentrations, and in the case of compound 5 in nano-molar concentration for leukemia. These anti-proliferative activity trends far exceed those of parent curcumin. It is noteworthy that three of these compounds are CUR—BF $_2$  adducts. Comparing the IC $_{50}$  data for compound 6 with the  $\alpha$ -carbonyl-monofluorinated analog 8 indicates increased activity as a result fluorine introduction, notably against breast cancer. Compound 6 (DMC) was previously tested as an anti-prostate cancer agent. (L. Lin, et al., *J. Med. Chem.*, 2006, 49, 3964-3972). The reported IC $_{50}$  values against PC3 and LNCap are near identical to those in the present study.

Some of the other fluorinated curcuminoids were also more active than their precursors, in particular against leukemia. The  $\alpha$ -carbonyl-difluorinated analogs 3 and 12 of FIG. 2 exhibited increased potency (against MOLT-4) as compared to their curcuminoid precursors 1 and 11. Overall, except for compound 11 of FIG. 2 which exhibited lower activity relative to curcumin, all others were more active

than parent curcumin, but those shown in FIG. 15 were found to be the most promising lead compounds.

TABLE 3

In vitro cell viability bioassay* of selected compounds of FIG. 2						
	Leukemia IC ₅₀ (μΜ) ^{a,b}		te Cancer (μΜ) ^{a,c}	Lung Cancer IC ₅₀ ( $\mu$ M) ^{$a,c$}	Breast Cancer $IC_{50} (\mu M)^{a,c}$	
Cell Line	MOLT-4	PC3	LNCap	A549	MDA231	
Curcuminoid						
Parent 1	19	9.0	9.7	18.0	11.5	
4	3.6*	7.4	13.0	20.0	6.2	
3	0.66**	15.0	28.0	26.0	2.2*	
10	1.5*	1.9*	4.3	7.3	1.0*	
11	28.0	14.0	30.0	29.0	20.0	
13	2.8*	38.0	7.0	60.0	12.0	
6	0.043***	1.0*	1.2*	7.1	0.28**	
5	0.56 (nM)****	3.2*	0.37**	1.5*	2.0*	
12	1.32*	nd	29.2	nd	6.7	
8+	0.076***	nd	0.19**	nd	0.023***	
7	1.07*	nd	21.3	nd	2.1*	
14	0.10**	nd	2.98*	nd	1.7*	
15	1.58*	nd	13.2	nd	20	

"Curcuminoids with:  $IC_{50}$  <4 micro-molar are considered active*;  $IC_{50}$  <1 micro-molar considered highly active**;  $IC_{50}$  <0.1 micro-molar considered potent***;  $IC_{50}$  values in the nano-molar range are considered highly potent****; compounds were chemically stable at r.t. in DMSO (solvent used for bioassay) " $IC_{50}$  is drug concentration that can inhibit 50% of cell growth

nd = not determined

The CUR—BF₂ adducts 5, 10, and 19, the  $(CF_3)_2$ —CUR 20 and the (CF₃)₂—CUR—BF₂ adduct 21 of FIG. 2 were screened at the National Cancer Institute using NCI-60 cell 35 one-dose protocol ( $10^{-5}$  M). Compounds 10, 19, and 21 of FIG. 2 exhibited relatively modest growth inhibition activities (10-20%) that were below the threshold criteria for further testing. The CUR-BF2 adduct 5 of FIG. 2, on the other hand, proved highly active with growth inhibition 40 (70%-80%) and cell death (up to 33%) and has been selected by NCI for further testing.

22

Computational Docking Study

In an effort to shed some light on the factors determining the bioactivity of these curcumin analogues, molecular docking calculations were performed in the active site of HER2. Human epidermal growth factor receptor 2 (HER2) is one of the tyrosine kinase receptors in EGFR family. which is known to play a central role in the pathogenesis of several human cancers. (N. Iqbal, et al., Mol. Biol. Int., 2014, 2014, 852748). Amplification or overexpression of HER2 occurs in breast, prostate, gastric/gastroesophageal, ovarian, endometrium, bladder, lung, colon, and head and neck cancers. Therefore, it is a drug target for cancer therapy focusing on inhibiting HER2 to reduce tumor growth. (N. Iqbal, et al., Mol. Biol. Int., 2014, 2014, 852748). Taking this into account, binding energies in HER2 were compared with the bioactivity data (IC₅₀ MDA231; breast cancer) in the search for correlations between the HER2 inhibitory activity and inhibition of cancer cells growth.

The curcuminoid derivatives fitted nicely in the tunnellike binding pocket of HER2, where they mainly established hydrophobic contacts. The more bioactive analogs (as in compound 14 of FIG. 2) interacted with the residues Leu726, Thr798, Lys753, Leu796, Thr862, Asp863, Val734, and Leu852, seen in FIGS. 10 and 11, similar to the potent HER2 tyrosine kinase domain (HER2-TK) inhibitor  $(2-\{2-[4-(\{5-chloro-6-[3-(trifluoromethyl))\}$ SYR127063 phenoxy|pyridin-3-yl\amino)-5H-pyrrolo[3,2-d]pyrimidin-5-yl]ethoxy}ethanol). In addition to its numerous hydrophobic interactions, SYR also formed hydrogen bonds with Met801, Asp863 and Asn850. A hydrogen bond with Met801 was also observed for the difluorinated curcuminoid 3 of FIG. 2. Table 4 provides a comparison between docking energies in HER2 and the measured IC50 values for MDA231, showing that curcuminoids-BF₂ adducts 10, 14, and 5 of FIG. 2 exhibit both favorable docking energy and cytotoxicity against breast cancer. Inhibition of tumor cellular proteasome has been suggested as the mechanism by which curcumin arrests the proliferation of acute promyelocytic leukemia (APL) cells. (K.-L. Tan, et al., ChemMed-Chem., 2012, 7, 1567-1579).

TABLE 4

Binding Energies in HER2 for Selected 0	Compounds of FIG.	2	
Compound	AutoDock 4.2	AutoDock Vina	IC ₅₀ MDA231 (Breast cancer)
SYR (native ligand)	-5.06 kcal/mol	-11.4 kcal/mol	
$H_3CO$ $OCH_3$ $OCH_3$ $OCH_3$	–5.05 kcal/mol	−8.2 kcal/mol ^a −7.9 kcal/mol ^b	0.023

^bCell viability was analyzed by the CellTiter-Glo ® Luminescent Cell Viability Assay

Cell viability was analyzed by the MTT assay

⁺contained circa 25% of the diketo-tautomer 9

TABLE 4-continued			
Binding Energies in HER2 for Selected Co  Compound	AutoDock 4.2	AutoDock Vina	IC ₅₀ MDA231 (Breast cancer)
H ₃ CO OCH ₃ OCH ₃ OCH ₃	-5.34 kcal/mol	-8.0 kcal/mol ^a -7.8 kcal/mol ^b	0.28
F F F F F F F F F F F F F F F F F F F	-4.08 kcal/mol	-10.6 kcal/mol	1.0
$H_3CO$ $OCH_3$ $OCH_3$ $OCH_3$	-4.75 kcal/mol ^a -4.36 kcal/mol ^b	-9.1 kcal/mol	1.7
$H_3CO$ $OCH_3$ $OCH_3$ $OCH_3$	-4.79 kcal/mol -4.42 kcal/mol	-9.6 kcal/mol	2.0
$_{\text{HO}}$ $_{\text{OCH}_3}$ $_{\text{OCH}_3}$ $_{\text{OCH}_3}$	-5.65 kcal/mol	-9.3 kcal/mol ^a -9.0 kcal/mol ^b	2.2

3

TABLE 4-continued

Binding Energies in HER2 for Selected Compounds of FIG. 2						
Compound	AutoDock 4.2	AutoDock Vina	IC ₅₀ MDA231 (Breast cancer)			
HO OCH3 OCH3	-6.18 kcal/mol ^a -5.61 kcal/mol ^b	-8.4 kcal/mol ^a -7.5 kcal/mol ^b	11.5			
$F_{3}$ C $F_{3}$ C $F_{3}$	-4.25 kcal/mol ^a -3.30 kcal/mol ^b	-10.5 kcal/mol ^a -10.4 kcal/mol ^b	NCI-60 cell screening modest activity			
F $F$ $F$ $F$ $F$ $F$	-4.46 kcal/mol	-10.5 kcal/mol ^a ,b -10.4 kcal/mol ^b	6.7			
F II	-4.50 kcal/mol	-10.3 kcal/mol	20			
F $F$ $F$	-4.34 kcal/mol	-9.9 kcal/mol	12.0			
$\begin{array}{cccccccccccccccccccccccccccccccccccc$	-5.56 kcal/mol	-9.5 kcal/mol	_			

TABLE 4-continued

Binding Energies in HER2 for Selected Compounds of FIG. 2						
Compound	AutoDock 4.2	AutoDock Vina	IC ₅₀ MDA231 (Breast cancer)			
$_{\mathrm{HO}}$ $_{\mathrm{OCH_{3}}}$ $_{\mathrm{OCH_{3}}}$ $_{\mathrm{OCH_{3}}}$	-5.78 kcal/mol	-8.5 kcal/mol ^a -8.1 kcal/mol ^b	6.2			
4						

^aMost stable binding mode.

Considering the high degree of potency against leukemia observed in the present study, in particular by 5, 6, 8, and 14 of FIG. 2, docking calculations were also performed in proteasome, as seen in Table 5. The structure of the 20S proteasome ( $\beta$ 5 and  $\beta$ 6 subunits) was obtained from the Protein Data Bank. Treatment with proteasome inhibitors

results in decrease proliferation, induction of apoptosis, and sensitization of a variety of tumor cells to chemotherapeutic agents and irradiation. Docking calculations for curcuminoids resulted in binding energies that were similar to parent curcumin itself, but judging from their  $\rm IC_{50}$  values these compounds are more active.

TABLE 5

Binding Energies in Proteasome for Selected Compoun	ds of FIG. 2	
Compound	AutoDock Vina (kcal/mol)	Leukemia MOLT-4 IC ₅₀ (μM)
HO OCH3 OCH3	-8.0	19.0

 $^{{}^}b\mathrm{Binding}$  pose most similar to SYR.

Binding Energies in Proteasome for Selected Compounds	s of FIG. 2	
Compound	AutoDock Vina (kcal/mol)	Leukemia MOLT-4 IC ₅₀ (μM)
F F F OCH ₃ OCH ₃ OCH ₃	-7.4	0.00056
H ₃ CO OCH ₃ OCH ₃	-7.2	0.076
$_{\rm H_3CO}$ $_{\rm OCH_3}$ $_{\rm OCH_3}$ $_{\rm OCH_3}$	-7.9	0.01
14		

Considering the high bioactivity and favorable docking energies of compounds 5, 6, 8, 10, and 14 of FIG. 2, their electrostatic potential maps were computed and are shown in FIG. 12 for a better visualization of the electronic properties of these molecules. Molecular electrostatic potential is a useful tool for interpreting and getting insight into the role played by electrostatic forces in the interactions between biomolecules and their ligands.

For this family of compounds, the most notable observation is the negative electrostatic potential developed by the  $_{55}$  BF $_{2}$  and the keto-enol moiety.

CUR-Inspired Compounds Effectiveness Against Cancer Various cancer cell lines were seeded into 384-well culture plates at  $2\times10^3$  cell/well and incubated at 5% CO $_2$ ,  $37^\circ$  C. The culture media was replaced with  $1\times10^{-5}$  M of  $_{60}$  curcuminoid; 1,7-bis(2,3,6-trimethoxyphenyl)hepta-1,4,6-triene-3,5-dione, 7-bis(3-benzothiophene)hepta-1,4,6-triene-3,5-dione, or D-793176. The cell line growth was measured. As seen in FIG. 19, 1,7-bis(2,3,6-trimethoxyphenyl)hepta-1,4,6-triene-3,5-dione slowed growth for all cancer cell lines, reducing growth to at least 50% that seen in non-treated cells. Further, the compound showed substantial

cell reductions for leukemia cells, as well as colon cancer, melanoma, renal, and breast cancer, as well as reduced growth or reduced growth and cell loss in prostate, non-small cell lung cancer, CNS cancer, ovarian cancer. Cell treatment with 1,7-bis(3-benzothiophene)hepta-1,4,6-triene-3,5-dione and D-793176 resulted in similar trends.

To confirm that the compounds targeted cancerous cells, and did not simply possess cytotoxic effects, the compounds were tested against cancer cells and non-cancerous cells. Peripheral blood mononuclear cells (PBMCs) were collected from healthy, i.e. non-cancerous, donors (CONTROL)

RPMI-8266 (Multiple myeloma cell line, MM) and PBCMs cells were seeded into 384-well culture plates at  $2\times10^3$  cell/well in quadruplicate, and incubated at 5% CO $_2$ ,  $37^{\circ}$  C. The culture media was replaced with compounds (ranges from 0-10,000 nM) and incubated for 72 h. Bortezomib was spiked in control. EC $_{50}$  of bortezomib in RPMI8266 is typically  $\sim\!10\text{-}16$  nM. CellTiter-Glo® 2.0 reagent was added at equal volume to the cell culture medium present in each well and the plate was left to incubate at room temperature for 10 minutes to stabilize the

luminescent signal. The plates were loaded onto a plate reader and luminescent signal/intensity from the 384-well plate read to provide  $IC_{50}$  value graphs, as seen in FIGS. 19-25.  $EC_{50}$  values were calculated as seen in Table 6 for run number 1 and Table 7 for run number 2.

TABLE 6

EC50 value calcu	ulations beginning with titr	ation of 10,000 nM.
Drug	RPMI8226 (nM)	PBMC (nM)
Drug 1	19	>30000
Drug 7	3890	>30000
Drug 13	26.33	>17647
Drug 17	26.39	>30000
Drug 18	1.3	>12335
Drug 20	1923	1267
Drug 25	27.69	>30000
U		

TABLE 7

EC50 value calculations beginning with titration of 30,0000 nM.					
Drug	RPMI8226 (nM)	PBMC (nM)			
Drug 1	23.5	>1000			
Drug 7	2920	>5000			
Drug 13	29.5	>1000			
Drug 17	13.3	>1000			
Drug 18	2.4	>1000			
Drug 20	1760	>5000			
Drug 25	47.2	>1000			
Bortezomib	10.6	60.5			

PBMC values between the two runs differ due to differences in the dose titration, which started at 10,000 nM in the first run, and which started at 30,0000 nM in the second run. 35 Additionally, variation in PBMC's  $\rm EC_{50}$  are at least partially due to donor differences.

Comparative Discussion and Summary

A series of fluorinated curcumins and curcumin-BF, adducts have been synthesized and characterized. The  $\alpha$ -car- 40 bonyl mono- and di-fluorinations were achieved by direct fluorination with Selectfluor, and ring fluorinated/trifluoromethylated CUR-BF2 adducts were assembled in onepot from the corresponding aldehydes. Structural features of the new curcuminoids were examined by multinuclear 45 NMR, and by X-ray analysis (for three CUR—BF2 adducts and a mono-fluorinated analog). A notable feature observed in the X-ray crystal structures is detection of intermolecular interactions via short H-F contacts. The IC₅₀ data from in-vitro cell growth inhibitory bioassay indicated that the 50 majority of curcuminoids were more active relative to parent curcumin, but those shown in FIG. 15 were clearly superior. The bioassay data along with the NCI-60 screening suggest that CUR—BF₂ complexes bearing activating substituents in the phenyl rings (as in compound 5 of FIG. 2) may be 55 promising drug candidates, and that introduction of F or CF₃ groups into the phenyl rings is not particularly beneficial. The finding that compound 8 of FIG. 2 is more potent than compound 6 of FIG. 2 implies that monofluorinaton at the  $\alpha$ -carbonyl position can be beneficial. The fact that activity 60 of F₂—CUR analogs (3, 12, 7, and 16 of FIG. 2) were not particularly impressive reinforces the earlier conclusions that the enolic tautomer is an important feature in binding of curcumin to proteins. (S. C. Gupta, et al., Nat. Prod. Rep. 2011, 28, 1937-1955; K.-L. Tan, et al., ChemMedChem., 65 2012, 7, 1567-1579). Model molecular docking calculations in the active site of HER2 indicated that the curcuminoid

32

derivatives can fit nicely in the tunnel-like binding pocket of HER2 by establishing hydrophobic contacts, leading to favorable docking energies.

In summary, the present study has provided notable structural clues that when brought to bear could lead to the synthesis of effective drug targets based on curcumin. Synthesis and characterization of other fluorocurcuminoids are ongoing in this laboratory and collaborative studies aimed at understanding how fluorination contributes to inhibition of cell viability are planned.

Experimental Section

General. Synthetic curcumin, fluorinated aldehydes (p-fluorobenzaldehye, 6-fluorovetraldehyde, vetraldehyde, and p-trifluoromethylbenzaldehyde), Selectfluor, and acety-15 lacetone were all high purity commercially available samples and were used without further purification. Regular solvents used for synthesis (MeCN, acetone, DCM, hexane, and EtOAc) were all of sufficient purity and were used as received. Column chromatography was performed on silica gel (63-200 mesh). NMR spectra were recorded on a 500 MHz instrument using CDCl₃, DMSO-d₆, or MeCN-d₃ as solvent. 19F NMR and 11B NMR spectra were referenced relative to external CFCl₃ and BF₃.Et₂O respectively. HRMS analyses were performed on an LC-MS instrument in 25 electrospray mode using DMSO as solvent. FT-IR spectra were recorded in ATR mode in solvent. Microwave reactions were performed in a miniature 400 W lab microwave in 5 mL vials with magnetic stirring. Melting points were measured in open capillaries and are not corrected.

Typical procedure for difluorination of curcuminoids: Selectfluor (2.2 equiv.) was added in one portion to a solution of the curcuminoid (0.75 mmol) in methanol (25 mL) at r.t. (at 55° C. in case of compounds 6 and 11 of FIG. 2) with efficient stirring under a nitrogen atmosphere for the requisite time (either 4 hrs at 55° C. or overnight for r.t.) until completion (TLC monitoring). The MeOH solvent was then removed in vacuo and the reaction mass was dissolved in DCM (3×10 mL), washed with deionized water (3×10), dried (sodium sulfate) and filtered through a coarse sintered glass funnel. The DCM was removed in vacuo and the crude mixture was purified by flash chromatography eluting with hexane and ethyl acetate (refer to analytical data), ramping of the elution solvent was employed in all cases.

Specific procedure—difluorination of 11 of FIG. 2: Selectfluor (2.5 eq, 1.04 mmol, 371 mg) was added in one portion to a solution of 11 (0.42 mmol, 131 mg) in methanol (20 mL) under a nitrogen atmosphere, and the mixture was stirred under mild reflux at 55° C. overnight. Completion of the reaction was confirmed by TLC and the solvent was removed in vacuo. The reaction mass was dissolved in DCM (3×10 mL) and washed with deionized water (3×10). The organic layer was dried (sodium sulfate), filtered through a coarse sintered glass funnel, and the solvent was removed in vacuo. The difluoro-derivative (compound 12) precipitated out of the crude reaction mixture as a white crystalline solid by addition of hexane/EtOAc (20%); 62 mg, 0.18 mmol, 42% yield.

Typical procedure for mono fluorination of curcuminoids of FIG. 2: Selectfluor (0.8 mmol, 1.05 equiv.) was added in one portion to a solution of the curcuminoid (0.75 mmol) in acetonitrile (25 mL) at 0° C. under a nitrogen atmosphere, and the mixture was stirred for 6 hours at this temperature, followed by overnight stirring at r.t. Upon completion (verified by TLC) the solvent was removed in vacuo and the reaction mass was dissolved in DCM (3×10 mL). The reaction mixture was washed with deionized water (3×10 mL), dried over sodium sulfate and filtered through a coarse

sintered glass funnel. The solvent was removed in vacuo and the crude reaction mixture was purified by flash chromatography eluting with hexane/ethyl acetate (refer to analytical data), ramping of the elution solvent was employed in all cases).

Specific procedure—monofluorination of 11 of FIG. 2: Selectfluor (0.81 mmol, 1.05 eq, 286 mg) was added in one portion to a solution of 11 (0.38 mmol, 119 mg) in acetonitrile (20 mL) at 0° C. under a nitrogen atmosphere, and the mixture was stirred for 6 hrs at this temperature, followed by overnight stirring at r.t. Upon completion (monitored by TLC), the acetonitrile was removed in vacuo and the reaction mass was dissolved in DCM (3×10 mL). Following the steps outlined in the typical procedure and flash chromatography (hexane/EtOAc (5%), the monofluorinated product 13 was obtained as a yellow solid (54 mg, 0.1635 mmol, 43% yield).

Synthesis of acetylacetone-difluoroboron adduct: Following a similar procedure described by Fraser et al, to a mixture of acetylacetone (10 mmol, 1 g) in dry DCM (50 20 mL, distilled from P₂O₅) under a nitrogen atmosphere BF₃.Et₂O (~48%; 2.126 g, 1.89 mL, 15 mmol, 1.5 equiv) was slowly added over a period of 5 minutes, and the reaction mixture was refluxed (41° C.) for 12 hrs. (S. Xu, et al., Inorg. Chem., 2013, 52, 3597-3610). Upon completion 25 of the reaction, the reaction mixture was allowed to come to room temperature and quenched with DI water (15 mL). It was transferred to a large separatory funnel, the DCM layer was separated, and the aqueous layer was discarded (the aqueous layer was quite acidic with a pH of about 1 or less). 30 The reaction mixture was subsequently washed several times with DI water (3×15 mL) until the aqueous layer had a pH of about 7. The organic layer was dried (sodium sulfate), filtered through a coarse sintered glass funnel, and the solvent was removed in vacuo to afford a brown crys- 35 talline solid (1.422 g, 9.6128 mmol, 96.0% yield), which was shown to be pure by NMR.

Typical procedure for the synthesis of curcuminoid-difluoroboron adducts: These compounds were synthesized by a slight modification of the procedure described by Rao and 40 Sudheer. (E. V. Rao, et al., Indian. J. Pharm. Sci., 2011, 73, 262-270). To a mixture of acetylacetone-BF, complex (6 mmol, 887 mg) in ethyl acetate (60 mL) under stirring and nitrogen atmosphere, the respective aldehyde (2.2 equivalence, 13.2 mmol) was added in one portion, followed by 45 N-butylamine (0.22 eq., 1.32 mmol, 96.5 mg, 130 μL) over a period of 20 minutes, with continuous stirring at room temperature overnight. The completion of the reaction was confirmed by TLC. The desired product precipitates from ethyl acetate. The reaction mixture was cooled to 0° C. in an 50 ice bath and the product was filtered, washed with cold (0° C.) ethyl acetate and dried for 30 minutes. The purity of this cut was exceptional (NMR) and no further purification was required (~60% isolated yield). The filtrate was transferred to a round bottom flask and concentrated under vacuum and 55 re-filtered to obtain a second cut which was slightly less pure by NMR (combined yield: typically >80%, except for compound 2 which was 64%).

Specific procedure—synthesis of curcuminoid-BF $_2$  adduct 10 of FIG. 2: To a mixture of acetylacetone-BF $_2$  (6 60 mmol, 887 mg) in ethyl acetate (60 mL) under stirring and nitrogen atmosphere, was added p-fluorobenzaldehyde (2.2 equivalence, 13.2 mmol, 1.638 g) in one portion, followed by slow addition (over 20 min) of N-butylamine (0.22 eq., 1.32 mmol, 96.5 mg, 130  $\mu$ L). The reaction mixture was 65 stirred continuously at room temperature overnight whereupon compound 10 precipitated from ethyl acetate. The

reaction mixture was cooled to  $0^{\circ}$  C. in an ice bath, filtered, and the product was washed with cold ( $0^{\circ}$  C.) ethyl acetate and dried for 30 minutes to afford compound 11 as a yellow solid (1.723 g, 4.78 mmol, 80% yield) which was confirmed by NMR to be highly pure.

34

General procedure for decomplexation of curcuminoid-BF₂: Using a modified microwave assisted method, the curcuminoid-BF₂ complex (0.3 mmol) and sodium oxalate (2 equiv) were added to a clean/dry microwave vial equipped with magnetic stirrer. (S. Raghavan, et al., Bioorg. Med. Chem. Lett., 2015, 25, 3601-3605). Aqueous methanol (5 mL, 8:2 MeOH/H₂O) was added and the vial was sealed with a crimp-able cap with septa using a crimping tool and the sealed vial was irradiated for 6 min at 140° C. The vial was cooled to room temperature and the cap removed. The reaction mixture was transferred to a round bottom flask and the methanol removed under vacuum. Upon addition of deionized-water (20 mL) a precipitate was formed which was collected by filtration, washed with 40 mL of deionizedwater and dried for 30 min. The resulting curcuminoid product was >98% pure (by NMR).

Typical procedure—decomplexation of curcuminoid-BF₂ adduct 10 of FIG. 2: The curcuminoid-BF₂ adduct 10 (0.28 mmol, 101 mg) and sodium oxalate (2 equiv, 0.56 mmol, 75 mg) were added to a clean/dry microwave vial equipped with magnetic stirrer. Upon addition of aqueous methanol (5 mL, 8:2 MeOH/H₂O) a suspension was formed. The vial was sealed and irradiated for 6 min at 140° C. The vial was cooled to r.t. and the sealed cap was removed. Removal of solvent and addition of deionized-water gave a precipitate which was washed and dried under vacuum to give compound 11 as a yellow solid (79 mg, 0.25 mmol, 90% yield) which was pure by NMR.

Microwave assisted formation of curcumin-BF₂ adduct using Selectfluor: To a clean dry microwave vial (5 mL) curcumin 1 (0.75 mmol, 276.3 mg) was added followed by acetone (5 mL) to dissolve the curcumin. Selectfluor (0.825 mmol, 292.3 mg, 1.1 equiv) was then added directly to the solution, and the vial was sealed with a crimp-able cap with septa using a crimping tool. The absorbance was set to very high and the mixture was irradiated at 200 W for 97 seconds until it reached a temperature of 138° C. and a pressure of 10 bar. The reaction was monitored by TLC at intervals by removing ~0.1 mL through the septa with a syringe and diluting in DCM. Upon completion, the acetone was removed in vacuo and reaction mass was dissolved in DCM, washed with deionized water (3×10 mL), dried (sodium sulfate) and filtered through a coarse sinter glass funnel. The solvent was removed in vacuo, and the crude mixture was purified by flash chromatography eluting with ethyl acetate/ hexane (40:60). The resulting curcumin-BF₂ complex 2 (128 mg, 0.3075 mmol, 41% yield) was pure as confirmed by NMR. For comparison, a 64% isolated yield was obtained for this decomplexation by using BF₃.Et₂O instead of Selectfluor.

Characterization Data for Compounds of FIG. 2

Curcumin-BF₂ adduct (2): Yield: 64% (using BF₃.Et₂O and 41% by using Selectfluor), red solid, mp>260° C. Rf 0.16 (40% EtOAc in hexane).  1 H NMR (CD₃CN, 500 MHz):  $\delta$  7.96 (d, J=16.0 Hz, 2H), 7.42 (br, s, 2OH), 7.37 (d, J=2.1 Hz, 2H), 7.30 (dd, J=8.2 and 2.1 Hz, 2H), 6.94 (d, J=8.6 Hz, 2H), 6.89 (d, J=16.0 Hz, 2H), 6.28 (s, 1H), 3.95 (s, 6H, 2OMe).  13 C NMR (CD₃CN, 125 MHz):  $\delta$  180.5, 151.4, 148.7, 147.6, 127.8, 128.0, 119.2, 116.2, 112.3, 102.4, 56.7.  19 F NMR (CD₃CN, 470 MHz):  $\delta$  -140.97 (s,  11 B-F), -140.91 (s,  10 B-F).  11 B NMR (CD₃CN, 160.3 MHz):  $\delta$  0.95 (s).

36

(1E,6E)-4,4-Difluoro-1,7-bis(4-hydroxy-3-methoxyphenyl)hepta-1,6-diene-3,5-dione (3): Yield: 33%, red solid, mp 117-118° C. Rf 0.53 (40% EtOAc in hexane). ¹H NMR  $(CD_3CN, 500 \text{ MHz}): \delta 7.85 \text{ (d, J=16.0 Hz, 2H)}, 7.35 \text{ (d, J=16.0 Hz, 2H)}$ J=1.5 Hz, 2H), 7.29 (br s, 2OH), 7.25 (dd, J=8.0 and 1.5 Hz, 5 2H), 7.12 (d, J=16 Hz, 2H), 6.88 (d, J=8.0 Hz, 2H), 3.90 (s, 6H, 2OMe).  13 C NMR (CD₃CN, 125 MHz):  $\delta$  186.5 (t,  2 J $_{CF}$ 26.7 Hz), 150.5, 148.8, 147.8, 126.2, 125.5, 115.2, 116.5, 111.1, 111.7 (t,  ${}^{1}J_{CF}$ =263.2 Hz), 58.9.  ${}^{19}F$  NMR (CD₃CN, 470 MHz): δ -115.3. HRMS (ESI): m/z [M+H]⁺ calcd for 10  $C_{21}H_{19}O_6F_2$ : 405.1149; found: 405.065. IR (cm⁻¹, CH₂Cl₂/ MeCN): 3415 (br, OH), 3182-2847 (C-H package), 1693 (CO), 1681, 1568, 1506, 1431, 1271, 1207, 1122, 1064.

(1E,4E,6E)-4-Fluoro-5-hydroxy-1,7-bis(4-hydroxy-3methoxyphenyl)hepta-1,4,6-trien-3-one (4): Yield: 52%, 15 purple solid, mp 154-155° C. Rf 0.60 (40% EtOAc in hexane). ¹H NMR (CD₃CN, 500 MHz): δ 14.1 (br, enolic OH), 7.63 (d, J=16 Hz, 2H), 7.31 (d, J=16 Hz, 2H), 7.20 (dd, J=8.5 and 1.5 Hz, 2H), 7.10 (dd, J=16 and 3.5 Hz, 2H), 7.05 (s, 2H, 2OH), 6.87 (d, J=8.0 Hz, 2H), 3.91 (s, 6H, 2OMe). 20  13 C NMR (CD₃CN, 125 MHz): 172.1 (d,  2 J $_{CF}$ =23 Hz), 149.5, 147.7, 143.0 (d,  ${}^{1}J_{CF}$ =238.0 Hz), 141.9 (d,  ${}^{3}J_{CF}$ =2.9 Hz), 127.4, 123.8, 115.1, 114.3, 110.7, 55.8. ¹⁹F NMR (CD₃CN, 470 MHz):  $\delta$  –176.5 (t, J $_{HF}$ =2.8 Hz). HRMS (ESI): m/z [M+H]⁺ calcd for C $_{21}$ H $_{20}$ O $_{6}$ F: 387.1243; found: 25 387.080. IR (cm $^{-1}$ , CH $_{2}$ Cl $_{2}$ /MeCN): 3417 (br, OH), 3062-2937 (C—H package), 1620 (CO), 1568, 1504, 1429. 1267, 1122, 1029.

Tetramethoxy-curcuminoid-BF2 complex (5): Yield 83%, purple solid, mp 224-226° C., Rf 0.16 (40% EtOAc in 30 hexane). ¹H NMR (DMSO-d₆, 500 MHz): δ 0.7.97 (d, J=16.0 Hz, 2H), 7.49 (d, J=2.0 Hz, 2H), 7.46 (dd, J=8.0 and 2.0 Hz, 2H), 7.11 (d, J=16 Hz, 2H), 7.07 (d, J=8.0 Hz, 2H),6.50 (s, 2H), 3.84 (s, 6H). ¹³C NMR (DMSO-d₆, 125 MHz): δ 179.5, 153.0, 149.6, 147.3, 127.6, 125.6, 119.3, 112.3, 35 111.7, 101.8, 56.3, 56.1. ¹⁹F NMR (DMSO-d₆, 470 MHz): δ –137.9 (s, ¹¹B-F), –137.8 (s, ¹⁰B-F). ¹¹B NMR (DMSO $d_6$ , 160.3 MHz):  $\delta$  0.90 (s). IR (cm⁻¹, CH₂Cl₂): 3003-2841 (CH package), 1610 (CO), 1529, 1508, 1263, 1136.

(1E,4E,6E)-5-Hydroxy-1,7-bis(3,4-dimethoxyphenyl) hepta-1,4,6-trien-3-one (6): Yield 94%, red solid, mp 122-125° C. Rf 0.375 (40% EtOAc in hexane). ¹H NMR (CDCl₃, 500 MHz):  $\delta \sim 14.8$  (br, enolic OH), 7.62 (d, J=16.0 Hz, 2H), 7.17 (dd, J=8.0 and 1.6 Hz, 2H), 7.09 (d, J=1.5 Hz, 2H), 6.89 (d, J=8 Hz, 2H), 6.51 (d, J=16 Hz, 2H), 5.85 (s, 1H), 3.94 45 (s, 6H), 3.93 (s, 6H).  13 C NMR (DMSO-d₆, 125 MHz):  $\delta$ 183.6, 151.4, 149.5, 140.9, 128.0, 123.5, 122.5, 112.1, 110.8, 101.5, 56.0, 56.1. HRMS (ESI): m/z [M+H]+ calcd for C₂₃H₂₅O₆: 397.1651; found: 397.140. IR (cm⁻¹, DCM/ CH₂Cl₂): 3005-2837 (CH package), 1624 (CO), 1581, 1510, 50 1462, 1259, 1136, 1022.

(1E,6E)-4,4-Difluoro-1,7-bis(3,4-dimethoxyphenyl) hepta-1,6-diene-3,5-dione (7): Yield: 40%, orange solid, mp 148-149° C. Rf 0.425 (40% EtOAc in hexane). ¹H NMR J=15.5 Hz, 2H), 6.90 (d, J=8.0 Hz, 2H), 3.95 (s, 6H, 2OMe), 3.96 (s, 6H, 2OMe). ¹³C NMR (CDCl₃, 125 MHz): δ 186.6 (t,  ${}^{2}J_{CF}$  26.8 Hz), 152.7, 149.4, 148.8, 126.7, 125.1, 115.6, 112.0 (t,  ${}^{1}J_{CF}$ =264.1 Hz), 111.0, 110.0, 59.0.  ${}^{19}F$  NMR 60  $(CDCl_3, 470 \text{ MHz}): \delta - 115.3 \text{ (s, }^{11}\text{B isotope)} \text{ and } -115.4 \text{ (s, }^{11}\text{B isotope)}$  10 B isotope). HRMS (ESI): m/z [M+H]⁺ calcd for  $C_{23}H_{23}O_6F_2$ : 433.1462; found: 433.0886. IR (cm⁻¹, CH₂Cl₂/DCM): 3003-2937 (CH package), 1681(CO), 1587, 1573, 1510, 1463, 1421, 1265, 1139.

(1E,4E,6E)-4-Fluoro-5-hydroxy-1,7-bis(3,4-dimethoxyphenyl)hepta-1,4,6-trien-3-one (8) and (1E,6E)-4-Fluoro-1, 7-bis(3,4-dimethoxyphenyl)hepta-1,6-diene-3,5-dione (9): Tautomeric mixture (75:25 ratio by ¹⁹F NMR). Yield 33%, red solid, mp 145-146° C. Rf 0.525 (40% EtOAc in hexane). Analytical data for 8.  1 H NMR (CDCl₃, 500 MHz):  $\delta \sim 14.0$ (br, enolic OH), 7.67 (d, J=16 Hz, 2H), 7.21 (dd, J=8.0 and 2.0 Hz, 2H), 7.14 (d, J=2 Hz, 2H), 6.99 (dd, J=16.0 and 3.5 Hz, 2H), 6.90 (d, J=8.5 Hz, 2H), 3.96 (s, OMe), 3.94 (s, OMe).  19 F NMR (CDCl $_3$ , 470 MHz):  $\delta$  –175.7 (s). Analytical data for 9:  ${}^{1}H$  NMR (CDCl₃, 500 MHz):  $\delta$  7.78 (d, J=16 Hz, 2H), 7.22 (dd, not fully resolved), 7.12 (d, J=2 Hz), 6.88 (d, J=8.5 Hz), 5.70 (d,  $J_{HF}$ =50 Hz), 3.93 (s, OMe), 3.94 (OMe, not fully resolved). ¹⁹F NMR (CDCl₃, 470 MHz):  $\delta$ -194.9 (d,  $J_{HF}$ =50 Hz). Data for 8 (a) and 9 (b):  13 C NMR  $(CDCl_3, 125 \text{ MHz}): 189.9 \text{ (d, } ^2J_{CF}=20 \text{ Hz})^b, 172.0 \text{ (d, }$  ${}^{2}\mathrm{J}_{CF} = 22 \ \mathrm{Hz})^{a}, \ 152.3, \ 151.4^{a}, \ 149.3, \ 149.2^{a}, \ 146.9 \ \mathrm{(d, }^{3}\mathrm{J}_{CF} = 2.7 \ \mathrm{Hz})^{b}, \ 143.0 \ \mathrm{(d, }^{1}\mathrm{J}_{CF} = 236 \ \mathrm{Hz})^{a}, \ 141.7 \ \mathrm{(d, }^{3}\mathrm{J}_{CF} = 3 \ \mathrm{Hz})^{a}, \ 128.0_{a}, \ 126.9^{b}, \ 123.2^{a}, \ 117.1^{b}, \ 115.0^{a}, \ 111.1^{a}, \ 111.0, \ \mathrm{(d, }^{3}\mathrm{J}_{CF} = 3 \ \mathrm{(d, }^{3}\mathrm{J}_{CF} = 3$  $109.9^a$ , 97.5 (d,  ${}^{1}J_{CF}$ =199 Hz) b , 56.0, 55.0. HRMS (ESI): m/z  $[M+H]^+$  calcd for  $C_{23}H_{24}O_6F$ : 415.1556; found: 415.120. IR (tautomeric mixture; cm⁻¹, CH₂Cl₂/CDCl₃): 3400 (br, OH), 2933, 2839, 1685 (CO), 1589, 1510, 1463, 1265, 1139, 1022.

Difluorocurcuminoid-BF2 adduct (10): Yield 80%, orange solid, mp 258-260° C. Rf 0.05 (5% EtOAc in hexane).  1 H NMR (acetone-d₆, 500 MHz):  $\delta$  8.07 (d, J=15.7 Hz, 2H), 7.96 (dd, J=8.5 and 7.0 Hz, 4H), 7.30 (t appearance, J=9.5 Hz, 4H), 7.13 (d, J=15.7 Hz, 2H), 6.65 (s, 1H). ¹³C NMR (acetone-d₆, 125 MHz):  $\delta$  181.7, 165.7 (d,  ${}^{1}J_{CF}$ =251.7 Hz), 146.3, 132.7 (d,  $J_{CF}$ =8.6 Hz), 131.9 (d,  $J_{CF}$ =3.9 Hz), 122.2, 117.2 (d, J_{CF}=22 Hz), 103.1. ¹⁹F NMR (acetone-d₆, 470 MHz):  $\delta$  –108.7 (m, 2F), –140.2 (s, ¹¹B-F), –140.1 (s,  $^{10}\mbox{B-F}).$   $^{11}\mbox{B}$  NMR (acetone-d₆, 160.3 MHz):  $\delta$  1.01 (s). IR , CH₂Cl₂): 3107, 3041, 2922, 2850, 1620 (CO), 1589, 1548, 1508, 1404, 1232, 1155.

(1E,4E,6E)-1,7-Bis(fluorophenyl)-5-hydroxy-hepta-1,4, 6-trien-3-one (11): Yield 90%, yellow solid, mp 158-160° C., Rf 0.325 (5% EtOAc in hexane). ¹H NMR (CDCl₃, 500 MHz):  $\delta \sim 15.9$  (br, enolic OH), 7.64 (d, J=16.0 Hz, 2H), 7.56 (dd, J=8.5 and 15.0 Hz, 4H), 7.10 (t appearance, J=8.5 ⁴⁰ Hz, 4H), 6.51 (d, J=15.9 Hz, 2H), 5.82 (s, 1H). ¹³C NMR (CDCl₃, 125 MHz):  $\delta$  183.1, 163.8 (d,  ${}^{1}J_{CF}$ =250.8 Hz), 139.4, 131.2 (d,  $J_{CF}$ =2.9 Hz), 129.9 (d,  $J_{CF}$ =8.6 Hz), 123.7, 116.1 (d,  $J_{CF}$ =22 Hz), 101.8. ¹⁹F NMR (CDCl₃, 470 MHz):  $\delta$  -109.7 (m). HRMS (ESI): m/z [M+H]⁺ calcd for  $C_{19}H_{15}O_2F_2$ : 313.1040; found: 3313.100. IR (cm⁻¹, DCM): 3066-2850 (CH package), 1631 (CO), 1593, 1508, 1414, 1234, 1150.

(1E,6E)-4,4-Difluoro-1,7-bis(4-fluorophenyl)hepta-1,6diene-3,5-dione (12): Yield 42%, white solid, mp 72-73° C., Rf 0.35 (5% EtOAc in hexane). ¹H NMR (CDCl₃, 500 MHz): δ 7.88 (d, J=16.5 Hz, 2H), 7.67-7.63 (m, 4H), 7.15-7.12 (m, 4H), 7.06 (d, J=16.5 Hz, 2H). ¹³C NMR  $(CDCl_3, 125 \text{ MHz}): \delta 186.7 \text{ (t, }^2J_{CF} 27.9 \text{ Hz)}, 164.9 \text{ (d,}$  $^{1}J_{CF}$ =254.7 Hz), 147.3, 131.4 (d,  $J_{CF}$ =8.5 Hz), 129.9 (d, (CDCl₃, 500 MHz):  $\delta$  7.87 (d, J=15.5 Hz, 2H), 7.24 (dd, 55 J_{CF}=3.9 Hz), 117.6 (d, J_{CF}=2.9 Hz), 116.4 (d, J_{CF}=22 Hz), J=8.0 and 2.0 Hz, 2H), 7.13 (d, J=2.0 Hz, 2H), 6.98 (d, 111.4 (t,  ${}^{1}J_{CF}$ =265.1 Hz).  ${}^{19}F$  NMR (CDCl₃, 470 MHz):  $\delta$ -106.2 (m, 2F), -115.3 (s, 2F). HRMS (ESI): m/z [M+H]⁺ calcd for  $C_{19}H_{13}O_2F_4$ : 349.0851; found: 349.040. IR (cm⁻¹, DCM/CDCl₃): 3078, 2929, 1697, 1608, 1585, 1508, 1417, 1234, 1159, 1112, 1099, 1058.

(1E,4E,6E)-4-Fluoro-1,7-bis(4-fluorophenyl)-5-hydroxyhepta-1,4,6-trien-3-one (13): Yield: 43%, yellow solid, mp 152-153° C. Rf 0.45 (5% EtOAc in hexane). ¹H NMR  $(CDCl_3, 500 \text{ MHz}): \delta \sim 13.8 \text{ (br, enolic OH)}, 7.68 \text{ (d, J=15.9)}$ Hz, 2H), 7.62 (dd, J=8.5 and 5.5. Hz, 4H), 7.12 (t appearance, J=8.5, 4H), 7.06 (dd, J=15.7 and 3.7 Hz, 2H). ¹³C NMR (CDCl₃, 125 MHz): 172.0 (d,  ${}^{2}J_{CF}$ =21.8 Hz), 164.0 (d,  ${}^{1}J_{CF}$ =251.6 Hz), 145.5, 143.1 (d,  ${}^{1}J_{CF}$ =238.4 Hz), 140.6 (d,  $J_{CF}$ =1.9 Hz), 131.2 (d,  $J_{CF}$ =2.9 Hz, 130.3 (d,  $J_{CF}$ =8.7 Hz), 116.8, 116.2 (d,  $J_{CF}$ =22.0 Hz).  ${}^{19}F$  NMR (CDCl₃, 470 MHz):  $\delta$  –108.9 (m, 2F), –175.2 (t, J=3.3 Hz, 1F). HRMS (ESI): m/z [M+H]+ calcd for C₁₉H₁₄O₂F₃: 331.0945; found: 5331.110. IR (cm⁻¹, DCM/CDCl₃): 3072, 2920, 1633, 1597, 1508, 1417, 1319, 1232, 1157.

Tetramethoxydifluoro-curcuminoid-BF $_2$  adduct (14): Yield 90%, red solid, mp 253-255. Rf 0.211 (40% EtOAc in hexane).  $^1\mathrm{H}$  NMR (DMSO-d $_6$ , 500 MHz):  $\delta$  8.05 (d, J=16.0 Hz, 2H), 7.46 (d, J=7.0 Hz, 2H), 7.16 (d, J=15.5 Hz, 2H), 7.08 (d, J=12 Hz, 2H), 6.65 (s, 1H).  $^{13}\mathrm{C}$  NMR (DMSO-d $_6$ , 125 MHz):  $\delta$  179.3, 157.2 (d,  $^1\mathrm{J}_{CF}$ =250 Hz), 153.9 (d, J $_{CF}$ =11.4 Hz), 145.9, 138.3 (d, J $_{CF}$ =2.9 Hz), 120.7 (d, J $_{CF}$ =5.7 Hz), 113.1 (d, J $_{CF}$ =11.4 Hz), 110.4 (d, J $_{CF}$ =3.8 Hz), 101.7, 100.7 (d, J $_{CF}$ =28.6 Hz), 56.5, 56.2.  $^{19}\mathrm{F}$  NMR (DMSO-d $_6$ , 470 MHz):  $\delta$  -119.0 (unresolved dd, 2F), -137.7 (s,  $^{11}\mathrm{B}$ -F), -137.6 (s,  $^{10}\mathrm{B}$ -F).  $^{11}\mathrm{B}$  NMR (DMSO-d $_6$ , 160.3 MHz):  $\delta$  0.89 (br, s). IR (cm $^{-1}$ , CH $_2\mathrm{Cl}_2$ ): 2954, 2922, 20 2852, 1714, 1597, 1514, 1462, 1278, 1193, 1001.

(1E,4E,6E)-5-Hydroxy-1,7-bis(3,4-dimethoxy-6-fluorophenyl)hepta-1,4,6-trien-3-one (15): Yield 94%, orange solid, mp 154-156° C. Rf 0.447 (40% EtOAc in hexane).  $^1\mathrm{H}$  NMR (CDCl₃, 500 MHz):  $\delta$  7.74 (d, J=16.0 Hz, 2H), 6.99  25  (d, J $_{HF}$ =7.5 Hz, 2H), 6.67 (d, J $_{HF}$ =12.5 Hz, 2H), 6.60 (d, J=16.5 Hz, 2H), 5.88 (s, 1H), 3.92 (s, 12H).  $^{13}\mathrm{C}$  NMR (CDCl₃, 125 MHz):  $\delta$  183.2, 156.6 (d,  $^1\mathrm{J}_{CF}$ =249.0 Hz), 151.8 (d, J $_{CF}$ =10.4 Hz), 145.6 (d, J $_{CF}$ =2.0 Hz), 133.0, 124.0 (d, J $_{CF}$ =6.6 Hz), 114.1 (d, J $_{CF}$ =13.3 Hz), 109.6 (d, J $_{CF}$ =4.8 Hz), 101.4, 100.2 (d, J $_{CF}$ =28.5 Hz), 56.4, 56.3.  $^{19}\mathrm{F}$  NMR (CDCl₃, 470 MHz):  $\delta$  -20.1 (dd, J $_{HF}$ =11.7 and 5.6 Hz). HRMS (ESI): m/z [M+H]+ calcd for C $_{23}\mathrm{H}_{23}\mathrm{O}_6\mathrm{F}_2$ : 433.1462; found: 433.142. IR (cm $^{-1}$ , DCM/CH $_2$ Cl $_2$ ): 3005-2835 (CH package), 1614 (CO), 1510, 1440, 1363, 1292, 1273, 1211, 1192, 1139, 1109.

(1E,6E)-4,4-Difluoro-1,7-bis(3,4-dimethoxy-6-fluoro-phenyl)hepta-1,6-diene-3,5-dione (16): Yield: 26%, brown solid, mp 162-163° C. Rf 0.526 (40% EtOAc in hexane).  $^{1}\mathrm{H}$  NMR (CDCl3, 500 MHz):  $\delta$  8.05 (d, J=16.0 Hz, 2H), 7.05 (d, J=16.0 Hz, 2H), 7.02 (d, J $_{HF}$ =6.7 Hz, 2H), 6.67 (d, J $_{HF}$ =11.6 Hz, 2H), 3.93 (s, 6H, OMe), 3.92 (s, 6H, OMe).  $^{13}\mathrm{C}$  NMR (CDCl3, 125 MHz):  $\delta$  186.7 (t,  $^{2}\mathrm{J}_{CF}$ =27.6 Hz), 158.0 (d,  $^{1}\mathrm{J}_{CF}$ =252.6 Hz), 153.8 (d, J $_{CF}$ =10.5 Hz), 145.8 (d, 45 J $_{CF}$ =2.0 Hz), 140.9, 117.0 (d, J $_{CF}$ =6.6 Hz), 113.1 (d, J $_{CF}$ =12.4 Hz), 111.7 (t,  $^{1}\mathrm{J}_{CF}$ =264.2 Hz, CF $_{2}$ ), 109.3 (d, J $_{CF}$ =3.8 Hz), 100.1 (d, J $_{CF}$ =28.6 Hz), 56.5, 56.4.  $^{19}\mathrm{F}$  NMR (CDCl3, 470 MHz):  $\delta$  –115.4 (s, 2F), –117.6 (dd, J $_{HF}$ =11.7 and 5.8 Hz, 2F). HRMS (ESI): m/z [M+H]+ calcd for 50 C $_{23}\mathrm{H}_{21}\mathrm{O}_{6}\mathrm{F}_{4}$ : 469.1274; found: 469.0499. IR (cm $^{-1}$ , CDCl3/DCM): 308, 2941, 1707, 1693, 1512, 1442, 1365, 1280, 1193.

 $\begin{array}{l} (1\mathrm{E},4\mathrm{E},6\mathrm{E})\text{-}4\text{-}\mathrm{Fluoro}\text{-}5\text{-}\mathrm{hydroxy}\text{-}1,7\text{-}\mathrm{bis}(3,4\text{-}\mathrm{dimethoxy}\text{-}6\text{-}\mathrm{fluorophenyl})\mathrm{hepta}\text{-}1,4,6\text{-}\mathrm{trien}\text{-}3\text{-}\mathrm{one}\ (17)\text{: Yield}\ 10\%, red\ 55\ \mathrm{solid},\ \mathrm{mp}\ 148\text{-}150^\circ\ \mathrm{C}.\ \mathrm{Rf}\ 0.579\ (40\%\ \mathrm{EtOAc}\ \mathrm{in}\ \mathrm{hexane}).\ ^1\mathrm{H}\ \mathrm{NMR}\ (\mathrm{CDCl}_3,\ 500\ \mathrm{MHz})\text{: }\delta\ 7.82\ (\mathrm{d},\ \mathrm{J}=16\ \mathrm{Hz},\ 2\mathrm{H}),\ 7.08\text{-}7.03\ (\mathrm{m},\ 4\mathrm{H}),\ 6.67\ (\mathrm{d},\ \mathrm{J}_{HF}=11.5\ \mathrm{Hz}),\ 3.93\ (\mathrm{s},\ \mathrm{OMe}),\ 3.942\ (\mathrm{s},\ \mathrm{OMe}).\ ^{13}\mathrm{C}\ \mathrm{NMR}\ (\mathrm{CDCl}_3,\ 125\ \mathrm{MHz})\text{: }172.0\ (\mathrm{d},\ ^2\mathrm{J}_{CF}=21\ \mathrm{Hz}),\ 156.9\ (\mathrm{d},\ ^1\mathrm{J}_{CF}=250\ \mathrm{Hz}),\ 152.2\ (\mathrm{d},\ \mathrm{J}_{CF}=10.4\ \mathrm{Hz}),\ 145.7,\ 60\ 143.1\ (\mathrm{d},\ \mathrm{J}_{CF}=238.5\ \mathrm{Hz}),\ 134.2,\ 116.8\ (\mathrm{d},\ \mathrm{J}_{CF}=5.8\ \mathrm{Hz}),\ 114.2\ (\mathrm{d},\ \mathrm{J}_{CF}=238.5\ \mathrm{Hz}),\ 134.2,\ 116.8\ (\mathrm{d},\ \mathrm{J}_{CF}=5.8\ \mathrm{Hz}),\ 114.2\ (\mathrm{d},\ \mathrm{J}_{CF}=12.4\ \mathrm{Hz}),\ 109.6\ (\mathrm{d},\ \mathrm{J}_{CF}=3.7\ \mathrm{Hz}),\ 100.3,\ 56.4.\ 56.3.\ ^{19}\mathrm{F}\ \mathrm{NMR}\ (\mathrm{CDCl}_3,\ 470\ \mathrm{MHz})\text{: }\delta\ -119.5\ (\mathrm{dd},\ \mathrm{J}_{HF}=11.7\ \mathrm{and}\ 6.6.\ \mathrm{Hz},\ 2\mathrm{F}),\ -175.3\ (\mathrm{distorted}\ \mathrm{t},\ \mathrm{J}=3.3\ \mathrm{Hz},\ 1\mathrm{F}).\ \mathrm{HRMS}\ (\mathrm{ESI})\text{: m/z}\ [\mathrm{M}+\mathrm{H}]^+\ \mathrm{calcd}\ \mathrm{for}\ \mathrm{C}_{23}\mathrm{H}_{22}\mathrm{O}_6\mathrm{F}_3\ 450.1368;\ found:\ 65\ 451.0632.\ \mathrm{IR}\ (\mathrm{cm}^{-1},\ \mathrm{CH}_2\mathrm{Cl}_2/\mathrm{CDCl}_3)\text{: }2922,\ 1608,\ 1548,\ 1504,\ 1367,\ 1276,\ 1213,\ 1157,\ 1066.\ \end{array}$ 

(1E,6E)-4-Fluoro-1,7-bis(3,4-dimethoxy-6-fluorophenyl) hepta-1,6-diene-3,5-dione (18): Yield 12% (by NMR).  119 F NMR (CDCl₃, 470 MHz):  $\delta$  –195.2 (d, J $_{HF}$ =50 Hz, 1F), –118.59 (m, 2F)

Bis-trifluoromethylcurcuminoid-BF₂ adduct (19): Yield 88%, yellow solid, mp>260° C. Rf 0.14 (10% EtOAc in hexane).  1 H NMR (DMSO-d₆, 500 MHz): δ 8.14 (d, J=15.8 Hz, 2H), 8.10 (d, J=8.5 Hz, 4H), 7.87 (d, J=8.0 Hz, 4H), 7.44 (d, J=15.8 Hz, 2H), 6.77 (s, 1H).  13 C NMR (DMSO-d₆, 125 MHz): δ 180.6, 145.2, 145.1, 137.7, 131.0 (q, J_{CF}=31.4 Hz), 130.1, 125.9 (q, J_{CF}=3.8 Hz), 124.1, 123.9 (q,  1 J_{CF}=272.7 Hz, CF₃), 103.3.  19 F NMR (DMSO-d₆, 470 MHz): δ -61.4 (s, CF₃), -136.5 ( 11 B-F), -136.4 ( 10 B-F).  11 B NMR (DMSO-d₆, 160.3 MHz): δ 0.96 (br,s). IR (cm⁻¹, DCM): 1620, 1529, 1514, 1404, 1321, 1166, 1111, 1064.

(1E,4E,6E)-1,7-Bis(4-trifluoromethyl-phenyl)-5-hydroxy-hepta-1,4,6-trien-3-one (20): Yield 88%, yellow solid, mp 153-154° C., Rf 0.56 (10% EtOAc in hexane).  1 H NMR (CDCl₃, 500 MHz): δ ~15.9 (br, enolic OH), 7.95 (d, J=8.0 Hz, 2H), 7.79 (d, J=8.0 Hz, 2H), 7.72 (d, J=15.9 Hz, 2H), 7.13 (d, J=15.8 Hz, 2H), 6.28 (s, 1H).  13 C NMR (CDCl₃, 125 MHz): δ 182.9, 138.3, 131.5 (q, J_{CF}=31.5 Hz), 128.9, 126.9, 125.7 (q, J_{CF}=4 Hz), 124.0 (q,  1 J_{CF}=271.8 Hz, CF₃), 102.6.  19 F NMR (CDCl₃, 470 MHz): δ -61.2 (s, CF₃). HRMS (ESI): m/z [M+H]⁺ calcd for C₂₁H₁₅O₂F₆: 413.0976; found: 413.087. IR (cm⁻¹, DCM): 2928, 1635 (CO), 1579, 1413, 1330, 1265, 11681128, 1066.

(1E,6E)-4,4-Difluoro-1,7-bis(4-trifluoromethyl-phenyl) hepta-1,6-diene-3,5-dione (21): Yield 36%, white solid, mp 75-76° C., Rf 0.72 (10% EtOAc in hexane).  $^1\mathrm{H}$  NMR (CDCl₃, 500 MHz):  $\delta$  7.93 (d, J=15.9 Hz, 2H), 7.76 (d, J=8.5 Hz, 4H), 7.71 (d, d, J=8.5 Hz, 4H), 7.19 (d, J=16 Hz, 2H).  $^{13}\mathrm{C}$  NMR (CDCl₃, 125 MHz):  $\delta$  186.6 (t,  $^2\mathrm{J}_{CF}$ =27.7 Hz), 146.6, 136.8, 133.2 (q,  $\mathrm{J}_{CF}$ =3.8 Hz), 129.3, 126.1 (q,  $\mathrm{J}_{CF}$ =3.8 Hz), 123.6 (q,  $^1\mathrm{J}_{CF}$ =272.7 Hz, CF₃), 120.0, 112.1 (t,  $^1\mathrm{J}$ =265.1 Hz, CF₂).  $^{19}\mathrm{F}$  NMR (CDCl₃, 470 MHz):  $\delta$  -63.1 (s, 6F, CF₃), -115.1 (s, 2F, CF₂). HRMS (ESI): m/z [M+H]^+ calcd for C₂₁H₁₃O₂F₈: 449.0787; found: 449.0145. IR (cm⁻¹, CDCl₃): 3080, 2933, 1699 (CO), 1608, 1577, 1417, 1319, 1168, 1124, 1066.

(1E,4E,6E)-4-Fluoro-1,7-bis(4-trifluoromethyl-phenyl)-5-hydroxy-hepta-1,4,6-trien-3-one (22): Yield 60% [crude yield, contained 20 (22%) and 19 (18%); 16% yield after recrystallization (purity by NMR was 70%, contained 19 (30%)], orange solid, mp 144-146° C. Rf 0.64 (10% EtOAc in hexane).  $^1{\rm H}$  NMR (CDCl $_3$ , 500 MHz):  $\delta$  ~13.5 (br, enolic OH), 7.22 (dd, J=15.5 and 3.7 Hz, 2H), 7.76-7-67 (unresolved-m, 10H).  $^{19}{\rm F}$  NMR (CDCl $_3$ , 470 MHz):  $\delta$  –62.8 (6F, CF $_3$ ), –173.9 (t, J $_{HF}$ =3.2 Hz, 1F). HRMS (ESI): m/z [M+H] $^+$  calcd for C $_{21}{\rm H}_{14}{\rm O}_{2}{\rm F}_{7}$ : 431.0882; found: 431.0804.

Bioassay Methods

The cell viability/anti-proliferative activity of the curcuminoids against PC3 (human androgen-insensitive prostate cancer cell line), LNCap (human-androgen sensitive prostate cancer cell line), A549 (lung cancer), and MDA231 (breast cancer) were determined by means of 3-(4,5-dimethyl-2-thiazolyl)-2,5-diphenyl-2H-tetrazolium bromide (MTT) assay (the tetrazolium salt was a commercial sample). (R. N. Khaybullin, et al., *Molecules*, 2014, 19, 18676-18689). The ability of the curcuminoids to affect proliferations of suspension cell lines (MOLT-4) was tested by the CellTiter-Glo® Luminescent Cell Viability Assay (purchased from Promega Madison, Wis., USA) to determine the number of viable cells in culture based on quantitation of the ATP present. The IC₅₀ values were obtained from fitting data with GraphPad software to determine the

growth inhibition in the presence of test compounds. (R. N. Khaybullin, et al., *Molecules*, 2014, 19, 18676-18689).

X-ray Crystallography

Suitable single crystals for X-ray diffraction studies were obtained for compounds 10, 5 and 8 of FIG. 2 from ethyl 5 acetate and for 14 from dichloromethane. Crystal data of the compounds were collected by exactly the same method by mounting a crystal onto a thin glass fiber from a pool of Fluorolube[™] and immediately placing it under a liquid N₂ cooled stream, on a Bruker AXS diffractometer upgraded 10 with an APEX II CCD detector. The radiation used is graphite monochromatized Mo K $\alpha$  radiation ( $\lambda$ =0.7107 Å). The lattice parameters are optimized from a least-squares calculation on carefully centered reflections. Lattice determination, data collection, structure refinement, scaling, and 15 data reduction were carried out using APEX2 Version 2014.11 software package. The data were corrected for absorption using the SCALE program within the APEX2 software package. The structure was solved using SHELXT. This procedure yielded a number of C. B. F and O atoms. 20 Subsequent Fourier synthesis yielded the remaining atom positions. The hydrogen atoms are fixed in positions of ideal geometry (riding model) and refined within the XSHELL software package. These idealized hydrogen atoms had their isotropic temperature factors fixed at 1.2 or 1.5 times the 25 equivalent isotropic U of the C atoms to which they were bonded. A few hydrogen atoms could not be adequately predicted via the riding model within the XSHELL software, these hydrogen atoms were located via difference-Fourier mapping and subsequently refined. The final refinement of 30 each compound included anisotropic thermal parameters on all non-hydrogen atoms. The crystal data for the compounds are given in Table 1. Packing diagrams and thermal ellipsoid plots along with selected interatomic distances and bond angles are included in supplementary data.

Computational Methods

Geometry optimizations of the curcumin derivatives were performed at the B3LYP³⁶/6-311+G(d,p) level with the Gaussian 09 package. Distribution of the electrostatic potential derived from the electron density was estimated by 40 energy calculations at the optimized structures. The programs AutoDock 4.2 and AutoDock Vina were employed to carry out automated molecular docking for estimating the interaction energy and modeling the binding modes between the curcuminoid ligands and the enzymes HER2 and pro- 45 teasome. The three-dimensional coordinates of the proteins were obtained from the Protein Data Bank (PDB codes 3PP0 (HER2) and 3SDK (20S proteasome)). (K. Aertgeerts, et al., J. Biol. Chem. 2011, 286, 18756-18765; C. Blackburn, et al., Bioorg. Med. Chem. Lett., 2010, 20, 6581-6586). Chain A of 50 HER2, and chains K (β5 subunit) and L (β6 subunit) of 20S proteasome were selected as target templates for the docking calculations. Co-crystalized ligands and crystallographic water molecules were removed. Addition of hydrogens, merger of non-polar hydrogens to the atom to which they 55 were linked, and assignment of partial charges were achieved with AutoDockTools. Merz-Kollman partial atomic charges were employed for proteins, and Gasteiger charges were assigned to ligands. The docking area was defined using the AutoDock module AutoGrid. The docking 60 area, defined using the AutoDock module AutoGrid, was constrained to a 30×26.2×30 Å box centered at the active site, providing proper space for rotational and translational movement of the ligands. With AutoDock 4.2, the Lamarckian genetic algorithm (LGA) was used, default parameters 65 were applied, and the maximum number of energy evaluations was set to  $1.0 \times 10^7$ . For each of the 100 independent

40

runs performed for each ligand a maximum number of  $2.7 \times 10^4$  genetic algorithm operations were generated on a single population of 150 individuals. Operator weights for crossover, mutation, and elitism were default parameters, 0.80, 0.02, and 1, respectively. The default parameters were used for Vina.

Example 2—Mono- and Di-Fluorinated CUR Inspired Compounds Possessing Non-Fluorinated Aryls

Curcuminoids were formed by forming a reflux solution from 10 mmol (1 g) acetylacetone ((3Z)-4-hydroxypent-3en-2-one) with in 50 mL dichloromethane (DCM, distilled from P₂O₅) under a nitrogen atmosphere for 12 hours. Boron trifluoride complexed to diethyl ether (BF₃.Et₂O, ~48%; 2.126 g, 1.89 mL, 15 mmol, 1.5 equiv) was slowly added over a period of 5 minutes and the reaction mixture was refluxed (41° C.) for 12 hrs, as seen in FIG. 4. The product, i.e. boron-difluoride adduct of acetylacetone, was cooled to room temperature and quenched with 15 mL deionized water. The DCM layer was separated, and the aqueous layer was discarded. The reaction mixture was subsequently washed several times with DI water (3×15 mL) until the aqueous layer had a pH of about 7. The organic product was isolated and 6 mmol (887 mg) of the boron-difluoride adduct of acetylacetone mixed with 2.2 equivalent (13.2 mmol) of an aryl aldehyde in 60 mL of an ethyl acetate in a nitrogen atmosphere. N-butylamine (0.22 eq., 1.32 mmol, 96.5 mg, 130 µL) was added over a period of 20 minutes, and the solution continuously stirred at room temperature overnight.

The aryl aldehyde can be phenyl, mono-substituted aryl, di-substituted aryl, or tri-substituted aryl. The reaction mixture was cooled to 0° C. in an ice bath and the product was filtered, washed with cold (0° C.) ethyl acetate and dried for 30 minutes. The filtrate was transferred to a round bottom flask and concentrated under vacuum. The resulting bis(aryl) hepta-1,6-diene-3,5-dione boron-difluoride adduct was used as is or reduced to remove the difluoroboride adduct.

The adduct was removed from non-fluorinated aryls by dissolving 0.3 mmol of the compound in 5 mL aqueous methanol (8:2 methanol to water) and adding 2 molar equivalents of sodium oxalate in a clean/dry microwave vial equipped with magnetic stirrer. The vial was sealed and subjected to microwave for 6 minutes using a miniature 400 W lab microwave at 140° C., to form a bis(aryl) hepta-1,6-diene-3,5-dione, i.e. curcuminoid. The reaction mixture was transferred to a round bottom flask and the methanol removed under vacuum. Upon addition of deionized-water (20 mL) a precipitate was formed which was collected by filtration, washed with 40 mL of deionized-water and dried for 30 min.

To difluorinate the curcuminoid backbone, 2.2 equivalents of Selectfluor (1-Chloromethyl-4-fluoro-1,4-diazoniabicyclo[2.2.2] octane bis(tetrafluoroborate); Sigma-Aldrich, Merck KgaA, Damrstadt, Germany) was added in one portion to a solution of the curcuminoid (0.75 mmol) in methanol (25 mL) at r.t. with efficient stirring under a nitrogen atmosphere for the requisite time (either 4 hrs at 55° C. or overnight for r.t.) until completion (TLC monitoring). The MeOH solvent was then removed in vacuo and the reaction mass was dissolved in DCM (3×10 mL), washed with deionized water (3×10 mL), dried (sodium sulfate) and filtered through a coarse sintered glass funnel. The DCM was removed in vacuo and the crude mixture was purified by

flash chromatography eluting with hexane and ethyl acetate (refer to analytical data), ramping of the elution solvent was employed in all cases.

To mono-fluorinate the curcuminoid backbone, except compounds possessing fluorinated aryls, 1.05 equivalents of 5 Selectfluor (0.8 mmol) was added in one portion to a solution of the curcuminoid (0.75 mmol) in acetonitrile (25 mL) at 0° C. under a nitrogen atmosphere, and the mixture was stirred for 6 hours at this temperature, followed by overnight stirring at r.t. Upon completion (verified by TLC) 10 the solvent was removed in vacuo and the reaction mass was dissolved in DCM (3×10 mL). The reaction mixture was washed with deionized water (3×10 mL), dried over sodium sulfate and filtered through a coarse sintered glass funnel. The solvent was removed in vacuo and the crude reaction 15 mixture was purified by flash chromatography eluting with hexane/ethyl acetate with ramping of the elution solvent was employed in all cases.

# Example 3—Mono- and Di-Fluorinated CUR Inspired Compounds Possessing Fluorinated Aryls

Curcuminoids were formed by forming a reflux solution from 10 mmol (1 g) acetylacetone ((3Z)-4-hydroxypent-3en-2-one) with in 50 mL dichloromethane (DCM, distilled 25 from P₂O₅) under a nitrogen atmosphere for 12 hours. Boron trifluoride complexed to diethyl ether (BF₃.Et₂O, ~48%; 2.126 g, 1.89 mL, 15 mmol, 1.5 equiv) was slowly added over a period of 5 minutes and the reaction mixture was refluxed (41° C.) for 12 hrs, as seen in FIG. 4. To form 30 fluorinated aryl compounds, a mixture of 6 mmol the borondifluoride adduct of acetylacetone (887 mg) was suspended in ethyl acetate (60 mL) under stirring and nitrogen atmosphere, A fluorinated aryl-aldehyde (2.2 equivalence, 13.2 mmol, 1.638 g) was added in one portion, followed by slow 35 addition of 0.22 equivalents N-butylamine (1.32 mmol, 96.5 mg, 130 μL) over 20 min. The reaction mixture was stirred continuously at room temperature overnight. The reaction mixture was cooled to 0° C. in an ice bath, filtered, and the product was washed with cold (0° C.) ethyl acetate and dried 40 for 30 minutes to afford the desired compound. The aryl aldehyde can be phenyl, mono-substituted aryl, di-substituted aryl, or tri-substituted aryl.

To remove the adduct from fluorinated aryls, the adduct was removed by dissolving 0.28 mmol of the compound 45 (101 mg) in 5 mL aqueous methanol (8:2 methanol to water) and adding 2 molar equivalents of sodium oxalate (0.56 mmol, 75 mg) in a clean/dry microwave vial equipped with magnetic stirrer. The vial was sealed and irradiated for 6 min at 140° C. in the microwave. The vial was cooled to r.t. and 50 solvent removed. Deionized-water was added to form a precipitate which was washed and dried under vacuum.

To difluorinate the heptene curcuminoid backbone of fluorinated aryl compounds, 2.5 equivalents of Selectfluor (1.04 mmol, 371 mg) was added in one portion to a solution of 0.42 mmol of a fluorinated aryl compound (131 mg) in methanol (20 mL) under a nitrogen atmosphere, the mixture was stirred under mild reflux at 55° C. overnight, and the solvent was removed in vacuo. The reaction mass was dissolved in DCM (3×10 mL) and washed with deionized 60 water (3×10 mL). The organic layer was dried (sodium sulfate), filtered through a coarse sintered glass funnel, and the solvent was removed in vacuo. The difluoro-derivative was precipitated out of the crude reaction mixture by addition of hexane/EtOAc (20%).

To mono-fluorinate the compounds possessing fluorinated aryls, 1.05 equivalents of Selectfluor (0.81 mmol, 286 mg)

42

was added in one portion to a solution of the compounds possessing fluorinated aryls (0.38 mmol, 119 mg) in acetonitrile (20 mL) at 0° C. under a nitrogen atmosphere, and the mixture was stirred for 6 hrs at this temperature, followed by overnight stirring at r.t. Upon completion (monitored by TLC), the acetonitrile was removed in vacuo and the reaction mass was dissolved in DCM (3×10 mL). Following the steps outlined in the typical procedure and flash chromatography (hexane/EtOAc (5%), the monofluorinated product was obtained.

# Example 4—Multiply-Substituted and CUR-Pyrazole and CUR-Isoxazole Compounds

Multiply-substituted curcuminoids shown in FIGS. 32-35 were synthesized from the corresponding aldehydes according to the general synthetic scheme outlined in FIG. 4. FIG. 36 represents binding affinities for CURs listed in FIG. 35. FIG. 37 depicts a table of tumor-cell specific cytotoxicity by cell viability assay to determine EC50 (concentration at which 50% of the cells remain viable). These assays indicated that curcuminoids 9 and 5 of FIG. 35 were highly effective against RPMI-8226 (multiple myeloma cell line) while exhibiting significantly less cytotoxicity in peripheral blood mononuclear cells (PBMCs) from healthy donors (non-tumor control cells). EC50 curve plots for compounds 5 (A) and 9 (B) of FIG. 35 respectively, are shown in FIG. 38A-B. A list of CURs from FIG. 35 with anti-tumor activity based on NCI-60 immunoassay is shown in FIG. 39.

Pyrazole and Isoxazoles

The pyrazole and oxazole analogs, as seen in the exemplary compounds depicted in FIGS. **41-43**, were synthesized by reaction of the curcuminoids with the corresponding phenyl-hydrazine or hydroxylamine hydrochloride according to the general methods outlined in FIG. **40**.

A general observation is that the studied compounds fitted quite well in the binding pockets of the examined enzymes. Several curcuminoid, CUR-pyrazoles, and CUR-isoxazoles exhibited very favorable binding affinities, particularly the analogs bearing CF3 groups; some of them exhibited even better binding energies than those corresponding to the known inhibitors employed in cancer therapy. Very good docking affinities were also observed for CURs with benzyloxy substituents. Binding affinities for CUR-pyrazoles, and CUR-isoxazoles are shown in FIG. 44.

General Procedure for the Synthesis of CUR-Pyrazoles from FIG.  ${\bf 43}$ 

With a microliter syringe phenyl-hydrazine (2 equiv.) was added to a suspension of CUR (1 equiv.) in glacial acetic acid (5 mL) and the mixture was heated to 70° C. on a hotplate with stirring. After 2 h, the suspension had fully dissolved and the reaction had gone to completion (confirmed by TLC showing a new fluorescent spot above the precursor). The reaction mixture was transferred to a large beaker with dichloromethane (20 mL) and the acid was neutralized by gradual addition of saturated sodium bicarbonate solution until no more gas was evolved. The pH of the aqueous phase was confirmed to be seven and the mixture was transferred to a separatory funnel. The DCM layer was separated and the aqueous phase was washed with DCM (3×50 mL). The DCM layer was dried over magnesium sulfate, filtered and the solvent was removed in vacuo to give the crude reaction mixture. The crude product was dissolved in hot iPrOH and allowed to cool to give the desired product in good purity (see below for exceptions).

Exceptions

CUR-pyrazole 23—a two solvent system of iPrOH/ hexane was used for recrystallization. CUR-pyrazoles 26, 29, 32, and 34—water was added to the hot reaction mixture until the mixture became cloudy. It was left to cool slowly and the desired product precipitated out of solution, the product was filtered and no further purification was needed. CUR-pyrazole 31—DCM extract was an oil which was crystallized from hexane. CUR-pyrazole 38—The oil from DCM extraction was purified by column chromatography with 10% EtOAc/hexane. CUR-pyrazole 39—the oil from DCM extraction was washed with hexane to produce a dark-red oil confirmed by NMR to be pure.

General procedure for the synthesis of CUR-isoxazoles of FIG. 43

Hydroxylamine hydrochloride (2 equiv.) was added to a suspension of CUR (1 equiv.) in ethanol (100 mL). Concentrated sulfuric acid (1 mL) was added slowly with efficient stirring and the reaction was setup to reflux and left by TLC (the product shows as a fluorescent spot). Once the reaction had mostly gone to completion, the solvent was removed in vacuo and the reaction was worked up by neutralization and separation as described in the pyrazole procedure. The crude reaction mixture was recrystallized to 25 give the CUR-isoxazoles. They were crystallized from iPrOH except 27 from FIG. 43 which was crystallized from chloroform.

Characterization Data for Compounds in FIGS. 32-35 and

CUR—BF2 adduct (2): Yield 68%, brown solid, Rf 0.43 (40% EtOAc in hexane). 1H NMR (DMSO-d6, 500 MHz): δ 7.97 (d, J=16.0 Hz, 2H), 7.63 (d, J=1.50 Hz, 2H), 7.49 (pseudo-d, 6H), 7.42 (t, J=8.0 Hz, 4H), 7.36 (t, J=7.5 Hz, 2H), 7.12 (s, 2H), 7.18 (d, J=15.9 Hz, 2H) 7.12 (d, J=7.5 Hz, 35 2H), 6.51 (s, 1H), 5.17 (s, 4H), 3.86 (s, 6H). 13C NMR (DMSO-d6, 125 MHz): δ 179.5, 153.3, 148.6, 147.2, 137.2, 128.9, 128.5, 127.5, 125.9, 119.4, 113.3, 112.6, 101.9, 70.4, 56.3. 19F NMR (DMSO-d6, 470 MHz):  $\delta$  –137.9 (s, 11B F), 1392, 1338, 1300, 1280, 1259, 1134, 1060, 1008.

(1E,4E,6E)-5-Hydroxy-1,7-bis(3-benzyloxy-4-methoxyphenyl)hepta-1,4,6-trien-3-one (3): Yield 87%, orange solid, mp 153-155° C., Rf 0.71 (40% EtOAc in hexane). 1H NMR (DMSO-d6, 500 MHz):  $\delta$  16.15 (br, enolic OH), 7.57 (d, 45 J=15.5 Hz, 2H), 7.49-7.47 (overlapping signals/unresolved, 6H), 7.42 (t, J=7.5 Hz, 4H), 7.35 (t, J=7.5 Hz, 2H), 7.29 (d, J=8.5 Hz, 2H), 7.05 (d, J=7.5 Hz, 2H), 6.83 (d, J=16.0 Hz, 2H), 6.10 (s, 1H), 5.16 (s, 4H), 3.82 (s, 6H). 13C NMR (DMSO-d6, 125 MHz): 8 183.7, 151.8, 148.5, 140.8, 137.4, 50 128.9, 128.4, 128.0, 123.8, 122.6, 112.6, 112.5, 101.5, 70.4, 56.5, 56.2. HRMS (ESI): m/z [M+H]+ calcd for C35H33O6: 549.22771; found: 549.23807. IR (cm-1): 3030-2841, 1627, 1593, 1512, 1456, 1512, 1456, 1413, 1338, 1274, 1259, 1226, 1165, 1134.

Curcuminoid-BF2 adduct 4: Yield 79%, brown solid, Rf 0.75 (40% EtOAc in hexane). 1H NMR (DMSO-d6, 500 MHz): δ 7.94 (d, J=15.5 Hz, 2H), 7.65 (d, J=1.5 Hz, 2H), 7.49 (d, J=7.0 Hz, 4H), 7.48-7.41 (m, 6H), 7.38-7.40 (m, J=15.5 Hz, 2H), 6.49 (s, 1H), 5.24 (s, 4H), 5.22 (s, 4H). 13C NMR (DMSO-d6, 125 MHz): δ 179.6, 152.4, 148.9, 147.1, 137.4, 137.1, 128.9, 128.9, 128.4, 128.2, 128.0, 128.0, 127.8, 125.7, 119.6, 114.4, 102.0, 70.5, 70.4. 19F NMR (DMSO-d6, 470 MHz):  $\delta$  –137.8 (s, 11B F), –137.9 (s, 10B F). IR (cm-1): 3026-3007 (CH package), 2358, 1622, 1556, 1504, 1456, 1433, 1306, 1277, 1260, 1136, 1063.

44

(1E,4E,6E)-5-Hydroxy-1,7-bis(3,4-dibenzyloxyphenyl) hepta-1,4,6-trien-3-one (5): Yield 88%, orange solid, mp 150-153° C., Rf 0.92 (40% EtOAc in hexane). 1H NMR (DMSO-d6, 500 MHz): 8 16.25 (br, enolic OH), 7.56 (d, J=15.5 Hz, 2H), 7.49 (d, J=9 Hz, 6H), 7.46 (d, J=7.5 Hz, 4H), 7.41-7.45 (overlapping/unresolved signals, 9H), 7.33 (m, 5H), 7.12 (d, =8J=8.5 Hz, 2H), 6.82 (d, J=15.5 Hz, 2H), 5.76 (s, 1H), 5.21 (s, 8H). 13C NMR (DMSO-d6, 125 MHz): δ 183.6, 150.8, 148.8, 140.7, 137.6, 137.4, 128.9, 128.4, 128.3, 128.1, 128.0, 123.6, 122.8, 114.5, 113.6, 101.6, 70.5, 70.3. HRMS (ESI): m/z [M+H]+ calcd for C47H41O6: 701.29031; found: 701.29706. IR (cm-1): 3034-2989, 2358, 1624, 1591, 1576, 1510, 1454, 1416, 1333, 1277, 1254, 1128, 1001.

Curcuminoid-BF2 adduct 6: Yield: 94%, violet-red solid, mp>240° C. Rf 0.28 (40% EtOAc in hexane). 1H NMR (DMSO-d6, 500 MHz):  $\delta$  8.04 (d, J=16.0 Hz, 2H), 7.64 (d, J=9.0 Hz, 2H), 7.09 (d, J=15.5 Hz, 2H), 6.96 (d, J=9.5 Hz, 2H), 6.55 (s, 1H), 3.91 (s, 6H), 3.89 (s, 6H), 3.77 (s, 6H). for 48 h after which the progress of the reaction was checked 20 13C NMR (DMSO-d6, 125 MHz): δ 179.7, 157.7, 154.1, 142.1, 141.3, 125.4, 120.9, 120.1, 109.2, 102.5, 62.0, 60.9, 56.7. 19F NMR (DMSO-d6, 470 MHz): δ –137.70 (s, 11B F), -137.64 (s, 10B F). IR (cm-1): 3009-2945, 2843, 1607, 1589, 1527, 1489, 1460, 1279, 1156.

(1E,4E,6E)-5-Hydroxy-1,7-bis(2,3,4-trimethoxyphenyl) hepta-1,4,6-trien-3-one (7): Yield: 79%, bright-orange solid, mp 104-106° C. Rf 0.59 (40% EtOAc in hexane). 1H NMR (CDC13, 500 MHz): 8 7.84 (d, J=16.5 Hz, 2H), 7.30 (d, J=9.5 Hz, 2H), 6.71 (d, J=8.5 Hz, 2H), 6.63 (d, J=16 Hz, 30 2H), 5.83 (s, 1H), 3.94 (s, 6H), 3.90 (s, 6H), 3.89 (s, 6H). 13C NMR (CDCl3, 125 MHz): δ 183.6, 155.4, 153.4, 142.4, 135.3, 123.4, 123.2, 122.2, 107.7, 101.3, 61.4, 60.9, 56.1. HRMS (ESI): m/z [M+H]+ calcd for C25H29O8: 457.18624; found: 457.19797. IR (cm-1): 2997-2839, 1620, 1589, 1487, 1454, 1413, 1298, 1134, 1091.

Curcuminoid-BF2 adduct 8: Yield: 91%, black solid, mp >240° C. Rf 0.21 (40% EtOAc in hexane). 1H NMR (DMSO-d6, 500 MHz):  $\delta$  8.22 (d, J=15.5 Hz, 2H), 7.15 (d, J=16.0 Hz, 2H), 6.33 (s, 4H), 6.40 (s, 1H), 3.93 (s, 12H), -138.0 (s, 10B F). IR (cm-1): 3001-2839, 1614, 1537, 1499, 40 3.89 (s, 6H). 13C NMR (DMSO-d6, 125 MHz): δ 179.3, 165.5, 162.6, 136.9, 119.7, 105.8, 102.7, 91.7, 56.7, 56.3.19F NMR (DMSO-d6, 470 MHz): δ –138.29 (s, 11B F), -138.23 (s, 10B F). IR (cm-1): 2920-2848, 1608, 1591, 1541, 1448, 1380, 1300, 1203, 1116.

 $(1E,\!4E,\!6E)\text{-}5\text{-}Hydroxy\text{-}1,\!7\text{-}bis(2,\!4,\!6\text{-}trimethoxyphenyl})$ hepta-1,4,6-trien-3-one (9): Yield: 85%, dark-purple solid, mp: 187-190° C. Rf 0.39 (40% EtOAc in hexane). 1H NMR (DMSO-d6, 500 MHz):  $\delta$  8.05 (d, J=16.0 Hz, 2H), 7.00 (d, J=16.5 Hz, 2H), 6.12 (s, 4H), 5.78 (s, 1H), 3.88 (s, 12H), 3.85 (s, 6H). 13C NMR (DMSO-d6, 125 MHz): δ 184.7, 162.6, 161.2, 131.0, 124.3, 106.6, 101.6, 90.5, 55.7, 55.4. HRMS (ESI): m/z [M+H]+ calcd for C25H29O8: 457.18624; found: 457.19797. IR (cm-1): 2959, 2918, 2849, 1593, 1454, 1317, 1202, 1404, 1155, 1115.

Curcuminoid-BF2 adduct 10: Yield: 74.0%, red-violet solid, mp>240° C. Rf 0.20 (40% EtOAc in hexane). 1H NMR (DMSO-d6, 500 MHz):  $\delta$  8.05 (d, J=16.5 Hz, 2H), 7.26 (s, 4H), 7.20 (d, J=14.5 Hz, 2H), 6.58 (s, 1H), 3.86 (s, 12H), 3.75 (s, 6H). 13C NMR (DMSO-d6, 125 MHz): δ 8H), 7.35-7.31 (m, 4H), 7.18 (d, J=8 Hz, 2H), 7.09 (d, 60 180.0, 153.6, 147.5, 141.5, 130.1, 121.1, 107.8, 102.2, 60.7, 56.6, 19F NMR (DMSO-d6, 470 MHz):  $\delta$  –137.71 (s, 11B F), -137.65 (s, 10B F). IR (cm-1): 3059-2837, 1622, 1564, 1504, 1469, 1504, 1469, 1340.

> (1E,4E,6E)-5-Hydroxy-1,7-bis(3,4,5-trimethoxyphenyl) hepta-1,4,6-trien-3-one (11): Yield: 96.0%, bright-orange solid, mp 181-182° C. Rf 0.47 (40% EtOAc in hexane). 1H NMR (CDC13, 500 MHz): δ 7.49 (d, J=15.5 Hz, 2H), 6.70

(s, 4H), 6.46 (d, J=15.5 Hz, 2H), 5.81 (s, 1H), 3.83 (s, 18H). 13C NMR (CDCl3, 125 MHz): δ 183.1, 153.4, 140.5, 140.0, 130.5, 123.3, 105.2, 101.6, 60.9, 56.1. HRMS (ESI): m/z [M+H]+ calcd for C25H29O8: 457.18624; found: 457.19880. IR (cm-1): 2941, 2836, 1631, 1579, 1501, 1451, 5 1413, 1234, 1120.

Curcuminoid-BF2 adduct 12: Yield 71%, brown solid, Rf 0.22 (40% EtOAc in hexane). 1H NMR (DMSO-d6, 500 MHz): δ 8.05 (d, J=15.5 Hz, 2H), 7.66 (d, J=2.0 Hz, 2H), 7.49 (dd, J=8.0 and 1.5 Hz, 2H), 7.28 (d, J=15.5 Hz, 2H), 10 7.23 (d, J=8.5 Hz, 2H), 6.64 (s, 1H), 3.86 (s, 6H), 2.28 (s, 6H). 19F NMR (DMSO-d6, 470 MHz):  $\delta$  –137.2 (s, 11B F), –137.2 (s, 10B F). 13C NMR (DMSO-d6, 125 MHz): δ 180.5, 168.8, 151.8, 146.8, 142.7, 133.5, 124.1, 123.3, 122.1, 113.7, 102.7, 56.5, 20.9. IR (cm-1): 3011-2848, 1768, 15 1755, 1614, 1544, 1499, 1417, 1361, 1300, 1254, 1207, 1150, 1119, 1055.

(1E,4E,6E)-5-Hydroxy-1,7-bis(4-acetoxy-3-methoxyphenyl)hepta-1,4,6-trien-3-one (13): Yield 80%, orange solid, mp 157-160° C., Rf 0.53 (40% EtOAc in hexane). 1H 20 NMR (CDCl3, 500 MHz): δ 7.60 (d, J=16.0 Hz, 2H), 7.14 (dd, J=8.5 and 2.0 Hz, 2H), 7.10 (d, J=1.8 Hz, 2H), 7.05 (d, J=16.0 Hz, 2H), 5.84 (s, 1H), 3.86 (s, 6H), 2.32 (s, 6H). 13C NMR (CDCl3, 125 MHz): δ 183.1, 168.8, 151.4, 141.3, 139.9, 134.0, 124.3, 123.3, 121.1, 111.5, 101.8, 55.9, 20.7. 25 HRMS (ESI): m/z [M+H]+calcd for C25H25O8: 453.15494; found: 453.15202. IR (cm-1): 3055-2841, 1755, 1628, 1599, 1504, 1411, 1368, 1301, 1250, 1211, 1029.

Curcuminoid-BF2 adduct 14: Yield 33%, yellow solid, Rf=0.64 (40% EtOAc in hexane). 1H NMR (acetone-d6, 30 500 MHz): δ 8.10 (d, J=15.5 Hz, 2H), 7.88 (d, J=7.5 Hz, 2H), 7.84 (s, 2H), 7.65 (t, J=8.0 Hz, 2H), 7.48 (dd, J=8.0 and 1.8 Hz, 2H), 7.28 (d, J=16 Hz, 2H), 6.38 (s, 1H). 19F NMR (acetone-d6, 470 MHz):  $\delta$  –58.6 (s, 6F), –139.6 (s, 11B F), 181.0, 149.6, 145.0, 136.7, 131.0, 128.2, 123.8, 123.3, 121.3, 120.5 (g, 1JCF=256 Hz, OCF3), 102.8. IR (cm-1): 2922, 2360, 1627, 1547, 1275, 1261, 1155, 1057.

(1E,4E,6E)-5-Hydroxy-1,7-bis(3-trifluoromethoxyphemp 68-70° C., Rf 0.79. 1H NMR (CDCl3, 500 MHz): δ 7.63 (d, J=16 Hz, 2H), 7.47 (d, J=9.0 Hz, 2H), 7.43 (t, J=7.0 Hz, 2H), 7.40 (s, 2H), 7.23 (d, J=7.5 Hz, 2H), 6.64 (d, J=16 Hz, 2H), 5.88 (s, 1H). 19F NMR (CDC13, 470 MHz):  $\delta$  –57.8 (s). 13C NMR (CDCl3, 125 MHz): δ 182.9, 149.7, 139.1, 45 137.0, 130.3, 126.6, 125.5, 122.3, 120.4 (q, 1JCF=257 Hz, OCF3), 120.0, 102.3. HRMS (ESI): m/z [M+H]+ calcd for C21H14F6O4: 445.08745; found: 445.09910. IR (cm-1): 3067, 1636, 1582, 1435, 1323, 1265, 1123.

0.87 (40% EtOAc in hexane). 1H NMR (acetone-d6, 500 MHz): δ 8.07 (d, J=16.0 Hz, 2H), 7.99 (m, 4H), 7.45 (d, J=7.5 Hz, 4H), 7.18 (d, J=16.0 Hz, 2H), 6.59 (s, 1H). 19F NMR (acetone-d6, 470 MHz):  $\delta$  –58.4 (s, 6F), –139.7 (s, 11B F), -139.7 (s, 10B F). 13C NMR (CDCl3, 125 MHz): 55 Hz, 1H), 6.65 (d, J=4.0 Hz, 1H), 6.63 (d, J=4.0 Hz, 1H), 3.90  $\delta$  180.9, 151.1, 145.0, 133.4, 131.3, 122.4, 121.4, 120.4 (q, 1JCF=257.0 Hz, OCF3), 102.5. IR (cm-1): 3117-2922, 1628, 1558, 1506, 1400, 1215, 1163, 1055, 1001.

(1E,4E,6E)-5-Hydroxy-1,7-bis(4-trifluoromethoxyphenvl)hepta-1,4,6-trien-3-one (17): Yield 94%, fluffy yellow 60 solid, mp 108-111° C., Rf 0.94 (40% EtOAc in hexane). 1H NMR (acetone-d6, 500 MHz): δ 7.88 (m, 4H), 7.73 (d, J=16.0 Hz, 2H), 7.42 (d, J=8.0 Hz, 4H), 6.95 (d, J=15.5 Hz, 2H), 6.17 (s, 1H). 19F NMR (acetone-d6, 470 MHz)  $\delta$  –58.5 (s). 13C NMR (CDC13 and acetone-d6, 125 MHz):  $\delta$  183.0, 65 150.3, 139.0, 133.6, 133.5, 129.5, 124.8, 121.2, 120.4 (q, 1JCF=257 Hz, OCF3), 102.1. HRMS (ESI): m/z [M+H]+

46

calcd for C21H15F6O4: 445.08747; found: 445.09909. IR (cm-1): 3048-2853, 1628, 1585, 1506, 1420, 1278, 1244, 1213, 1141 1109.

Curcuminoid-BF2 adduct 18: Yield 48%, yellow solid, Rf 0.91 (40% EtOAc in hexane), 1H NMR (DMSO-d6, 500 MHz): δ 8.11 (d, J=16.0 Hz, 2H), 8.02 (d, J=8.5 Hz, 4H), 7.83 (d, J=8.5 Hz, 4H), 7.40 (d, J=16.0, 4H), 6.74 (s, 1H). 19F NMR (DMSO-d6, 470 MHz):  $\delta$  –41.4 (s, 6F), –136.6 (s, 11B F), -136.6 (s, 10B F). 13C NMR (DMSO-d6, 125 MHz): δ 180.8, 145.7, 137.1, 136.8, 131.0, 129.9 (q, 1JCF=308 Hz, SCF3), 126.9, 124.3, 103.6. IR (cm-1): 3005-2870, 2361, 2342, 1625, 1562, 1523, 1408, 1277, 1260, 1152, 1105, 1080, 1056.

(1E,4E,6E)-5-Hydroxy-1,7-bis(4-trifluoromethylthiophenyl)hepta-1,4,6-trien-3-one (19): Yield 93%, yellow solid, m.p 128-130° C. Rf 0.93 (40% EtOAc in hexane). 1H NMR (CDCl3, 500 MHz): 8 7.67 (d, J=8 Hz, 4H), 7.65 (d, J=15.5 Hz, 2H), 7.58 (d, J=15.5 Hz, 4H), 6.68 (d, J=15.5 Hz, 2H), 5.88 (s, 1H), 19F NMR (CDCl3, 470 MHz):  $\delta$  –42.3 (s, 6F). 13C NMR (CDCl3, 125 MHz): δ 182.9, 139.1, 137.3, 136.5, 129.4 (q, 1JCF=308 Hz, SCF3), 128.8, 126.1, 126.0, 102.5. HRMS (ESI): m/z [M+H]+ calcd for C21H15F6O2S2: 477.04177; found: 477.05480. IR (cm-1): 3005-2990, 1630, 1566, 1521, 1404, 1275, 1260, 1167, 1103, 1082, 1049.

Curcumin-BF2 adduct 20: Yield: 57.0%, yellow solid, mp>240° C. Rf 0.56 (40% EtOAc in hexane). 1H NMR (DMSO-d6, 500 MHz): δ 7.99 (d, J=16.0 Hz, 2H), 7.88 (m, 2H), 7.51 (m, 2H), 7.31 (d, J=16.0 Hz, 2H), 6.89 (s, 1H). 19F NMR (DMSO-d6, 470 MHz):  $\delta$  –128.8 (m, 2F), –134.7 (m, 2F), -136.5 (s, 11B F), -136.6 (s, 10B F), -160.3 (m, 2F). IR (cm-1): 2953-2848, 1625, 1597, 1552, 1512, 1479, 1467, 1303, 1159, 1138, 1061.

(1E,4E,6E)-5-Hydroxy-1,7-bis(2,3,4-trifluorophenyl) -139.6 (s, 10B F). 13C NMR (acetone-d6, 125 MHz): δ 35 hepta-1,4,6-trien-3-one (21): Yield: 93.0%, yellow solid, mp: 156-158° C. Rf 0.89 (40% EtOAc in hexane). 1H NMR (DMSO-d6, 500 MHz):  $\delta$  7.68 (d, J=15.5 Hz, 2H), 7.88 (m, 2H), 7.51 (m, 2H), 7.31 (d, J=16.0 Hz, 2H), 6.89 (s, 1H). 19F NMR (DMSO-d6, 470 MHz):  $\delta$  –128.8 (m, 2F), –134.7 (m, nyl)hepta-1,4,6-trien-3-one (15): Yield 73%, yellow solid, 40 2F), -136.5 (s, 11B F),-136.6 (s, 10B F),-160.3 (m, 2F). 13C NMR (CDCl3, 125 MHz): δ 182.7, 152.0 (ddd, 1JCF=256 Hz, 2JCF=10 Hz, 3JCF=2.9 Hz), 150.4 (ddd, 1JCF=256 Hz, 2JCF=10 Hz, 3JCF=3.0 Hz), 140.4 (td, 1JCF=253 Hz, 2JCF=15.2 Hz), 131.8, 127.2 (m), 123.1 (m), 120.8 (m), 112.7 (m), 102.5. HRMS (ESI): m/z [M+H]+ calcd for C19H11F6O2: 385.06632; found: 385.07822. IR (cm-1): 2955-2851, 1625, 1597, 1508, 1464, 1303, 1298, 1132, 1036.

3,5-bis-(6-Fluoro-3,4-dimethoxystyryl)-1-phenylpyra-Curcuminoid-BF2 adduct 16: Yield 17%, yellow solid, Rf 50 zole (22): Yield 85%, pale yellow solid, mp 142-144° C., Rf 0.55 (40% EtOAc in hexane). 1H NMR (CDC13, 500 MHz): δ 7.53 (m, 4H), 7.42 (m, 1H), 7.32 (d, J=16.0 Hz, 1H), 7.22 (d, J=16.5 Hz, 1H), 7.13 (d, J=16.5 Hz, 1H), 7.09 (d, J=7.0 Hz, 1H), 6.92 (s, 1H), 6.85 (d, J=7.0 Hz, 1H), 6.82 (d, J=16.0 (s, 3H), 3.88 (s, 3H), 3.88 (s, 3H), 3.84 (s, 3H). 19F NMR (CDC13, 470 MHz)  $\delta$  -123.3 (dd, J=11.3 and 6.5 Hz, 1F),-124.9 (dd, J=11.8 and 6.6 Hz, 1F). 13C NMR (CDCl3, 125 MHz) δ 155.3 (d, 1JCF=245.0 Hz), 154.9 (d, 1JCF=244.0 Hz), 151.4, 150.2 (d, JCF=9.5 Hz), 149.6 (d, JCF=10.4 Hz), 145.5, 142.6, 139.4, 129.2, 128.0, 125.2, 124.9 (d, JCF=2.9 Hz), 122.7 (d, JCF=2.8 Hz), 120.1 (d, JCF=3.9 Hz), 116.0 (d, JCF=13.3 Hz), 115.5 (d, JCF=5.7 Hz), 115.4, 115.3, 109.0 (d, JCF=5.8 Hz), 108.0 (d, JCF=4.8 Hz), 100.7, 100.3 (d, JCF=20.1 Hz), 100.0 (d, JCF=20.0 Hz), 56.5, 56.3, 56.2, 56.2. HRMS (ESI): m/z [M+H]+ calcd for C29H27F2N2O4: 505.19389; found: 505.19228. IR

(cm-1) 3057-2833, 1616, 1597, 1506, 1464, 1440, 1408, 1379, 1356, 1318, 1274, 1234, 1209, 1192, 1171, 1105.

3,5-bis-(6-Fluoro-3,4-dimethoxystyryl)-1-(4-trifluoromethoxyphenyl)pyrazole (23): Yield: 42.0%, Yellowbrown solid, mp 80-83° C., Rf=0.74 (40% EtOAc/Hexane). 5 1H NMR (CDCl3, 500 MHz): δ 7.60 (d, with additional unresolved splitting, J=8.5 Hz, 2H), 7.37 (d, J=8.5 Hz, 2H), 7.32 (d, J=16.5 Hz, 1H), 7.21 (d, J=16.5 Hz, 1H), 7.11 (d, J=16.5 Hz 1H), 7.08 (d, J=3.0 Hz, 1H), 6.91 (s, 1H), 6.85 (d. J=6.5~Hz,~1H),~6.79~(d,~J=16.0~Hz,~1H),~6.65~(d,~J=12.0~Hz,~102H), 3.90 (s, 3H), 3.89 (s, 6H), 386 (s, 3H). 19F NMR (CDCl3, 470 MHz):  $\delta$  -57.9 (s, 3F), -123.0 (dd, J=6.6 Hz and 10.8 Hz, 1F), -124.7 (dd, J=6.6 Hz and 11.8 Hz, 1F). 13C NMR (CDCl3, 125 MHz) δ 155.4 (d, J=245 Hz), 154.9 (d, 1JCF=244 Hz), 151.7, 150.4 (d, JCF=9.5 Hz), 149.7 (d, 15 JCF=9.5 Hz), 148.4, 145.5 (q, JCF=1.9 Hz), 142.7, 138.0, 126.4, 125.6 (d, JCF=1.9 Hz), 123.1 (d, JCF=2.9 Hz), 121.7, 120.4 (q, JCF=259 Hz, OCF3), 119.8 (d, JCF=4.7 Hz), 115.8 (d, JCF=13.3 Hz), 115.2, 115.1 (d, JCF=5.8 Hz), 109.8 (d, JCF=4.7), 108.1 (d, JCF=4.7 Hz), 101.2, 100.4, 100.2 (d, 20 JCF=3.9 Hz) 100.0, 56.5, 56.3, 56.2, 56.2. HRMS (ESI): m/z [M+H]+ calculated for C30H26F5O5N2: 589.17619; found: 589.15726. IR (cm-1): 3078-2835, 1616, 1506, 1464, 1454, 1358, 1254-1107 (unresolved bands).

3,5-bis-(6-Fluoro-3,4-dimethoxystyryl)-1-(3-trifluoromethylphenyl)pyrazole (24): Yield 60%, pale yellow solid, mp 130-134° C., Rf 0.65 (40% EtOAc in hexane). 1H NMR (CDC13, 500 MHz): 8 7.87 (s, 1H), 7.78 (m, 1H), 7.67 (m, 2H), 7.33 (d, J=17.0 Hz, 1H), 7.24 (d, J=16.5 Hz, 1H), 7.11 (d, J=17.0 Hz, 1H), 7.09 (s, 1H), 6.94 (s, 1H), 6.85 (d, J=6.5 30 Hz, 1H), 6.82 (d, J=16.5 Hz, 1H), 6.67 (d, J=1.0 Hz, 1H), 6.64 (d, J=1.5 Hz, 1H), 3.91 (s, 3H), 3.89 (s, 3H), 3.89 (s, 3H), 3.86 (s, 3H). 19F NMR (CDC13, 470 MHz):  $\delta$  -62.7 (s, 3F), -123.3 (dd, J=11.2 and 6.6 Hz, 1F),-124.7 (dd, J=11.8 and 7.1 Hz, 1F). 13C NMR (CDC13, 125 MHz): δ 155.4 (d, 35 1JCF=245 Hz), 155.0 (d, 1JCF=244 Hz), 152.1, 150.5 (d, 2JCF=9.5 Hz), 149.8 (d, 2JCF=9.5 Hz), 145.6 (d, JCF=2.9 Hz), 145.5 (d, JCF=1.9 Hz), 142.8, 139.9, 131.8 (q, 2JCF3=33.4 Hz), 129.9, 128.1, 125.7 (d, JCF=1.9 Hz), 123.4 (d, JCF=3.9 Hz), 123.6 (q, 1JCF3=272.7 Hz), 121.1 40 (q, JCF=3.9 Hz), 119.6 (d, JCF=4.8 Hz), 115.7 (d, 2JCF=13.3 Hz), 115.1 (d, 2JCF=12.4 Hz), 114.8 (d, JCF=6.7 Hz), 108.6 (d, JCF=4.8 Hz), 108.0 (d, JCF=4.8 Hz), 101.4, 100.3 (d, JCF=22.0 Hz), 100.1 (d, JCF=21.0 Hz), 56.3, 56.3, 56.2, 56.2. HRMS (ESI): m/z [M+H]+ calcd for 45 C30H26F5N2O4: 573.18127; found: 573.19228. IR (cm-1): 3071-2839, 1613, 1504, 1450, 1373, 1273, 1172, 1126, 1103, 1072, 1033.

3,5-bis-(6-Fluoro-3,4-dimethoxystyryl)-1-(3,5-difluorophenyl) pyrazole (25): Yield: 53%, Mustard yellow solid, 50 mp 115-117° C., Rf 0.66 (40% EtOAc/Hexane). 1H NMR (ĈDCl3, 500 MHz): δ 7.31 (d, J=16.5 Hz, 1H), 7.22 (d, J=16.5 Hz, 1H), 7.16 (dd, J=7.7 Hz and 2.5 Hz, 2H), 7.07 (d, J=16.5 Hz, 1H), 7.07 (d, J=7.5 Hz, 1H), 6.89-6.83 (unre-1H), 3.91 (s, 3H), 3.90 (s, 3H), 3.89 (s, 3H), 3.88 (s, 3H). 19F NMR (CDCl3, 470 MHz): δ –107.7 (t appearance, J=8.5 Hz, 2F), -122.9 (dd, J=6.7 Hz and 5.2 Hz, 1F), -124.6(dd, J=7.1 Hz and 4.7 Hz, 1F). 13C NMR (CDCl3, 125 MHz): δ 163.0 (d, 1JCF=249 Hz), 162.9 (d, 1JCF=250 Hz), 60 156.4, 155.9, 154.5, 154.0, 152.1, 150.5 (d, JCF=10.6 Hz), 149.8 (d, JCF=10.4 Hz), 145.6 (d, J=2.9 Hz), 145.5 (d, J=2 Hz) 142.8, 141.5 (t, 3JCF=12.3 Hz), 126.1 (d, JCF=1.9 Hz), 123.5 (d, JCF=2.9 Hz), 119.5 (d, JCF=4.8 Hz), 115.7 (d, JCF=13.0 Hz), 115.0, 114.9, 109.2 (d, JCF=4.7 Hz), 108.2, 65 108.1, 108.0 (d, JCF=7.7 Hz), 103.0 (t, 2JCF=24.6 Hz), 101.9, 100.2 (t, 2JCF=28.6 Hz), 56.5, 56.3, 56.2, 56.1.

48

HRMS (ESI): m/z [M+H]+ calculated for C29H25N2O4F4: 541.17505; found: 541.15787. IR (cm-1): 3053-2986, 1620, 1512, 1466, 1360, 1325, 1263, 1194, 1123.

3,5-bis-(6-Fluoro-3,4-dimethoxystyryl)-1-(4-cyanophenyl)pyrazole (26): Yield: 81%, yellow solid. mp 91-93° C., Rf 0.61 (40% EtOAc/Hexane). 1H NMR (CDC13, 500 MHz): δ 7.8 (d, J=8.5 Hz, 2H), 7.72 (d, J=8.5 Hz, 2H), 7.32 (d, J=16.5 Hz, 1H), 7.22 (d, J=16.5 Hz, 1H), 7.08 (d, J=17.0 Hz, 1H), 7.08 (s, 1H), 6.92 (s, 1H), 6.86 (s, 1H), 6.83 (d, J=16.5 Hz, 1H), 6.66 (dd, J=6.0 Hz and 11.7 Hz, 2H), 3.91 (s, 3H), 3.90 (s, 3H), 3.89 (s, 3H), 3.87 (s, 3H). 19F NMR (CDC13, 470 MHz):  $\delta$  –122.6 (dd, J=6.6 Hz and 12.5 Hz, 1F), -124.6 (dd, J=8.5 Hz and 11.5 Hz, 1F). 13C NMR (CDCl3, 125 MHz): δ 155.5 (d, 1JCF=245 Hz), 155.0 (d, 1JCF=244 Hz), 152.6, 150.6 (d, J=9.5 Hz), 149.9 (d, J=10.4 Hz), 145.6 (d, JCF=1.8 Hz and 4.7 Hz), 145.60 (d, J=4.7 Hz), 142.9, 133.3, 126.4, 124.8, 123.8 (d, J=2.9 Hz), 119.4 (d, J=4.6 Hz), 118.2, 115.6 (d, J=13.0 Hz), 115.0 (d, J=7.5 Hz), 114.9 (d, J=13.3 Hz), 110.9, 109.4 (d, J=4.7 Hz), 108.1 (d, J=4.7 Hz), 102.5, 100.4, 100.2 (d, J=3.7 Hz), 100.0, 56.6, 56.3, 56.7, 56.2. HRMS (ESI): m/z [M+H]+ calcd. for C30H26O4F2N3: 530.18914; found 530.19228. IR (cm-1): 3055-2835, 2227, 1605, 1335, 1506, 1450, 1410, 1337, 1360, 1313, 1275, 1103, 1033.

3,5-bis-(6-Fluoro-3,4-dimethoxystyryl)-isoxazole Yield 60%, pale yellow solid, mp 158-160° C., Rf 0.55 (40%) EtOAc in hexane). 1H NMR (acetone-d6, 500 MHz): δ 7.45 (d, J=16.5 Hz, 1H), 7.40 (d, J=17.0 Hz, 1H), 7.35 (d, J=7.0 Hz, 1H), 7.33 (d, J=6.5 Hz, 1H), 7.18 (d, J=16.5 Hz, 1H), 7.16 (d, J=17.0 Hz, 1H), 6.91 (s, 1H), 6.87 (d, J=9.5 Hz, 1H), 6.86 (d, J=9.5 Hz, 1H), 3.91 (s, 3H), 3.90 (s, 3H), 3.89 (s, 6H). 19F NMR (CDCl3, 470 MHz)  $\delta$  –122.2 (dd, J=11.8 and 5.7 Hz, 1F), -124.0 (dd, J=11.8 and 8.5 Hz, 1F). 13C NMR (acetone-d6, 125 MHz): 8 168.6, 162.3, 155.6 (d, 1JCF=244.0 Hz), 155.3 (d, 1JCF=244.0 Hz), 151.7 (d, JCF=10.6 Hz), 151.4 (d, JCF=10.6 Hz), 146.3 (d, JCF=1.9 Hz), 127.6 (d, JCF=2.9 Hz), 126.4 (d, JCF=3.8 Hz), 115.8 (d, JCF=4.8 Hz), 114.6 (d, JCF=12.4 Hz), 114.3, 114.2, 113.1 (d, JCF=5.7 Hz), 109.4 (d, JCF=4.8 Hz), 109.2 (d, JCF=4.8 Hz), 100.4 (d, JCF=9.5 Hz), 100.1 (d, JCF=10.4 Hz), 98.2, 55.8 (2 OMe), 55.6, 55.6. HRMS (ESI): m/z [M+H]+ calcd for C23H22F2NO5: 430.14660; found: 430.15628. IR (cm-1): 3061-2837, 1643, 1618, 1510, 1464, 1440, 1414, 1369, 1310, 1279, 1211, 1192, 1105.

3,5-bis-(4-Trifluoromethylthiostyryl)-1-phenylpyrazole (28): Yield 30%, pale yellow solid, mp 119-121° C., Rf 0.94 (40% EtOAc in hexane). 1H NMR (acetone-d6, 500 MHz): δ 7.79-7.68 (unresolved overlapping signals, 7H), 7.62 (d, J=4.0 Hz, 4H). 7.53 (m, 1H), 7.40 (d, J=16.5 Hz, 1H), 7.39 (d, J=16.5 Hz, 1H), 7.36 (d, J=17.0 Hz, 1H), 7.23 (s, 1H), 7.19 (d, J=16.5 Hz, 1H). 19F NMR (acetone-d6, 470 MHz): δ -43.8 (s, 3F), -43.9 (s, 3F). 13C NMR (CDCl3, 125 MHz): δ 150.6, 142.0, 140.4, 139.7, 139.6, 136.7, 136.7, 130.6, 129.9 (q, 1JCF3=308.1 Hz), 129.8 (q, 1JCF3=307.1 solved m, 4H), 6.67 (d, J=6.5 Hz, 1H), 6.64 (d, J=7.0 Hz, 55 Hz), 129.4, 128.7, 128.1, 127.9, 127.6, 125.2, 123.3, 122.9, 122.2, 118.0, 102.3. HRMS (ESI): m/z [M+H]+ calcd for C27H19F6S2N2: 549.08938; found 549.08770. IR (cm-1): 3047, 1597, 1535, 1497, 1404, 1373, 1319, 1265, 1157, 1080.

> 3,5-bis-(4-trifluoromethylthiostyryl)-1-(3-trifluoromethylphenyl)pyrazole (29): Yield: 30%, pale yellow solid, mp 121-122° C., Rf 0.95 (40% EtOAc in hexane). 1H NMR (CDC13, 500 MHz):  $\delta$  7.88 (s, 1H), 7.74-7.64 (unresolved, 7H), 7.57 (d, J=8.5 Hz, 2H), 7.46 (d, J=9.0 Hz, 2H), 7.24 (pseudo-s, 2H), 7.17 (d, J=16.0 Hz, 1H), 6.96 (s, 1H), 6.92 (d, J=16.5 Hz, 1H). 19F NMR (CDC13, 470 MHz):  $\delta$  -42.6 (s, 3F), -42.7 (s, 3F), -62.7 (3F). 13C NMR (CDCl3, 125

MHz): δ 151.3, 142.0, 139.7, 139.4, 138.6, 136.7, 136.7, 132.2 (q, JCF=33.4 Hz), 131.7, 130.8, 130.7, 130.0, 129.8, 128.2, 127.5, 127.4, 124.9 (q, JCF=3.8 Hz), 124.3 (unresolved q), 124.8 (unresolved q), 124.3 (unresolved q), 122.3 (q, JCF=3.9 Hz), 122.2, 116.9, 102.6. HRMS (ESI): m/z 5 [M+H]+ calcd for C28H18F9S2N2: 617.07677; found 617.08770. IR (cm-1) 3065-3036, 1910, 1593, 1537, 1495, 1468, 1375, 1333, 1111, 1013.

3,5-bis-(4-Trifluoromethylthiostyryl)-isoxazole Yield 41%, yellow needle like crystals, mp 165-167° C., Rf 10 0.95 (40% EtOAc in hexane). 1H NMR (CDC13, 500 MHz): δ 7.69 (d, J=7.0 Hz, 4H), 7.58 (d, J=8.5 Hz, 4H), 7.38 (d, J=16.5 Hz, 1H), 7.23 (d, J=15.0 Hz, 1H), 7.19 (d, J=15.5 Hz, 1H), 7.04 (d, J=16.5 Hz, 1H), 6.56 (s, 1H). 19F NMR (CDCl3, 470 MHz)  $\delta$  –42.5 (s, 3F), –42.5 (s, 3F). 13C NMR 15 (CDCl3, 125 MHz) δ 167.9, 161.6, 138.3, 137.9, 136.7, 134.3, 133.5, 129.5 (q, 1JCF3=310.0 Hz), 127.9, 127.8, 125.0, 124.7, 118.3, 114.9, 99.5. HRMS (ESI): m/z [M+H]+ calcd for C21H14F6S2NO: 474.04210; found: 474.05261. IR (cm-1): 2922, 1637, 1591, 1588, 1510, 1492, 1421, 1155, 20 421, 13279.; found: 421, 08770. IR (cm-1): 3048, 2338,

3,5-bis-(4-Fluorostyryl)-1-phenylpyrazole (31): Yield: 55%, light yellow solid, mp 109-111° C. Rf 0.91 (40% EtOAc in hexane). 1H NMR (CDCl3, 500 MHz): δ 7.54-7.37 (unresolved 9H), 7.20 (d, J=17.0 Hz, 1H), 7.13-7.03 25 (complex m, 6H), 7.11 (d, J=16.5 Hz, 1H), 7.10 (d, J=16.0 Hz, 1H), 7.07 (d, J=10.0 Hz, 1H), 7.05 (d, J=10.0 Hz, 2H), 6.86 (s, 1H), 6.80 (d, J=16.0 Hz, 1H). 19F NMR (CDC13, 470 MHz): δ -112.6 (m, 1F), -113.8 (m, 1F). 13C NMR (CDCl3, 125 MHz): δ 162.8 (d, 1JCF=248 Hz), 162.5 (d, 30 1JCF=248 Hz), 151.0, 142.2, 139.3, 133.2 (d, J=3.8 Hz), 132.5 (d, J=3.7 Hz), 131.2, 129.6, 129.3, 128.3, 128.3, 128.1, 128.1, 128.0, 125.4, 120 (d, J=2.0 Hz), 115.9, 115.9, 115.8, 115.7, 115.6, 115.2 (d, J=2.9 Hz), 101.0. HRMS (ESI): m/z [M+H]+ calcd for C25H19N2F2: 385.15163; 35 found: 385.15430. IR (cm-1): 3066, 3042, 1713, 1597, 1533, 1504, 1458, 1375, 1225, 1157.

3,5-bis-(4-Fluorostyryl)-1-(4-trifluoromethoxyphenyl) pyrazole (32): Yield: 37%, light-brown solid, mp 155-156° C. Rf 0.95 (40% EtOAc in hexane). 1H NMR (CDC13, 500 40 MHz): δ 7.57-7.55 (m, 2H), 7.50-7.46 (m, 2H), 7.41-7.38 (m, 4H), 7.18 (d, J=16.5 Hz, 1H), 7.11 (d, J=16.5 Hz, 1H), 7.04-7.08 (m, 5H), 6.84 (s, 1H), 6.75 (d, J=16.5 Hz, 1H). 19F NMR (CDCl3, 470 MHz):  $\delta$  –57.9 (q, 3F), –112.3 (m, 1F), -113.7 (m, 1F). 13C NMR (CDC13, 125 MHz): δ 162.8 45 (d, 1JCF=248 Hz), 162.5 (1JCF, J=248 Hz), 151.4, 148.5 (d, J=2.0 Hz), 142.3, 137.9, 133.1 (d, J=3.7 Hz), 132.4 (d, J=2.7 Hz), 131.8, 129.9, 128.3 (d, J=37.0 Hz), 128.2 (d, J=37.0), 126.6, 121.8, 120.4 (q, 1JCF=257.5 Hz), 119.8 (d, J=2 Hz), 116.0, 115.8 (d, J=3.7 Hz), 115.6, 114.7 (d, J=2.9 Hz), 101.4. 50 HRMS (ESI): m/z [M+H]+ calcd for C26H18N2F5O: 469.13393.; found: 469.12278. IR (cm-1): 3040, 2924, 1597, 1534, 1504, 1373, 1258, 1211, 1157, 1103, 1011.

3,5-bis-(4-Fluorostyryl)-1-(3-trifluoromethylphenyl) 98-100° C. Rf 0.92 (40% EtOAc in hexane). 1H NMR (CDCl3, 500 MHz): δ 7.88 (s, 1H), 7.74-7.64 (m, 3H), 7.51 (dd, J=9.0 and 5.5 Hz, 2H), 7.40 (dd, J=9.0 and 5.5 Hz, 2H), 7.21 (d, J=16.5 Hz, 1H), 7.13 (d, J=16.5 Hz, 1H), 7.12-7.05 (m, 5H), 6.88 (s, 1H), 6.77 (d, J=16.0 Hz, 1H). 19F NMR 60 (CDCl3, 470 MHz): δ –62.7 (q, 3F), –112.2 (m, 1F), –113.6 (m, 1F). 13C NMR (CDCl3, 125 MHz): δ 162.8 (d, J=248.0 Hz), 162.5 (d, J=248.0 Hz), 151.7, 142.3, 139.8, 133.0 (d, JCF=3.7 Hz), 132.3 (d, J=2.5 Hz), 132.2, 130.1, 129.9, 128.4, 128.3, 128.2, 128.1, 128.0, 124.5 (q, JCF=3.9 Hz), 65 123.5 (q, 1JCF3=273 Hz), 122.2 (q, JCF=3.7 Hz), 119.7, 116.0, 115.9, 115.8, 115.6, 114.5 (d, J=2.0 Hz), 101.5.

HRMS (ESI): m/z [M+H]+ calcd for C26H18N2F5: 453.13901.; found: 453.12278. IR (cm-1): 3068, 3041, 1599, 1537, 1506, 1467, 1454, 1337, 1332, 1226, 1157, 1122, 1069.

3,5-bis-(4-Fluorostyryl)-1-(3,4-difluorophenyl)pyrazole (34): Yield: 51%, light-yellow solid, mp 169-170° C. Rf 0.95 (40% EtOAc in hexane). 1H NMR (CDC13, 500 MHz): δ 7.50-7.47 (m, 2H), 7.44-7.41 (m, 2H), 7.18 (d, J=16.5 Hz, 1H), 7.14-7.00 (m, 8H), 6.88 (td, J=9 Hz and 2 Hz, 1H), 6.84 (s, H), 6.81 (d, J=16.0, 1H). 19F NMR (CDC13, 470 MHz):  $\delta$  –107.4 (m, 2F), –112.0 (m, 1F), –113.5 (m, 1F). 13C NMR (CDC13, 125 MHz): δ 163.1, (d, 1JCF=250 Hz), 163.0 (d, 1JCF=250 Hz), 162.9 (d, 1JCF=250 Hz), 162.6 (d, 1JCF=250 Hz), 151.7, 142.4, 141.2 (t, 3JCF=13.8 Hz), 132 (d, JCF=3.7 Hz), 132.3, 132.2 (d, JCF=2.9 Hz), 130.4, 128.4 (d, JCF=7.7 Hz), 128.1 (d, JCF=8.5 Hz), 119.5 (d, JCF=2 Hz), 116.0, 115.9, 115.8, 115.7, 114.4 (d, JCF=1.8 Hz), 108.5, 108.4, 108.3, 108.2, 103.3 (t, 2JCF=25.7 Hz), 102.2. HRMS (ESI): m/z [M+H]+ calcd for C25H17N2F4: 1883, 1604, 1504, 1481, 1334, 1227, 1157, 1119.

3,5-bis-(4-Fluorostyryl)-1-(4-cyanophenyl)pyrazole (35): Yield: 52%, light-brown solid, mp 209-211° C. Rf 0.89 (40% EtOAc in hexane). 1H NMR (DMSO, 500 MHz): δ 8.03 (dt, J=9.0 and 2.5 Hz, 2H), 7.76 (dt, J=9.0 and 2.5 Hz, 2H), 7.69-7.62 (m, 4H), 7.33 (d, J=16.5 Hz, 1H), 7.31 (d, J=16.5 Hz, 1H), 7.23-7.19 (m, 5H), 7.16 (d, J=16.5 Hz, 1H), 7.01 (d, J=16.5 Hz, 1H). 19F NMR (DMSO, 470 MHz):  $\delta$ -112.7 (m, 1F), -113.6 (m, 1F). 13C NMR (DMSO, 125 MHz): δ 162.6 (d, 1JCF=246 Hz), 162.3 (d, 1JCF=245 Hz), 152.1, 142.9, 134.2, 134.1, 133.5, 133.0, 132.7, 130.6, 129.5 (d, J=8.5 Hz), 129.0 (d, J=8.5 Hz), 125.4, 124.3, 120.2, 118.8, 116.2 (d, J=6.8 Hz), 116.1 (d, J=6.6 Hz), 115.3, 110.3, 103.4. HRMS (ESI): m/z [M+H]+ calcd for C26H18N3F2: 410.14688.; found: 410.15787. IR (cm-1): 3030-3008, 2227, 1600, 1537, 1504, 1373, 1225, 1157.

3,5-bis-(4-Fluorophenylstyryl)-isoxazole (36): Yield: 42%, white solid, mp 158-160° C., Rf 0.93 (40% EtOAc in hexane). 1H NMR (CDC13, 500 MHz): δ 7.53-7.50 (m, 4H), 7.33 (d, J=16.5 Hz, 1H), 7.15 (d, J=16.5 Hz, 1H), 7.12-7.07 (m, 4H), 7.05 (d, J=17.0 Hz, 1H), 6.89 (d, J=16.0 Hz, 1H), 6.48 (s, 1H). 19F NMR (CDC13, 470 MHz):  $\delta$  –111.4 (m, 1F), -111.9 (m, 1F). 13C NMR (CDCl3, 125 MHz): δ 168.1, 163.2 (d, 1JCF=250 Hz), 163.0 (d, 1JCF=250 Hz), 161.9, 134.5, 133.7, 132.0 (d, JCF=4.0 Hz), 131.7 (d, JCF=3.9 Hz), 128.9, 128.8, 128.7, 128.6, 116.1, 116.0, 115.9, 115.8, 115.7, 112.7 (d, J=1.9 Hz), 98.4. HRMS (ESI): m/z [M+H]+ calcd for C19H14ONF2: 310.10435.; found: 310.12278. IR (cm-1): 1651, 1593, 1564, 1508, 1433, 1232, 1159.

3,5-bis-(4-Trifluoromethylstyryl)-1-phenylpyrazole (37): Yield: 39%, mp 137-139° C. Rf 0.93 (40% EtOAc in hexane). 1H NMR (CDC13, 500 MHz): δ 7.62-7.47 (unresolved m, 13H), 7.30 (d, J=17 Hz, 1H), 7.24 (d, J=17.0 Hz, 1H), 7.16 (d, J=17.0 Hz), 6.97 (d, J=16.8 Hz), 6.95 (s, 1H). pyrazole (33): Yield: 33%, light orange-brown solid, mp 55 19F NMR (CDCl3, 470 MHz): δ -62.4 (s, CF3), -62.6 (s, CF3). 13C NMR (CDC13, 125 MHz): δ 150.6, 141.8, 140.5, 139.7, 139.2, 130.8, 130.1 (q, J=32.5 Hz), 129.3 (q, J=33.0 Hz), 129.4, 129.2, 128.4, 126.8, 126.6, 125.4, 123.1, 123.0, 122.7, 117.7, 101.9. HRMS (ESI): m/z [M+H]+ calcd for C27H19N2F6: 485.14524 found: 485.15710. IR (cm-1): 3067, 3043, 1614, 1597, 1501, 1458, 1408, 1319, 1161, 1107, 1064, 1014.

> 3,5-bis-(2,3,4-Trimethoxy-styryl)-1-phenylpyrazole (38): Yield: 52%, light orange oil, Rf 0.60 (40% EtOAc in hexane). 1H NMR (CDCl3, 500 MHz): δ 7.55-7.48 (m, 4H), 7.42-7.40 (m, 2H), 7.33 (d, J=8.5 Hz, 1H), 7.32 (d, J=16.4 Hz, 1H), 7.14 (d, J=16.5 Hz, 1H), 7.13 (d, J=9 Hz, 1H), 6.94

(s, 1H), 6.88 (d, J=16.5 Hz, 1H), 6.73 (d, J=8.5 Hz, 1H), 6.67 (d, J=8.5 Hz, 1H), 3.95 (s, 3H), 3.91 (s, 3H), 3.91 (s, 3H), 3.89 (s, 6H), 3.87 (s, 3H). 13C NMR (CDCl3, 125 MHz): δ 153.9, 153.4, 152.0, 151.9, 151.8, 143.0, 142.5, 142.4, 139.6, 129.2, 127.8, 127.0, 125.4, 125.0, 124.3, 123.5, 121.4, 120.9, 119.8, 114.9, 107.9, 107.7, 100.4, 61.4, 61.3, 60.9, 56.1. HRMS (ESI): m/z [M+H]+ calcd for C31H33N2O6: 529.23386; found: 529.22805. IR (cm-1): 3044-2837, 1713, 1593, 1533, 1495, 1456, 1406, 1371, 1096, 1042, 1007.

3,5-bis-(2,3,4-Timethoxy-styryl)-1-(4-trifluoromethoxyphenyl) pyrazole (39): Yield: 44%, dark-red oil, Rf 0.78 (40% EtOAc in hexane). 1H NMR (CDC13, 500 MHz): δ 7.61-7.59 (m, 2H), 7.42 (d, J=16.5 Hz, 1H), 7.37-7.26 (m, 4H), 7.16 (d, J=8.9 Hz, 1H), 7.13 (d, J=16.5 Hz, 1H), 6.92 (s, 1H), 6.84 (d, J=16.5 Hz, 1H), 6.73 (d, J=9.0 Hz, 1H), 6.68 (d, J=8.0 Hz, 1H), 3.96 (s, 3H), 3.92 (s, 3H), 3.92 (s, 3H), 3.90 (s, 6H), 3.89 (s, 3H). 19F NMR (CDCl3, 470 MHz): δ -57.9 (s, OCF3). 13C NMR (CDCl3, 125 MHz):  $\delta$  154.1, 20 isoxazole derivatives were performed at the B3LYP/6-31G* 153.5, 152.2, 152.1, 151.8, 148.2, 143.1, 142.5, 142.4, 138.1, 127.7, 126.6, 125.5, 124.1, 123.2, 123.1 (q, J=266 Hz), 121.7, 121.5, 121.0, 119.4, 114.3, 107.9, 107.7, 100.9, 61.4, 61.3, 60.9, 56.0. HRMS (ESI): m/z [M+H]+ calcd for C32H32N2O7F3: 613.21616.; found: 613.23494. IR (cm- 25 1): 3041-2839, 1595, 1510, 1495, 1464, 1408, 1375, 1294, 1257, 1222, 1165, 1091.

3,5-bis-(2,3,4-Trimethoxystyryl)-isoxazole (40): Yield: 39%, light-brown solid, mp: 136-137° C. Rf 0.62 (40%) EtOAc in hexane). 1H NMR (CDCl3, 500 MHz): δ 7.53 (d, 30 J=16.5 Hz, 1H), 7.38 (d, J=16.5 Hz, 1H), 7.33 (d, J=9.0 Hz, 1H), 7.28 (d, J=9.0 Hz, 1H), 7.08 (d, J=16.5 Hz, 1H), 6.96 (d, J=16.5 Hz, 1H), 6.73, (d, J=9.0 Hz, 1H), 6.72 (d, J=8.0 Hz, 1H), 6.51 (s, 1H), 3.95 (s, 3H), 3.94 (s, 3H), 3.90 (s, 12H). 13C NMR (CDCl3, 125 MHz): δ 168.9, 162.6, 154.5, 35 154.3, 152.5, 152.1, 142.5, 142.3, 130.1, 129.7, 123.0, 122.7, 121.9, 121.4, 115.3, 112.4, 107.8, 107.7, 97.7, 61.5, 61.4, 60.9, 60.9, 56.2, 56.1. HRMS (ESI): m/z [M+H]⁺ calcd for C25H28NO7: 454.18658; found: 454.19296. IR (cm-1): 3055-2995, 1643, 1593, 1574, 1557, 1493, 1462, 1433, 40 1412, 1281, 1092, 1038.

3,5-bis-(3,4,5-Trimethoxy-styryl)-1-phenylpyrazole (41): Yield: 77%, pale-orange solid, mp: 144-146° C. Rf 0.35 (40% EtOAc in hexane). 1H NMR (CDC13, 500 MHz): δ 7.55-7.50 (m, 4H), 7.43 (t, J=7.5 Hz, 1H), 7.15 (d, J=16.5 45 Hz, 1H), 7.11 (d, J=16.5 Hz, 1H), 7.07 (d, J=16.0 Hz, 1H), 6.86 (s, 1H), 6.78 (d, J=16.5 Hz, 1H), 6.77 (s, 2H), 6.64 (s, 2H), 3.91 (s, 6H), 3.88 (s, 3H), 3.87 (s, 6H), 3.87 (s, 3H). 13C NMR (CDCl3, 125 MHz): δ 153.5, 153.4, 151.1, 142.3, 139.4, 138.7, 138.0, 132.8, 132.5, 132.1, 129.3, 128.0, 50 125.2, 119.9, 115.0, 104.0, 103.5, 101.0, 61.0, 56.2, 56.1. HRMS (ESI): m/z [M+H]+ calcd for C31H33N2O6: 529.23386.; found: 529.22805. IR (cm-1): 2940, 2832, 2361, 1582, 1497, 1458, 1412, 1373, 1327, 1234, 1118.

3,5-bis-(3,4,5-Trimethoxy-styryl)-1-(4-trifluoromethoxy- 55 phenyl) pyrazole (42): Yield: 31%, dark-orange solid, mp: 140-142° C. Rf 0.61 (40% EtOAc in hexane). 1H NMR (CDC13, 500 MHz):  $\delta$  7.61-7.58 (m, 2H), 7.38 (d, J=8.0 Hz, 2H), 7.15 (d, J=16.5 Hz, 1H), 7.09 (d, J=16.0 Hz, 1H), 7.07 (d, J=16.5 Hz, 1H), 6.85 (s, 1H), 6.67 (s, 2H), 6.72 (d, J=16.5 60)Hz, 1H), 6.64 (s, 2H), 3.91 (s, 6H), 3.89 (s, 6H), 3.88 (s, 3H), 3.87 (s, 3H). 19F NMR (CDC13, 470 MHz):  $\delta$  -57.9 (s, OCF3). 13C NMR (CDCl3, 125 MHz): 8 153.5, 153.4, 151.4, 148.4, 142.4, 138.9, 138.2, 137.9, 133.2, 132.6, 131.8, 131.1, 126.5, 121.8, 120.5 (q, J=258 Hz), 119.5, 65 114.4, 104.0, 103.6, 101.5, 61.0, 61.0, 56.2, 56.1. HRMS (ESI): m/z [M+H]+ calcd for C32H32N2O7F3: 613.21616;

52

found: 613.22805. IR (cm-1): 3001-2837, 1581, 1504, 1465, 1415, 1377, 1301, 1240-1101, 1005.

3,5-bis-(3,45-Trimethoxystyryl)-1-(3,4-difluorophenyl) pyrazole (43): Yield: 32%, light-brown solid, mp: 54-56° C., Rf 0.62 (40% EtOAc in hexane). 1H NMR (DMSO-d6, 500 MHz): δ 7.15-7.06 (unresolved, 5H), 6.88 (tt, JHF=8.5 Hz, JHH=2.5 Hz, 1H), 6.85 (s, 1H), 6.80 (d, J=16.5 Hz, 1H), 6.77 (s, 2H), 6.67 (s, 2H), 3.92 (s, 6H), 3.90 (s, 6H), 3.89 (s, 3H), 3.88 (s, 3H). 19F NMR (CDC13, 470 MHz):  $\delta$  –107.5 (t, J=8.0 Hz). 13C NMR (CDC13, 125 MHz): δ 163.0, (d, 1JCF=250 Hz), 162.8 (d, 1JCF=250 Hz), 153.5, 152.0, 143.1, 141.7 (t, 3JCF=12.0 Hz), 138.6, 138.0, 134.2, 132.7, 132.2, 132.0, 119.7, 115.0, 108.6, 108.4, 105.0, 104.4, 103.5 (t, 2JCF=26.0 Hz), 103.1, 60.6, 60.5, 56.4, 56.3. HRMS (ESI): m/z [M+H]+ calcd for C31H31N2O6F2: 565.21502; found: 565.22207. IR (cm-1): 3080-2837, 1621, 1581, 1505, 1464, 1414, 1346, 1331, 1242, 1122.

Computational Methods

Geometry optimizations of the curcumin, pyrazole, and level with the Gaussian 09 package. Automated molecular docking calculations with the program AutoDock Vina were carried out for estimating the interaction energies and modeling the binding modes of the studied compounds as ligands for a series of enzymes involved in diverse carcinogenic processes (HER2, proteasome, VEGFR2, BRAF, and BCL-2). The three-dimensional coordinates of the proteins were obtained from the Protein Data Bank (PDB codes 3PPO (HER2), 3SDK (20S proteasome), 4AG8 (VEGFR2), 4XV2 (BRAF), and 4LVT (BCL-2)). Chain A of HER2, VEGFR2, BRAF and BCL-2, and chains K (β5 subunit) and L (β6 subunit) of 20S proteasome were selected as target templates for the docking calculations. Co-crystalized ligands and crystallographic water molecules were removed. Addition of hydrogens, merger of non-polar hydrogens to the atom to which they were linked, and assignment of partial charges were achieved with Auto-DockTools. Docking areas were constrained to a 30×30×30 Å box centered at the active site, providing proper space for rotational and translational movement of the ligands.

X-Ray Crystallography

Suitable single crystals for X-ray diffraction studies were obtained for 2, and 4 from chloroform and 15, 17, 19 and 21 from methanol. Crystal data of compounds 2, 4, 15, 17, 19 and 21 of FIG. 43 were collected by exactly the same method by mounting a crystal onto a thin glass fiber from a pool of FluorolubeTM and immediately placing it under a liquid N2 cooled stream, on a Bruker AXS diffractometer upgraded with an APEX II CCD detector. The radiation used is graphite monochromatized Mo K $\alpha$  radiation ( $\lambda$ =0.7107 Å). The lattice parameters are optimized from a leastsquares calculation on carefully centered reflections.

Lattice determination, data collection, structure refinement, scaling, and data reduction were carried out using APEX2 Version 2014.11 software package. The data were corrected for absorption using the SCALE program within the APEX2 software package. The structures were solved using SHELXT. This procedure yielded a number of the C, B, F, S and O atoms. Subsequent Fourier synthesis yielded the remaining atom positions. The hydrogen atoms are fixed in positions of ideal geometry (riding model) and refined within the XSHELL software package. These idealized hydrogen atoms had their isotropic temperature factors fixed at 1.2 or 1.5 times the equivalent isotropic U of the C atoms to which they were bonded. A few hydrogen atoms could not be adequately predicted via the riding model within the XSHELL software. These hydrogen atoms were located via

difference-Fourier mapping and subsequently refined. The final refinement of each compound included anisotropic thermal parameters on all non-hydrogen atoms.

Bioassay Methods NCI-60 Assay

Samples were submitted to the National Cancer Institute (NCI of NIH) Developmental Therapeutics anticancer screening program (DTP) for human tumor cell line assay by NCI-60 screening against leukemia, lung, colon, and CNS cancers, as well as melanoma, ovarian, renal, prostate, and 10 breast cancers. Compounds are initially tested at a single dose of 10-5 molar. Data are reported as mean graph of percent growth (GP). Growth inhibition is shown by values between 0 and 100 and lethality by values less than zero. Compounds that meet selection criteria based on one-dose 15 assay are then tested against 60 cell panel at five concentrations.

Cell Viability Assay to Determine EC50

Cells (2×103 cell/well) were incubated with compounds (concentration range 0-30000 nM) in a 384-well plate for 72 20 h in a CO2 incubator (5% CO2, 37° C.). Cell lines and PBCMs (peripheral blood mononuclear cells from healthy donors as non-cancer CONTROL) were seeded in quadruplicate (technical replicates). CellTiter-Glo® 2.0 reagent equal to the volume of cell culture medium present in each 25 well was added and the plate was left to incubate at room temperature for 10 min to stabilize the luminescent signal. Luminescent signal/intensity from the 384-well plate was read on a plate reader. Cells/cell lines used: BCWM.1 (Waldenstrom macroglobulinemia cell line, WM); RPMI- 30 8266 (Multiple myeloma cell line, MM); RS4; 11 (Acute lymphoblastic leukemia, ALL)* reported to be dependent on Bcl-2 protein.

Example 5—Heterocyclic Compounds Including Indole-Based, Benzothiophene-Based and Benzofuran-Based CUR-BF2 Adducts and CUR Compounds and their Pyrazoles

CUR compounds based on indole, benzothiophene, and benzofuran along with their aryl-pyrazoles were synthesized. Exemplary indole-based curcuminoid compounds, thiocyano-curcuminoid compounds and difluoroboron-curcuminoid adducts are shown in FIG. 45 and exemplary 45 benzothiophene-curcuminoid compounds, benzofuran-curcuminoid compounds, and difluoroboron-curcuminoid adducts are shown in FIG. 46. S-methylated curcuminoid di-cation salts were formed using a variation of the synthetic methods, as seen in FIG. 47

Computational/docking studies were performed on 20 heterocyclic CUR—BF₂ and CUR compounds to compare binding efficiency to target proteins involved in specific cancers, namely HER2, proteasome, VEGFR, BRAF, and BCL-2 versus known inhibitor drugs. The majority pre- 55 sented very favorable binding affinities that were comparable and in some cases more favorable than the knowninhibitors. The indole-based CUR—BF₂ and CUR compounds and their bis-thiocyanato derivatives exhibited high anti-proliferative and apoptotic activity by in-vitro 60 bioassay against a panel of 60 cancer cell lines, and more specifically against multiple myeloma (MM) cell lines (KMS11, MM1.S, and RPMI-8226) with significantly lower IC50s versus healthy PBMC cells. The indole-based CUR-BF₂ adducts and their bis-thiocyanato derivatives exhibited 65 significantly higher anti-proliferative activity in human colorectal cancer cells (HCT116, HT29, DLD-1, RKO, SW837,

54

and Caco2) compared to parent curcumin, while showing significantly lower cytotoxicity in normal (CCD112CoN and CCD841CoN).

The inventors used the earlier described one-pot method in Example 1 for the synthesis of CUR—BF₂ adducts for the synthesis of heterocyclic analogues starting with the corresponding aldehydes. In the majority of cases, the CUR-BF₂ adducts precipitated from ethyl acetate after overnight stirring at r.t. as detailed below.

- 1) Synthesis of Indole-Based CUR-BF2 Adducts and **CUR** Compounds
- a) From indole 5-aldehyde: The initial crop that precipitated out of EtOAc was a tautomeric mixture of 2a-BF₂ and 2-BF₂ in 60:40 ratio by NMR (FIG. **48**). By adding, some more base to the filtrate and continuing stirring overnight a second crop was produced that proved to be the enolic tautomer 2-BF₂. In independent runs 2-BF₂ was isolated as the sole product by using 0.66 equivalent of base after overnight stirring.

When a portion of crop 1 (CUR—BF₂ tautomeric mixture) was subjected to microwave (MW)-assisted decomplexation, a tautomeric mixture of the corresponding CURs 2a and 2 were obtained with the enolic tautomer 2 predominating. Decomplexation of another portion of the tautomeric mixture similarly resulted in a tautomeric mixture in which 2 was major. Finally, MW-assisted decomplexation of the 2-BF₂ furnished compound 2 purely as the enol tautomer in 94% isolated yield (FIG. 49).

- b) From indole 4-aldehyde: In initial studies (on a 500 mg scale), no precipitate was formed after 3 days mixing at r.t. Removal of EtOAc gave a dark residue which after washing with diethyl ether was shown by NMR to be a tautomeric mixture of enolic and the diketo forms in 4:1 ratio. By addition of more base and by using less EtOAc in a subsequent reaction, 3-BF₂ precipitated solely as the enol tautomer. The MW-assisted decomplexation cleanly gave the corresponding curcuminoid 3 as an enolic compound in 77% isolated yield (FIG. 50).
- c) Synthesis of bis-Thiocyanato-Derivatives of Indole-A novel series of heterocyclic CUR—BF2 adducts and 40 Based CUR—BF2 and CUR compounds: There is considerable current interest in the introduction of thiocyano group into bioactive compounds, and this has in turn stimulated a search for new thiocyanation methods. (T. Castanheiro, et al., Chem. Soc. Rev. 2016, 45, 494; G. Malik, et al., Chem. Sci., 2017, 8, 8050-8060; D. Wu, et al., J. Org. Chem. 2018, 83, 1576-1583). Development of a new method in this laboratory for facile introduction of SCN and SeCN groups into medicinally important heterocycles, enabled the synthesis of bis-thiocyanato CUR—BF2 and CUR compounds starting from the SCN-substituted benzaldehydes (FIG. 51).

Since attempts to obtain X-ray quality crystals from the CUR—BF₂ or CUR compounds in this class did not meet with success, their structure were optimized by DFT. Two representative examples (4-BF₂ and 5-BF₂) are shown (FIG. 52) while two others are shown in FIG. 53.

d) From N-Methylindole-3-aldehyde: Following our standard protocol, in a small scale experiment N-methylindole-5-carboxaldehyde reacted to give the 1,3-diketo tautomer 6a-BF₂ as a deep-purple solid which was harvested in two crops in 22% combined yield (FIG. 54). The MW-assisted decomplexation of 6a-BF2 cleanly furnished the corresponding curcuminoid 6a solely as the 1,3-diketo-tautomer in 64% isolated yield.

A second synthesis (FIG. 55) employing less ethyl acetate produced two crops, the first crop precipitated overnight (a red solid) as a 4:1 tautomeric mixture, and a second crop was harvested (after addition of more base to the filtrate and

stirring at r.t. for 2 days) which was solely the enolic 6-BF₂ (a green solid). Decomplexation of 6-BF₂ required multiple runs in the MW, followed by re-crystallization from methanol, to cleanly furnish compound 6 as a bright-red solid

2) Synthesis of Heterocyclic Benzothiophene- and Benzofuran-Based CUR-BF2 and CUR Compounds and their Aryl-Pyrazoles

Following the general one-pot method described in Example 4, the corresponding CUR—BF, adducts and CUR compounds in FIG. 56 were synthesized starting from the corresponding aldehydes. NMR spectra confirmed the sole presence of the enolic tautomers in every case.

With the goal to determine the significance of the ketoenolic moiety in bioactivity for this class of compounds, a small library of aryl-pyrazoles 10-15 were also synthesized (FIG. 57) following the earlier reported method.

Computational Docking Study

Molecular docking calculations were carried out with the aim to shed light on factors governing the biological activity of the heterocyclic curcuminoids. Binding affinities in the active site of various proteins involved in carcinogenic mechanisms were determined, and computed binding energies were compared with those of the corresponding known inhibitors (Table 8). The proteins selected for docking studies comprise a variety of oncogenic processes, described

Human epidermal growth factor receptor 2 (HER2), which is one of the tyrosine kinase receptors in EGFR family, has a crucial role in the evolution of several human cancers. (N. Iqbal, et al., Mol. Biol. Int., 2014, 2014, 852748). It is a target for therapies pointing to inhibition of HER2 to reduce tumor growth, since amplification or overexpression of this protein appears in breast, prostate, gastric/ gastroesophageal, ovarian, endometrium, bladder, lung, colon, and head and neck cancers. (N. Iqbal, et al., Mol. Biol. Int., 2014, 2014, 852748). It has been suggested that inhibition of tumor cellular proteasome is the mechanism by which curcumin prevents the proliferation of acute promy-

elocytic leukemia (APL) cells. (K.-L. Tan, et al., ChemMed-Chem 2012 7, 1567-1579). Treatment with proteasome inhibitors causes a decrease in proliferation, induction of apoptosis and sensitization of diverse tumor cells by chemotherapeutic drugs and irradiation. (S. B. Wan, et al., Int. J. Mol. Med., 2010, 26, 447-455). The vascular endothelial growth factor receptor (VEGFR) tyrosine kinases are clinically confirmed target of inhibitors applied in the renal cell carcinoma therapy. (M. McTigue, et al., Proc. Natl. Acad. Sci. USA, 2012, 109, 18281-18289). The treatment of metastatic melanoma significantly evolved by selective inhibition of BRAF, as oncogenic activation of this protein stimulates cancer cell growth. (C. Zhang, et al., Nature, 2015, 526, 583-586). The connection of proteins in the BCL-2 family (crucial regulators of normal apoptosis) with tumor initiation, disease progression and drug resistance makes them crucial targets for antitumor therapy. (A. J. Souers, et al., Nat. Med., 2013, 19, 202-208). BCL-2 is over-expressed in acute and chronic leukemias and presents a central role in the survival of multiple lymphoid malignancies. (A. J. Souers, et al., Nat. Med., 2013, 19, 202-208). The studied CUR—BF₂ and CUR compounds were able to fit nicely into the binding pocket of the considered proteins, and several compounds revealed markedly favored binding affinities (Table 8). In proteasome, VEGFR, and in BCL-2, several CUR derivatives presented enhanced binding energies in comparison with known inhibitors that are used in chemotherapy. It is noteworthy that docking energy for the 1,3diketo tautomer (as in 2aBF₂) is also predicted to be highly favorable, suggesting that in case of tautomeric mixtures both tautomers are capable of favorable docking interactions. Binding interactions for the compounds exhibiting highly favorable docking energies in the active site of each protein are displayed in FIG. 58. The principle interactions observed are hydrophobic contacts between the atoms of the ligands and the protein residues (red radial lines). In addition, hydrogen bond interactions were found between F and N ligand atoms and hydrogen bond donor groups in neighboring protein residues. FIG. 59 depicts a 3D representation of 3-BF₂ in BC1-2.

56

TABLE 8

Binding Energ	ies				
	AutoDock Vina (kcal/mol) ^a				
Heterocyclic Compounds	HER2	Proteasome	VEGFR	BRAF	BCL-2
Known inhibitor	-11.4 (SRY)	-7.8 (Bortezomib) -7.8 (Ixazomib) -8.5 (Carfilzomib)	-9.2 (Axitinib) -10.8 (Sorafenib) -8.9 (Lenvatinib)	-9.3 (Vemurafenib) -12.9 (Dabrafenib)	-8.3 (Navitoclax) -8.2 (Venetoclax)
H N N H	-11.0	-9.6	-11.7	-10.2	-8.6
H N N H	-10.8	-10.4	-12.6	-10.6	-8.7

Binding Ener	gies				
		Au	toDock Vina (	kcal/mol)a	
Heterocyclic Compounds	HER2	Proteasome	VEGFR	BRAF	BCL-2
Known inhibitor	-11.4 (SRY)	-7.8 (Bortezomib) -7.8 (Ixazomib) -8.5 (Carfilzomib)	-9.2 (Axitinib) -10.8 (Sorafenib) -8.9 (Lenvatinib)	-9.3 (Vemurafenib) -12.9 (Dabrafenib)	-8.3 (Navitoclax) -8.2 (Venetoclax)
H H H	-10.5 H	-10.3	-12.5	-10.7	-9.4
H SCN SCN SCN SCN	-10.4 H	-9.9	-12.4	-10.9	-8.3
H SCN SCN SCN	-8.9 H	-10.1	-11.5	-9.8	-9.4
HN H	-10.1	-9.6	-10.5	-10.2	<b>-7.7</b>
HN H	-10.2	-10.5	-11.7	-10.3	-9.4
SCN OF B NCS NH	-9.3	-10.8	-10.0	-10.1	-7.7

Binding Energy	gies					
	AutoDock Vina (kcal/mol) ^a					
Heterocyclic Compounds	HER2	Proteasome	VEGFR	BRAF	BCL-2	
Known inhibitor	-11.4 (SRY)	-7.8 (Bortezomib) -7.8 (Ixazomib) -8.5 (Carfilzomib)	-9.2 (Axitinib) -10.8 (Sorafenib) -8.9 (Lenvatinib)	-9.3 (Vemurafenib) -12.9 (Dabrafenib)	-8.3 (Navitoclax) -8.2 (Venetoclax)	
SCN H NCS NH	-8.7	-9.4	-9.4	-9.2	-6.6	
$H_3C$ $H_3C$ $H_3C$ $CH_3$	-9.0	-9.6	-9.9	-9.5	-9.3	
$H_3C$ $H_3C$ $H_3C$ $H$ $CH_3$	-9.4	-10.1	-11.2	-10.2	-9.2	
$H_3C$ $H$	-9.6	-10.5	-11.8	-10.7	-8.5	
$\begin{array}{cccccccccccccccccccccccccccccccccccc$	-10.2	-9.4	-10.8	-10.9	-9.0	

TABLE 8-continued  Binding Energies						
	AutoDock Vina (kcal/mol) ^a					
Heterocyclic Compounds	HER2	Proteasome	VEGFR	BRAF	BCL-2	
Known inhibitor	-11.4 (SRY)	-7.8 (Bortezomib) -7.8 (Ixazomib) -8.5 (Carfilzomib)	-9.2 (Axitinib) -10.8 (Sorafenib) -8.9 (Lenvatinib)	-9.3 (Vemurafenib) -12.9 (Dabrafenib)	-8.3 (Navitoclax) -8.2 (Venetoclax)	
$\begin{array}{cccccccccccccccccccccccccccccccccccc$	-11.7	-10.5	-11.4	-11.1	-8.7	
S H O H O S	-9.8	-9.3	-10.4	-9.6	-8.8	
S H S	-10.5	-9.9	-11.1	-10.4	-8.5	
S H O S S S S S S S S S S S S S S S S S	-9.8	-8.9	-11.2	-9.5	-8.0	
S H S S	-10.7	-9.1	-12.7	-10.8	-7.7	

Binding Energies								
	AutoDock Vina (kcal/mol) ^a							
Heterocyclic Compounds	HER2	Proteasome	VEGFR	BRAF	BCL-2			
Known inhibitor	-11.4 (SRY)	-7.8 (Bortezomib) -7.8 (Ixazomib) -8.5 (Carfilzomib)	-9.2 (Axitinib) -10.8 (Sorafenib) -8.9 (Lenvatinib)	-9.3 (Vemurafenib) -12.9 (Dabrafenib)	-8.3 (Navitoclax) -8.2 (Venetoclax)			
F B F	-11.6	-10.0	-13.3	-11.0	-8.0			
H O O O	-9.9	-9,9	-11.7	-10.1	-8.2			

^aMost stable binding mode.

^bBinding energies in bold = more favorable than known inhibitors

## In-Vitro Bioassay Study

thesized in the present study along with representative aryl-pyrazoles were initially tested for their anti-proliferative activity by the NCI-60 in-vitro assay. Among these, the indole-based CUR-BF2 and CUR compounds, and in particular their bis-thiocyanato-derivatives (FIG. 60), exhibited 40 notable anti-proliferative and apoptotic activity in a number of cell lines in several types of cancers, as reflected in either low or negative growth percent values respectively under standard 10⁻⁵ molar concentration. Subsequent five-dose assay on these compounds (performed at the NCI) showed 45 significant anti-proliferative activity remaining at 10⁻⁶ molar concentrations, followed by a rapid drop at lower concentrations. Among the N-methyl-indole derivatives and the benzothiophene- and benzofuran-derived CUR—BF, and CUR compounds only 7-BF₂ of FIG. **60** showed notable 50 anti-proliferative activity, while the corresponding arylpyrazoles proved to be ineffective.

Compounds shown in FIG. 60 were subsequently tested to determine their ability to induce cytotoxicity in a small panel of hematologic cancer cell lines in comparison to healthy 55 KMS11 and MM1.S cells, notable apoptosis (54% and 15%, (non-cancer) peripheral blood mononuclear cells (PBMCs). The indole-CUR and CUR—BF, compounds exhibited significant cytotoxicity in multiple myeloma (MM) cancer cells, with little to no cell death noted in healthy donor PBMCs.

Further bioassay studies focused on an expanded panel of MM cell lines that capture some of the genetic variability as seen in MM patients. Notably, these MM cell lines included MM1.S cells (TP53 wild type), KMS11 cells (TP53 biallelic deletion) and RPMI-8226 cells (c-MYC dependent). Among 65 these select group of heterocyclic curcuminoids, 3-BF₂ and 2 of FIG. 60 exhibited remarkable tumor-selective activity

with median IC₅₀ concentration in the aforementioned MM The heterocyclic CUR—BF2 and CUR compounds syn- 35 cell lines of 2.1 uM and 1.4 uM, respectively. They also showed notable MM-cell specific cytotoxicity with mean activity of 33.7-fold (range, 4-2,445-fold) greater in the MM cell lines relative to healthy PBMCs (FIG. 61). It is noteworthy that the MM standard-of-care agent, bortezomib (a proteasome inhibitor) has an in vitro tumor-specificity profile of roughly 2-3-fold (IC₅₀ in MM cells  $\sim$ 2 nM and IC₅₀ of PBMCs is ~4-6 nM).

> Next, the ability of these hit compounds to induce cell death was assessed through apoptosis at 1.25 uM and 2.5 uM concentrations for 24 h (FIG. 73). With 3-BF₂ of FIG. 60, significant apoptosis in MM1.S (34% and 47%), KMS-11 (75% and 79%), and RPMI-8226 (39% and 60%) cells occurred relative to healthy donor PBMCs, treated with the same concentrations (23-28% apoptosis observed). Next, the MM cells and PBMCs were tested with CUR-analog 2, showing that in line with cell proliferation assay data (FIG. 61), RPMI-8226 cells were most sensitive to this compound with 32% and 65% of cells undergoing apoptosis at

> 1.25 uM and 2.5 uM concentrations. In contrast, in respectively) was seen only at a 10 uM concentration. For comparison, the same MM cell lines were exposed to venetoclax (FDA-approved anti-Bcl-2 inhibitor, activator of apoptosis) at 1.25, 2.5, 5 uM and at 10 uM concentration, showing a median apoptosis of 15%; with ~10% cell death seen in healthy donor PBMCs (FIG. 72).

> Compounds shown in FIG. 60 along with two other CUR—BF, compounds from FIG. 73 were subsequently tested for their anti-proliferative activity and cytotoxicity in colorectal cancer (CRC) cells and in normal colon cells in comparison to parent curcumin. The CUR-BF2 adducts and in particular, the bis-SCN derivatives exhibited signifi-

cantly higher anti-cancer activity (growth inhibition) compared to curcumin, while the corresponding CUR compounds were less effective. Moreover, in comparison to parent curcumin, the CUR—BF₂ adducts were noticeably more toxic to cancer cells than to normal colon cells (see 5 FIG. 61 and FIG. 74).

In summary, the inventors have synthesized a series of new heterocyclic CUR—BF₂ and CUR compounds based on indole, benzothiophene and benzofuran were synthesized and characterized. Whereas computational docking studies showed that a fairly large subset of these compounds are capable of favorable docking interactions with several key proteins involved in carcinogenic mechanisms, bioassay studies pointed to a smaller subset and in particular two curcuminoids (3-BF₂ and 2) with favorable cytotoxicity 15 characteristics as potential hit compounds. Guided by the initial NCI-60 data, the anti-proliferative and apoptotic efficacy of the CUR—BF₂ and CUR compounds (FIG. 74) were studied in colorectal cancer (CRC) cells. The CUR-BF₂ adducts, and in particular the bis-SCN derivatives, 20 exhibited significantly higher anti-cancer activity compared to curcumin. Moreover, these compounds proved to possess more cancer cell-specific cell growth inhibition and lower toxicity to normal cells.

#### Experimental Section

General: The substituted benzaldehydes used in this study were all high purity commercially available samples and were used without further purification. Regular solvents used for synthesis and isolation (MeCN, acetone, DCM, hexane, and EtOAc) were all of sufficient purity and were 30 used as received. NMR spectra were recorded on a 500 MHz instrument using CDCl₃, DMSO-d₆ or acetone-d₆ as solvent. ¹⁹F NMR were referenced relative to external CFCl₃. HRMS analyses were performed on a Finnigan Quantum ultra-AM in electrospray mode using methanol as solvent. 35 Microwave reactions were performed in Biotage miniature 400 W lab microwave in 5 mL vials with magnetic stirring. FT-IR spectra were recorded in ATR mode (as thin films formed via DCM evaporation). Melting points were measured in open capillaries and are not corrected.

General procedure for the synthesis of curcuminoid-BF₂ adducts: To a mixture of acetyl acetone-BF2 complex (1 equiv.) in ethyl acetate (minimal) under stirring and nitrogen atmosphere, the respective aldehyde (2.2 equiv.) was added in one portion, followed by dropwise addition of N-butyl 45 amine (0.22 equiv.) over a period of 20 minutes. The CUR—BF₂ adduct precipitated out of EtOAc upon overnight stirring at r.t. The reaction mixture was subsequently cooled to 0° C. and the product was filtered, washed with cold (0° C.) EtOAc and dried under high vacuum, typically 50 trien-3-one (2): Yield 94%, red-brown powder, mp decomfor 1 h.

Variations thereof—in cases where the product had precipitated but the yield was poor <40%, the reaction mixture was returned to the flask with additional N-butyl amine (0.22 equiv.), and the reaction mixture was left to stir for an 55 additional 48 hours whereupon additional product precipitated out of EtOAc. This was required for all of the indolebased curcuminoids, and for 8-BF₂. (FIG. **56**) For 7-BF₂ the crude mixture was left in the freezer for 2 days to harvest an additional crop. (FIG. 56)

General procedure for the decomplexation of CUR-BF2: The curcuminoid-BF₂ complex (1 equiv.) and sodium oxalate (2 equiv.) were added to a 5 mL microwave vial equipped with a magnetic stirrer bar. Aqueous MeOH (5 mL, 8:2 MeOH:H₂O) was added and the vial was sealed with a 65 crimp cap with septa. The sealed vial was irradiated at 100 W for 6 min at 140° C. with stirring set at 900 rpm.

66

Decomplexation resulted in significant color change. The vial was cooled, the cap removed, and the reaction mixture was filtered, washed with de-ionized water, and the product was dried for 15 min on the sinter and then under high vacuum.

Variations thereof: 7-BF₂ of FIG. 56 required 4 equivalents of sodium oxalate to fully decomplex in the microwave at 145° C. for 10 minutes.

Synthesis of the Aryl-pyrazole derivatives 10-15 of FIG. 57: these were synthesized by reacting the corresponding CUR compound with aryl-pyrazoles in acetic acid using the previously described procedure in Example 4.

Representative Procedure: Curcuminoid 7 of FIG. 56 (60 mg, 0.155 mmol, 1 equiv.) was added to a small Erlenmeyer flask along with 5 mL of glacial acetic acid, and phenyl hydrazine (67 mg, 0.62 mmol, 4 equiv.) was then added. The reaction mixture was placed on a hotplate with stirring at 80° C. for 2 hours. Following overnight mixing at r.t, the reaction mixture was reheated to 80° C. and H₂O was slowly added until the solution was almost turbid. The flask was then removed from the heat and left to cool in an ice-bath. The product precipitated by cooling in an ice-bath. It was washed with 3×5 mL portions of H₂O, and dried on high vacuum for an hour to give 36 mg of a light-brown solid.

Variations: in the reaction with substituted phenyl hydrazines only 2 equivalents of the phenyl hydrazine was used. For compound 15 of FIG. 57, the product had to be further purified by re-crystallization from Et2O/hexane.

Characterization Data for Compounds in FIGS. 48-51, 54-57, 60 and 64

Indole-5-Curcuminoid-BF₂ adduct (2-BF₂): Yield 65%, brown powder. R_f 0.11 (40% EtOAc in hexane). ¹H NMR (acetone- $d_6$ , 500 MHz):  $\delta$  10.65 (br s, 2H), 8.18 (d, J=16.0 Hz, 2H), 8.11 (s, 2H), 7.67 (dd, J=8.5 Hz and 1.5 Hz, 2H), 7.56 (d, J=8.5 Hz, 2H), 7.45 (unresolved dd, J=3 Hz, 2H), 7.04 (d, J=15.5 Hz, 2H), 6.62 (d, J=3.0 Hz, 2H), 6.45 (s, 1H). ¹³C NMR (DMSO-d₆, 125 MHz): δ 178.7, 148.7, 138.2, 128.2, 127.3, 125.6, 124.6, 122.0, 117.5, 112.5, 102.7, 101.2.  19 F NMR (acetone-d₆, 470 MHz):  $\delta$  -141.1 (s, 40 ¹¹B-F), -141.2 (s, ¹⁰B-F). IR (cm⁻¹): 3418, 3005-2989, 1602, 1564, 1497, 1456, 1355, 1300, 1275, 1260, 1171, 1149, 1124, 1043.

Indole-5-Curcuminoid-BF₂ adduct (2a-BF₂) (1,3-diketo tautomer in a mixture with 2-BF₂):  $R_f 0.26$  (40% EtOAc in hexane):  1 H NMR (acetone-d₆, 500 MHz):  $\delta$  8.16 (d, J=16.0 Hz, 2H), 8.09 (unresolved, 2H), 7.61 (overlapping dd, 2H), 7.44 (unresolved, 2H), 7.0 (d, J=16.0 Hz, 2H), 6.61 (unresolved, 2H), 6.43 (s, 2H).

(1E,4E,6E)-5-Hydroxy-1,7-bis(indole-5)hepta-1,4,6poses at 250° C.,  $R_f 0.38$  (40% EtOAc in hexane). ¹H NMR (DMSO- $d_6$ , 500 MHz):  $\delta$  11.35 (s, 2H), 7.90 (s, 2H), 7.74 (d, J=16.0 Hz, 2H), 7.52 (d, J=8.5 Hz, 2H), 7.44 d, 8.0 Hz, s, 2H), 7.40 (br, s, 2H), 6.82 (d, J=16.0 Hz, 2H), 6.50 (br s, 2H), 6.11 (s, 1H). ¹³C NMR (DMSO-d₆, 125 MHz): δ 183.7, 142.8, 137.7, 128.5, 127.2, 126.4, 122.8, 121.4, 121.1, 112.6, 102.9, 101.4. IR (cm⁻¹): 3385, 2988, 2365, 1622, 1521, 1472, 1418, 1339, 1274, 1260, 1124. HRMS (ESI):  $m/z [M+H]^+$  calcd for  $C_{23}H19O_2N_2$ : 355.1446; found: 60 355.1396.

Indole-4-Curcuminoid-BF2 adduct (3-BF2): Yield 29%, black solid, R_e 0.16 (40% EtOAc in hexane). ¹H NMR (acetone- $d_6$ , 500 MHz):  $\delta$  10.75 (s, 2H, br), 8.45 (d, J=16.0 Hz, 2H), 7.68 (d, 8.0 Hz, 2H), 7.64-7.62 (overlapping dd, and d, 4H), 7.27 (t, J=8.0 Hz, 2H), 7.25 (d, J=7.5 Hz, 2H), 6.95 (d, J=3.5 Hz, 1H), 6.94 (s, 1H, br), 6.57 (s, 1H). ¹³C NMR (DMSO-d₆, 125 MHz): δ 179.7, 146.4, 137.1, 128.8,

127.4, 125.9, 124.0, 121.7, 121.1, 116.7, 102.4, 101.0. ¹⁹F NMR (acetone-d₆, 470 MHz):  $\delta$  –140.6 (s, ¹¹B-F), –140.7 (s, ¹⁰B-F). IR (cm⁻¹): 3431, 3412, 2951-2930, 1613, 1597, 1541, 1483, 1433, 1389, 1354, 1296, 1153, 1119, 1044.

67

(1E,4E,6E)-5-Hydroxy-1,7-bis(indole-4)hepta-1,4,6trien-3-one (3): Yield 77%, dark-brown solid, mp 201-204° C.,  $R_c 0.42$  (40% EtOAc in hexane). ¹H NMR (methanol-d₄, 500 MHz): δ 8.08 (d, J=15.5 Hz, 2H), 7.47 (d, J=8.5 Hz, 2H), 7.40-7.39 (unresolved doublets, 4H), 7.17 (t, J=7.5 Hz, 2H), 6.94 (d, J=15.5 Hz, 2H), 6.85 (dd, J=2.5 and 1 Hz, 2H), 10 6.13 (s, 1H).  $^{13}\mathrm{C}$  NMR (methanol-d₄, 125 MHz):  $\delta$  183.7, 140.0, 136.9, 127.1, 126.5, 125.9, 123.3, 121.0, 119.9, 113.3, 101.1, 99.7. HRMS (ESI): m/z [M+H]⁺ calcd for  $C_{23}H_{19}O_2N_2$ : 355.1446; found: 355.1294. IR (cm⁻¹): 3418, 3269-2872, 1620, 1557, 1416, 1344, 1277, 1201, 1141, 15

3-Thiocyanato-Indole-5-Curcuminoid-BF₂ (4-BF₂): Yield 49%, reddish-orange solid,  $R_f$  0.05 (40% EtOAc in hexane). ¹H NMR (DMSO-d₆, 500 MHz): δ 12.3 (s, 2H), 8.24 (d, J=15.5 Hz, 2H), 8.25 (s, 2H), 8.11 (d, J=2.5 20 Hz, 2H), 7.83 (dd, J=8.5 Hz and 1.5 Hz, 2H), 7.63 (d, J=8.5 Hs, 2H), 7.25 (d, J=15.5 Hz, 2H), 6.74 (s, 1H). ¹³C NMR (DMSO-d₆, 125 MHz): δ 179.8, 148.3, 138.6, 128.5, 128.1, 124.3, 121.7, 119.9, 114.2, 112.6, 102.0, 91.9. ¹⁹F NMR (DMSO-d₆, 470 MHz):  $\delta$  –137.5 (s, ¹¹B-F), –137.6 (s, 25 ¹⁰B-F). IR (cm⁻¹): 3417, 2916, 2848, 2152, 1739, 1612, 1552, 1541, 1500, 1382, 1300, 1058.

(1E,4E,6E)-5-Hydroxy-1,7-bis(3-thiocyanoindole-5) hepta-1,4,6-trien-3-one (4): Yield 73%, red solid, mp decomposes at 250° C.,  $R_c 0.08$  (40% EtOAc in hexane). ¹H 30 NMR (DMSO- $d_6$ , 500 MHz):  $\delta$  16.3 (s, 1H, br), 12.21 (d, J=2 Hz, 2H), 8.06 (d, J=2.5 Hz, 2H), 8.03 (s, 2H), 7.86 (d, J=16.0 Hz, 2H), 7.70 (d, J=9.0 Hz, 2H), 7.58 (d, J=8.5 Hz, 2H), 6.96 (d, J=16.0 Hz, 2H), 6.30 (s, 1H). ¹³C NMR 128.4, 123.3, 123.1, 119.6, 114.0, 112.7, 101.6, 91.2. HRMS (ESI):  $m/z [M+H]^+$  calcd for  $C_{25}H_{16}O_2N_4S_2$ : 469.56574; found: 469.47375. IR (cm⁻¹): 3300, 2924, 2152, 1705, 1622, 1604, 1273, 1138, 1124, 958.

3-Thiocyanato-Indole-4-Curcuminoid-BF₂ (5-BF₂): Yield 62%, dark-brown powder,  $R_f$  0.09 (40%) EtOAc in hexane). ¹H NMR (acetone-d₆, 500 MHz): δ 9.34 (d, J=15.0 Hz, 2H), 8.14 (d, 2.0 Hz, 2H), 7.90 (d, J=7.0 Hz, 2H), 7.77 (d, J=7.0 Hz, 2H), 7.42* (t, J=8.0 Hz, 2H), 7.27* (d, J=16.5 Hz, 2H), 6.71 (s, 1H) [NH signal is observed in 45 DMSO- $d_6$  at  $\delta$  12.39 (s, 2H) in which signals marked with * are overlapping]. ¹³C NMR (DMSO-d₆, 125 MHz): δ 180.0, 142.8, 138.0, 137.5, 126.9, 125.9, 123.7, 122.5, 121.7, 117.3, 113.1, 103.1, 90.4. ¹⁹F NMR (DMSO-d₆, 470 MHz):  $\delta$  -137.5 (s, ¹¹B-F), -137.6 (s, ¹⁰B-F). IR (cm⁻¹): 50 3395, 3335, 2154, 2156, 1616, 1601, 1555, 1541, 1508, 1493, 1410, 1275, 1161, 1128, 1062.

(1E,4E,6E)-5-Hydroxy-1,7-bis(3-thiocyano-indole-4) hepta-1,4,6-trien-3-one (5): Yield 82%, red powder, decomposes at 250° C., R_f 0.10 (40% EtOAc in hexane). ¹H NMR 55 (DMSO- $d_6$ , 500 MHz):  $\delta$  12.27 (s, 2H), 9.00 (d, J=15.5 Hz, 2H), 8.12 (d, J=2 Hz, 2H), 7.74 (d, J=8.0 Hz, 2H), 7.61 (d, J=8.0 Hz, 2H), 7.33 (t, J=7.5 Hz, 2H), 7.04 (d, J=16.0 Hz, 2H), 6.24 (s, 1H). ¹³C NMR (DMSO-d₆, 125 MHz): δ 183.6,  $137.9,\ 136.9,\ 136.7,\ 127.8,\ 125.6,\ 125.3,\ 123.7,\ 120.3,\ 60$ 115.4, 113.3, 102.6, 90.0. IR (cm⁻¹): 3313, 2155, 1624, 1602, 1396, 1275, 1119. HRMS (ESI): m/z [M+H]+ calcd for C₂₅H₁₇O₂N₄S₂: 469.07929; found: 469.3449

N-methyl-Indole-3-Curcuminoid-BF₂ adduct (6-BF₂): Yield 60%, dark-green solid, R_f 0.32 (40% EtOAc in 65 hexane).  1 H NMR (acetone-d₆, 500 MHz):  $\delta$  8.20 (d, J=15.5 Hz, 2H), 8.10 (d, J=7.5 Hz, 2H), 8.03 (s, 2H), 7.58 (d, J=8.5

Hz, 2H), 7.38 (dt, J=7 Hz and 1 Hz, 2H), 7.33 (dt, J=7 Hz and 1 Hz, 2H), 6.90 (d, J=15.5 Hz, 2H), 6.39 (s, 1H), 4.0 (s, 6H). ¹³C NMR (acetone-d₆, 125 MHz):  $\delta$  178.1, 139.3, 138.9, 138.0, 126.0, 123.4, 122.0, 120.7, 115.0, 113.2, 110.9, 100.1, 32.8. ¹⁹F NMR (acetone- $d_6$ , 470 MHz):  $\delta$  –142.0 (s, ¹¹B-F), -141.9 (s, ¹⁰B-F). IR (cm⁻¹): 1599, 1557, 1501, 1456, 1445, 1422, 1389, 1371, 1340, 1371, 1287, 1251, 1153, 1124, 1072.

68

(1E,4E,6E)-5-Hydroxy-1,7-bis(N-methyl-indole-3)hepta-1,4,6-trien-3-one (6); Yield 98%, bright-red powder, mp 195-198° C., R_f 0.54. ¹H NMR (acetone-d₆, 500 MHz): δ 8.04 (d, J=8 Hz, 2H), 7.91 (d, J=16.0 Hz, 2H), 7.78 (s, 2H), 7.52 (d, J=8.5 Hz, 2H), 7.33 (t, J=7 Hz, 2H), 7.26 (t, J=8.5 Hz, 2H), 6.77 (d, J=15.5 Hz, 2H), 6.04 (s, 1H), 3.92 (s, 6H). ¹³C NMR (acetone-d6, 500 MHz): δ 183.8, 138.5, 134.4, 133.5, 126.1, 122.7, 121.1, 120.3, 118.9, 112.5, 110.4, 100.1, 32.5. HRMS (ESI): m/z [M+H]+ calcd for C₂₅H₂₃O2N₂: 383.17595; found: 383.16476. IR (cm⁻¹): 3100 to 2824, 1746, 1715, 1607, 1556, 1519, 1494, 1454, 1421, 1373, 1330, 1255, 1157, 1126, 1070.

N-methyl-Indole-3-Curcuminoid-BF, adduct (1,3-diketo tautomer; 6a-BF₂): Yield 22%, deep-purple solid, R_f 0.44 (40% EtOAc in hexane). ¹H NMR (DMSO-d₆, 500 MHz): δ 8.31 (d, J=15.5 Hz, 2H), 8.26 (s, 2H), 8.12 (d, J=7 Hz, 2H), 7.62 (d, J=8 Hz, 2H), 7.39 (t, J=7 Hz, 2H), 7.33 (t, J=7 Hz, 2H), 6.85 (d, J=15.5 Hz, 2H), 6.40 (s, 2H), 3.89 (s, 6H). ¹³C NMR (DMSO-d₆, 125 MHz): δ 186.3, 181.0, 143.8, 141.4, 139.1, 125.7, 124.2, 123.1, 121.3, 113.0, 112.8, 112.0, 100.4, 34.0, 23.9. ¹⁹F NMR (DMSO-d₆, 470 MHz):  $\delta$  –137.6 (s, ¹¹B-F), -137.5 (s, ¹⁰B-F). IR (cm⁻¹): 3055, 2988, 1620, 1558, 1516, 1375, 1294, 1263, 1169, 1063.

(1E,6E)-1,7-bis(N-methyl-indole-3)hepta-1,6-dien-3,5dione (6a): Yield 64%, light-red powder, mp 126-128° C., R 0.72 (40% EtOAc in hexane). ¹H NMR (CDCl₃, 500 MHz): (DMSO-d₆, 125 MHz):  $\delta$  183.7, 141.8, 138.0, 135.0, 128.6, 35  $\delta$  7.93 (d, J=8 Hz, 2H), 7.85 (d, J=15.5 Hz, 2H), 6.49 (d, J=15.5 Hz, 2H), 5.41 (s, 2H), 3.82 (s, 6H). ¹³C NMR (CDCl₃, 125 MHz): δ 194.7, 180.5, 138.2, 134.0, 133.2, 126.0, 123.0, 121.3, 120.5, 117.7, 112.8, 110.1, 99.9, 33.2, 26.3. HRMS (ESI): m/z [M+H]+ calcd for C₂₅H₁₂O₂N₂: 383.17595; found: 383.16467. IR (cm⁻¹): 3098 to 2914, 1716, 1626, 1534, 1422, 1375, 1263, 1159, 1132, 1072.

Benzothiophene-3-Curcuminoid-BF₂ adduct (7-BF₂): Yield: 70%, bright-orange solid, mp  $>240^{\circ}$  C. R_c 0.81 (40%) EtOAc in hexane). ¹H NMR (DMSO-d₆, 500 MHz): δ 8.75 (s, 2H), 8.33 (d, J=20 Hz, 2H), 8.34 (s, 2H), 8.14 (d, J=8.0 Hz, 2H), 7.58 (t, J=7.5 Hz, 2H), 7.52 (t, J=7.5 Hz, 2H), 7.30 (d, J=16.0 Hz, 2H), 6.97 (s, 1H). ¹³C NMR (DMSO-d₆, 125 MHz): δ 180.2, 140.5, 138.5, 136.9, 135.8, 132.1, 126.1, 124.0, 123.0, 121.7, 110.0, 102.3. ¹⁹F NMR (DMSO-d₆, 470 MHz):  $\delta$  –137.4 (s, ¹¹B-F), –137.3 (s, ¹⁰B-F).

(1E,4E,6E)-5-Hydroxy-1,7-bis(benzo[b]thiophen-3-yl) hepta-1,4,6-trien-3-one (7): Yield: 85%, orange solid, mp: 159-160° C. R_€ 0.74 (40% EtOAc in hexane). ¹H NMR (DMSO-d₆, 500 MHz): δ 8.43 (s, 2H), 8.22 (d, J=7.5 Hz, 2H), 8.09 (d, J=7.5 Hz, 2H), 8.79 (d, J=16.5 Hz, 2H), 7.53 (t, J=7.5 Hz, 2H), 7.48 (t, J=7.5 Hz, 2H), 7.05 (d, J=16.5 Hz, 2H), 6.44 (s, 1H). ¹³C NMR (DMSO-d₆, 125 MHz): δ 183.7, 140.4, 137.3, 132.4, 132.1, 130.6, 125.7, 125.2, 123.8, 122.7, 102.0. HRMS (ESI): m/z [M+H]+ calcd for  $C_{23}H_{17}O_2S_2$ : 389.06700; found: 389.06055. IR (cm⁻¹): 3093 to 2852, 1614, 1489, 1421, 1269, 1134, 958.

Benzothiophene-2-Curcuminoid-BF2 adduct (8-BF2): Yield 28%, black solid,  $R_c 0.85$  (40% EtOAc in hexane). ¹H NMR (DMSO-d₆, 500 MHz): δ 8.38 (d, J=15.5 Hz, 2H), 8.11 (s, 2H), 8.06 (d, J=8.0 Hz, 2H), 7.97 (d, J=7.5 Hz, 2H), 7.51 (dt, J=7.5 and 1.5 Hz, 2H), 7.46 (dt, J=8.0 and 1.5 Hz, 2H), 6.89 (d, J=15 Hz, 2H), 6.83 (s, 1H). ¹³C NMR

1325, 1277, 1263, 1168, 1126, 1093, 1067, 1022.

(DMSO-d₆, 125 MHz): δ 179.5, 141.4, 140.5, 140.0, 139.8, 133.8, 128.1, 125.9, 123.4, 122.5, 110.0, 103.5. ¹⁹F NMR (DMSO-d₆, 470 MHz):  $\delta$  -137.2 (s, ¹¹B-F), -137.3 (s, ¹⁰B-F). IR (cm⁻¹): 3057 to 2851, 1599, 1533, 1485, 1385, 1283, 1136, 1051.

(1E,4E,6E)-5-Hvdroxy-1,7-bis(benzo[b]thiophen-2-vl) hepta-1,4.6-trien-3-one (8): Yield 93%, orange solid, R_c0.92 (40% EtOAc in hexane). ¹H NMR (DMSO-d₆, 500 MHz): δ 16.0 (br s, 1H), 8.00 (d, J=7.5 Hz, 2H), 7.97 (d, J=16 Hz, 2H), 7.90 (d, J=7.0 Hz, 2H), 7.87 (s, 2H), 7.45 (dt, J=7.5 and 2 Hz, 2H), 7.41 (dt, J=7.5 and 2.0 Hz, 2H), 6.65 (d, J=16 Hz, 2H), 6.36 (s, 1H). HRMS (ESI): m/z [M+H]+ calcd for C₂₃H₁₇O₂S₂: 389.06700; found: 389.05377.

Benzofuran-2-Curcuminoid-BF 2 adduct (9-BF2): Yield: 15 70%, dark-red solid, mp>240° C. R_f 0.84 (40% EtOAc in hexane).  1 H NMR (CDCl₃, 500 MHz):  $\delta$  7.91 (d, J=15.0 Hz, 2H), 7.65 (d, J=7.5 Hz, 2H), 7.53 (dd, J=8.5 Hz, 2H), 7.45 (dt, J=7.0 Hz and 1.0 Hz, 2H), 7.23 (dt, J=7.0 Hz and 1.0 Hz, 2H), 7.14 (s, 2H), 6.88 (d, J=15.5 Hz, 2H), 6.16 (s, 1H). ¹³C ₂₀ 1223, 1119. NMR (CDCl₃, 125 MHz): δ 179.3, 156.4, 152.3, 132.8, 128.5, 127.9, 123.9, 122.5, 120.9, 115.5, 111.6, 103.5. ¹⁹F NMR (CDCl₃, 470 MHz):  $\delta$  –140.15 (s, ¹¹B-F), –140.1 (s, ¹⁰B-F). IR (cm⁻¹): 2918, 1614, 1557, 1508, 1396, 1348, 1288, 1155, 1124, 1057, 947.

(1E,4E,6E)-5-Hydroxy-1,7-bis(benzo[b]furan-2-yl) hepta-1,4,6-trien-3-one (9): Yield: 88% yellow-orange solid, mp: 178-180° C. R_f 0.92 (40% EtOAc in hexane). ¹H NMR (acetone-d₆, 500 MHz): δ 7.73 (dd, J=7.5 and 1.5 Hz, 2H), 7.67 (d, J=15.0 Hz, 2H), 7.59 (d, J=7.5 Hz, 2H), 7.44 (dd, 30 J=7.5 and 1.5 Hz, 2H), 7.31 (dt, J=7.5 and 1.7 Hz, 2H), 7.31 (s, 2H), 6.91 (d, J=15.0 Hz, 2H), 6.31 (s, 1H). ¹³C NMR (CDCl₃, 125 MHz): 8 182.5, 155.7, 153.1, 128.6, 127.2, 126.5, 124.6, 123.4, 121.7, 111.4, 111.3, 103.3. HRMS (ESI): m/z  $[M+H]^+$  calcd for  $C_{23}H_{17}O_4$ : 357.11268; found: 35 1126, 1011. 357.10632. IR (cm⁻¹): 3080, 2953, 1608, 1557, 1516, 1348, 1286, 1256, 1200.

3,5-bis((E))-(benzo[b]thiophen-3-yl)vinyl)-1-phenyl-1Hpyrazole (10): Yield: 50%, light-brown/orange solid, mp: 141-143° C., R₆ 0.87 (40% EtOAc in hexane). ¹H NMR 40 (CDCl₃, 500 MHz): δ 8.10 (d, J=8.0 Hz, 1H), 7.94 (d, J=8.0 Hz, 1H), 7.90 (d, J=8.0 Hz, 1H), 7.89 (d, J=8.0 Hz, 1H), 7.39-7.47 (m, unresolved, 6H), 7.62-7.52 (m, unresolved, 7H), 7.31 (d, J=16.0 Hz, 1H), 7.01(s, 1H), 6.98 (d, J=16.5 Hz, 1H). ¹³C NMR (CDCl₃, 125 MHz): δ 151.2, 142.5, 45 140.5, 139.3, 127.7, 137.4, 133.8, 133.2, 129.4, 128.2, 125.5, 124.8, 124.6, 124.6, 124.5, 124.4, 123.4, 123.1, 123.0, 122.6, 122.1, 121.8, 121.5, 116.7, 101.0. HRMS (ESI): m/z [M+H]⁺ calcd for  $C_{29}H_{20}N_2S_2$ : 461.11462.; found: 461.10458. IR (cm⁻¹): 3028, 3010, 1694, 1645, 1633, 50 1603, 1494, 1440, 1404, 1373, 1249, 1153, 1028.

3,5-bis((E))-(benzo[b]thiophen-3-yl)vinyl)-1-(3-(trifluoromethyl)phenyl)-1H-pyrazole (11): Yield 63.0%, lightbrown solid, mp: 95-96° C.,  $R_f$ 0.91 (40% EtOAc in hexane). ¹H NMR (CDCl₃, 500 MHz): δ 8.11 (d, J=8.5 Hz, 1H), 7.96 55 (d, J=8.5 Hz, 1H), 7.95 (s, 1H), 7.91 (d, J=8.0 Hz, 2H), 7.79 (d, J=7.5 Hz, 1H), 7.78 (d, J=7.5 Hz, 1H), 7.72 (d, J=7.5 Hz, 1H), 7.67 (d, J=7.5 Hz, 1H), 7.64 (s, 1H), 7.56 (d, J=15.5 Hz, 1H), 7.54 (s, 1H), 7.50-7.40 (m, unresolved, 5H), 7.30 (d, J=16.5 Hz, 1H), 7.03 (s, 1H), 6.97 (d, J=16.5 Hz, 1H). ¹³C 60 NMR (CDCl₃, 125 MHz): δ 151.9, 142.7, 140.6, 140.6, 139.9, 137.6, 137.3, 133.7, 133.0, 132.0 (q,  ${}^{1}J_{CE}=250 \text{ Hz}$ ), 130.0, 128.3, 125.5, 124.9, 124.7, 124.7 124.6, 124.4, 124.0, 123.5, 123.1, 123.0, 122.9, 122.2 (q,  $J_{CF}$ =3.5 Hz), 122.1, 121.8, 121.2, 116.0, 101.7. ¹⁹F NMR (CDCl₃, 470 MHz): δ -62.60 (s, CF₃). HRMS (ESI): m/z [M+H]⁺ calcd for  $C_{30}H_{19}N_2F_3$ : 529.102001.; found: 529.10034. IR (cm⁻¹):

70 3067, 1699, 1614, 1597, 1497, 1456, 1423, 1377, 1360,

3,5-bis((E))-(benzo[b]thiophen-3-yl)vinyl)-1-(3,5-difluorophenyl)-1H-pyrazole (12): Yield: 50%, yellow solid, mp: 178-179° C. R_f 0.85 (40% EtOAc in hexane). ¹H NMR  $(CDCl_3, 500 \text{ MHz}): \delta 8.09 \text{ (d, J=8.0 Hz, 1H)}, 7.97 \text{ (d, J=8.0 Hz, 1H)}$ Hz, 1H), 7.91 (d, J=8.0 Hz, 1H), 7.90 (d, J=7.5 Hz, 1H), 7.62 (s, 1H), 7.58 (s, 1H), 7.53 (d, J=16.0 Hz, 1H), 7.39-7.40 (unresolved region, 5H), 7.27-7.19 (unresolved region, 2H), 7.00 (d, J=17.0 Hz, 2H), 6.98 (s, 1H), 6.89 (tt, J=5.5 Hz and 2.5 Hz, 1H).  13 C NMR (CDCl₃, 125 MHz):  $\delta$  163.1 (d,  ${}^{1}J_{CF}$ =249.0 Hz), 163.0 (d,  ${}^{1}J_{CF}$ =249.0 Hz), 152.0, 142.7, 141.4 (t,  ${}^{3}J_{CF}$ =12.3 Hz), 140.6, 140.5, 137.6, 137.3, 133.6, 133.0, 125.5, 124.9, 124.7, 124.7, 124.5, 123.9, 123.7, 123.1, 123.0, 122.9, 122.1, 121.7, 121.1, 116.0, 108.4, 103.3 (t,  ${}^2\mathrm{J}_{CF}$ =25.7 Hz), 102.3.  ${}^{19}\mathrm{F}$  NMR (CDCl $_3$ , 470 MHz):  $\delta$ -107.37 (m, 2F). HRMS (ESI): m/z [M+H]+ calcd for  $C_{29}H_{19}N_2S_2F_2$ : 497.09577; found: 497.08199. IR (cm⁻¹): 3080, 1620, 1597, 1539, 1481, 1462, 1425, 1304, 1263,

3,5-bis((E))-(benzofuran-2-yl)vinyl)-1-phenyl-1H-pyrazole (13): Yield: 67%, yellow solid, mp: 149-151° C. R_f 0.95 (40% EtOAc in hexane). ¹H NMR (CDCl₃, 500 MHz): δ 7.57-7.47 (unresolved region, 8H), 7.54 (d, J=8.0 Hz, 2H), 7.35 (d, J=17.5 Hz, 1H), 7.30-7.26 (complex region, 2H), 7.21 (t, J=8.0 Hz, 2H), 7.18 (d, J=16.5 Hz, 1H), 7.09 (d, J=15.5 Hz, 1H), 7.00 (d, J=16.0 Hz, 1H), 6.87 (s, 1H), 6.73 (s, 1H), 6.71 (s, 1H). ¹³C NMR (CDCl₃, 125 MHz): δ 155.0, 155.0, 154.8, 153.9, 150.4, 141.9, 139.2, 129.4, 129.1, 128.8, 128.3, 125.6, 125.2, 124.7, 123.1, 122.9, 121.5, 121.1, 120.9, 119.9, 118.6, 116.3, 111.0, 106.9, 105.5, 102.2. HRMS (ESI): m/z  $[M+H]^+$  calcd for  $C_{29}H_{21}N_2O_2$ : 429.16030; found: 429.15786. IR (cm⁻¹, CH₂Cl₂): 3055, 2924, 1713, 1597, 1497, 1451, 1366, 1288, 1250, 1188,

3,5-bis((E))-(benzofuran-2-yl)vinyl)-1-(3,5-difluorophenyl)-1H-pyrazole (14): Yield: 54%, yellow solid, mp: 158-160° C. R_f 0.91 (40% EtOAc in hexane). ¹H NMR (CDCl₃, 500 MHz): δ 7.57-7.54 (overlapping pair of doubles, triplet appearance, 2H), 7.50-7.46 (overlapping pair of doubles, triplet appearance, 2H), 7.34-7.15 (unresolved region, 8H), 7.14 (d, J=16.0 Hz, 1H), 7.06 (d, J=16 Hz, 1H), 6.93 (tt, J=9.0 Hz and 2.0 Hz, 1H), 6.86 (s, 1H), 6.78 (s, 1H), 6.74 (s, 1H). ¹³C NMR (CDCl₃, 125 MHz): δ 163.1 (d,  $^{1}J_{CF}$ =249.0 Hz), 163.0 (d,  $^{1}J_{CF}$ =249.0 Hz) 155.2, 155.0, 154.5, 153.5, 151.1, 142.1, 141.2 (t, ³J_{CF}=12.4 Hz), 129.0, 128.8, 125.5, 124.9, 123.2, 123.0, 121.2, 121.1, 121.0, 120.8, 119.2, 115.4, 111.1, 111.0, 108.6, 107.5, 105.9, 103.5 (t,  ${}^{2}J_{CF}$ =25.7 Hz), 103.2.  ${}^{19}F$  NMR (CDCl₃, 470 MHz):  $\delta$ -107.4 (m, 2F). HRMS (ESI): m/z [M+H]+ calcd for  $C_{29}H_{19}N_2O_2F_2$ : 465.14146; found: 465.13156. IR (cm⁻¹): 3086 to 2926, 1620, 1600, 1562, 1526, 1481, 1450, 1381, 1348, 1329, 1285, 1254, 1225, 1196, 1118.

3,5-bis((E))-(benzofuran-2-yl)vinyl)-1-(3-(trifluoromethoxy)phenyl)-1H-pyrazole (15): Yield: 22%, light brown solid, mp: 128-129° C. R, 0.96 (40% EtOAc in hexane). ¹H NMR (CDCl₃, 500 MHz): δ 7.63 (overlapping pair of doubles, 2H), 7.57 (d, J=7.5 Hz, 1H), 7.56 (d, J=8.0 Hz, 1H), 7.50 (d, 8 Hz, 1H), 7.46-7.42 (unresolved, 3H), 7.35-7.22 (complex region, 5H), 7.18 (d, J=16.0 Hz, 1H), 7.07 (d, J=16.0 Hz, 1H), 7.03 (d, J=16.0 Hz, 1H), 6.89 (s, 1H), 6.77 (s, 1H), 6.73 (s, 1H). ¹³C NMR (CDCl₃, 125 MHz): δ 150.3, 150.2, 149.9, 148.9, 146.1, 143.9, 137.3, 133.0, 124.3, 124.0, 122.0, 120.6, 120.0, 118.4, 118.2, 117.1, 116.6, 116.4, 116.1, 115.5, 114.0, 111.0, 106.3, 106.3, 102.5, 101.0, 97.8. ¹⁹F NMR (CDCl₃, 470 MHz): δ 57.83 (s, OCF3). HRMS (ESI): m/z  $[M+H]^+$ 

 $C_{30}H_{20}N_2O_3F_3$ : 513.14260.; found: 513.13940. IR (cm⁻¹): 3116 to 2926, 1717, 1668, 1609, 1564, 1510, 1452, 1371, 1384, 1254, 1205, 1161, 1033, 1015.

## Computational Methods

B3LYP/6-31G* geometry optimizations were performed 5 with the Gaussian 09 suite of programs. Molecular docking calculations were carried out with the program AutoDock Vina for modeling the binding modes and gauging the interaction energies of the studied compounds as ligands for HER2, proteasome, VEGFR2, BRAF, and BCL-2 proteins. The three-dimensional coordinates of the proteins were obtained from the Protein Data Bank (PDB codes 3PP0 (HER2), 3SDK (20S proteasome), 4AG8 (VEGFR2), 4XV2 (BRAF), and 4LVT (BCL-2)). (T. Castanheiro, et al., Chem. 15 Soc. Rev. 2016, 45, 494; G. Malik, et al., Chem. Sci., 2017, 8, 8050-8060; D. Wu, et al., J. Org. Chem. 2018, 83, 1576-1583; A. Vyas, et al., Curr. Pharm. Des. 2013, 19, 2047-2069; G. R. Pillail, et al., Cancer Letters 2004, 208, 163-170; A. L. Loprestil, et al., J. Psychopharmacology 20 2012, 26, 1512-1524; D. Perrone, et al., Experimental and Therapeutic Medicine 2015, 10, 1615-1623; M. Mimeault, et al., Chin. Med. 2011, 6, 31; C. Cheng, et al., RSC Adv. 2017, 7, 25978-25986; L. Zhang, et al., Environ. Tox. Pharm. 2016, 48, 31-38; M. M. Yallapu, et al., Colloids and Surfaces 25 B: Biointerfaces 2010, 79, 113-125; J. Liu, et al., Curr. Pharm.Des. 2013, 19, 1974-1993)

Chain A of HER2, VEGFR2, BRAF and BCL-2, and chains K ( $\beta$ 5 subunit) and L ( $\beta$ 6 subunit) of 20S proteasome were selected as target templates for the docking calculations. Co-crystallized ligands and crystallographic water molecules were removed. Addition of hydrogens, merger of non-polar hydrogens to the atom to which they were attached, and assignment of partial charges were computed with AutoDockTools. Docking areas were constrained to a 35 30×30×30 Å box centered at the active site, which provided suitable space for rotational and translational movement of the ligands.

## Bioassay Methods

NCI-60 assay: Samples were submitted to the National 40 Cancer Institute (NCI of NIH) Developmental Therapeutics anticancer screening program (DTP) for human tumor cell line assay by NCI-60 screening against leukemia, lung, colon, and CNS cancers, as well as melanoma, ovarian, renal, prostate, and breast cancers. Compounds are initially 45 tested at a single dose of 10⁻⁵ molar. Data are reported as mean graph of percent growth (GP). Growth inhibition is shown by values between 0 and 100 and lethality by values less than zero. Compounds that meet selection criteria based on one-dose assay are then tested against 60 cell panel at five 50 concentrations

Cell Viability assay to determine EC50: Cells  $(2\times10^3)$ cell/well) were incubated with the compounds (concentration range 0-30000 nM) in a 384-well plate for 72 hours in a CO₂ incubator (5% CO₂, 37° C.). Cell lines and PBCMs 55 (peripheral blood mononuclear cells from healthy donors as non-cancer CONTROL) were seeded in quadruplicate (technical replicates). CellTiter-Glo® 2.0 reagent equal to the volume of cell culture medium present in each well was added and the plate was left to incubate at room temperature 60 for 10 minutes to stabilize the luminescent signal. Luminescent signal/intensity from the 384-well plate was read on a plate reader. Cells/cell lines used: BCWM.1 (Waldenstrom macroglobulinemia cell line, WM); RPMI-8266 (Multiple myeloma cell line, MM); RS4; 11 (Acute lymphoblastic 65 leukemia, ALL). For Apoptosis study cells were treated with the indicated agents and concentrations (FIG. 74) for 24 h

72

and stained with annexin-V and propidium iodide (PI), followed by flow cytometry analysis.

Cell culture. Colorectal cancer and normal colon cell lines were obtained from ATCC (Manassas, Va.). Cells were maintained in DMEM medium (Life Technologies, Carlsbad, Calif.) supplemented with 10% fetal bovine serum (Life Technologies), 1% non-essential amino acids (Life Technologies), 1% penicillin-streptomycin (Life Technologies), and 1% glutamine (Life Technologies) at 37° C. and 5% CO₂.

Cell viability. Cells were seeded in 96-well plates with approximately 5.0×10³ cells/well and incubated in RPMI1640 medium (supplemented with 10% fetal bovine serum and 1% glutamine) for 24 hours. Cells were then treated with RPMI1640 medium containing CURs (10 μM) or vehicle (DMSO) for 48 hours and the number of viable cells determined using CellTiter-FluorTM cell viability assay kit (Promega, Madison Wis.). The fluorescence (excitation 400 nm, emission 505 nm) was detected using infinite M200 Pro microplate reader (TECAN).

Luciferase reporter gene assay. Cells stably transfected with luciferase reporter gene containing AHR binding elements were cultured with DMEM media containing 10  $\mu$ M CURs or 0.1% DMSO for 6 hours. The luciferase activity was measured using the dual luciferase reporter assay system (Promega) according to manufacturer's instructions, and infinite M200 Pro microplate reader (TECAN).

### Example 6—Deuterated CUR Compounds

Synthesis of a library of deuterated CUR—BF₂ and CUR compounds has been accomplished and bioassay data are being collected. These studies aim to determine if deuterated analogs are metabolitically more stable.

Deuterated compounds were formed from aryl-aldehydes or fluorinated aryl-aldehydes, as seen in FIG. 78. The aryl aldehyde was mixed with deuterated water and deuterated sulfates and placed into a microwave vial equipped with magnetic stirrer. The vial was sealed and irradiated for 6 min at 140° C. in the microwave. The vial was cooled to r.t. and solvent removed. The deuterated curcuminoids, such as those shown in FIGS. 76 and 77, were synthesized according to the general protocols outlined in Examples 2 and 3 above, starting with the deuterated aldehydes. A new library of deuterated CUR-BF2 and CUR compounds were synthesized along with their corresponding non-deuterated analogs for side by side study of their bio-activity, by replacing the -OCH₃ groups with —OCD₃ as shown in FIG. **76**. In other examples H/D exchange has been achieved in the aromatic rings. The NCI-60 data on a hexa-deuterated analog is shown in FIG. 79.

#### Conclusion

The inventors have synthesized numerous CUR-inspired compounds which have shown anti-proliferative activity against multiple cancer cells lines. These compounds can be used in drug development for cancer treatments.

In the preceding specification, all documents, acts, or information disclosed does not constitute an admission that the document, act, or information of any combination thereof was publicly available, known to the public, part of the general knowledge in the art, or was known to be relevant to solve any problem at the time of priority.

The disclosures of all publications cited above are expressly incorporated herein by reference, each in its entirety, to the same extent as if each were incorporated by reference individually.

20

It will be seen that the advantages set forth above, and those made apparent from the foregoing description, are efficiently attained and since certain changes may be made in the above construction without departing from the scope of the invention, it is intended that all matters contained in the foregoing description or shown in the accompanying drawings shall be interpreted as illustrative and not in a limiting sense.

It is also to be understood that the following claims are intended to cover all of the generic and specific features of the invention herein described, and all statements of the scope of the invention which, as a matter of language, might be said to fall therebetween. Now that the invention has been described,

What is claimed is:

1. A composition comprising formula (I):

$$\begin{array}{c} R_1 \\ R_2 \\ R_3 \end{array} \qquad \begin{array}{c} R_4 \\ R_6 \\ R_7 \end{array} \qquad \begin{array}{c} R_5 \\ R_7 \\ R_3 \end{array} \qquad \begin{array}{c} R_1 \\ R_2, \\ R_3 \end{array}$$

where * is a double bond or a single bond;

wherein * is a double bond when at least one of  $R_6$  and  $_{30}$   $R_7$  is unsubstituted or a single bond when  $R_6$  is fluorine or hydrogen and  $R_7$  is fluorine;

where • is a double bond or a single bond;

wherein • is a double bond when * is a single bond; where R₁ is o-OCH₃, m-OCH₃, o-F, or H; where R₂ is o-OCH₃, m-OCH₃, H, m-OCF₃, m-F,

at a meta position, a pyrrole formed with  $R_1$  or  $R_3$ , or a thiocyanate-substituted pyrrole formed with  $R_1$  or  $R_3$ ;

where R₃ is p-F, p-OCH₃, m-CF₃, p-CF₃, p-SCF₃, p-OH, m-OCF, p-OCF,

at a para position, or

at a para position;

where  $\hat{R}_4$  is O associated with a difluoroboron adduct formed with  $R_5$ ;

where  $R_5$  is O associated with a difluoroboron adduct formed with  $R_4$ ;

where  $R_6$  is H, F, or unsubstituted forming a double bond at  $\bullet$ ;

where  $R_7$  is H, or F.

2. The composition of claim 1, further comprising at least one deuterated substituent on the aryl.

3. The composition of claim 2, wherein the at least one deuterated substituent is deuterated methoxy.

**4**. The composition of claim **3**, wherein the deuterated methoxy is R—O-CD₃.

5. The composition of claim 1, further comprising at least one deuterated substitution on the aryl.

6. The composition of claim 5, wherein the at least one deuterated substitution is a plurality of deuterated substitutions.

7. The composition of claim 6, wherein the plurality of deuterated substitutions is at the meta positions.

* * * * *